

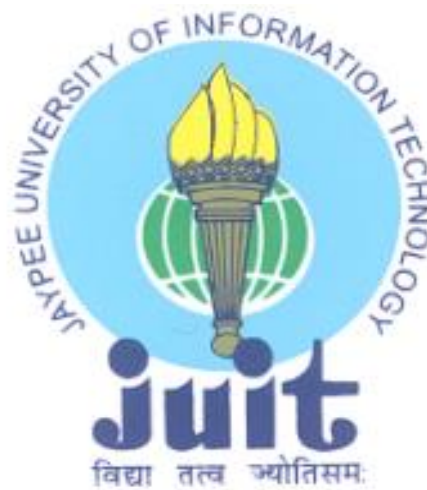
A LOW POWER WEARABLE ECG MODULE FOR HEART RATE VARIABILITY CLASSIFICATION SYSTEM

Thesis submitted in fulfillment of the requirements for the Degree of

DOCTOR OF PHILOSOPHY

By

KIRTI



Department of Electronics and Communication Engineering
JAYPEE UNIVERSITY OF INFORMATION TECHNOLOGY
WAKNAGHAT, DISTRICT SOLAN, H.P., INDIA

November, 2020

@ Copyright JAYPEE UNIVERSITY OF INFORMATION TECHNOLOGY, WAKNAGHAT
November, 2020
ALL RIGHT RESERVED

Dedicated to
My
Beloved Parents and
Husband

TABLE OF CONTENTS

Contents	Page No.
DECLARATION BY THE SCHOLAR	i
SUPERVISOR'S CERTIFICATE	ii
LIST OF ABBREVIATIONS AND ACRONYMS	v
LIST OF FIGURES	vii
LIST OF TABLES	x
ABSTRACT	xii
CHAPTER 1	
INTRODUCTION	2
1.1 HUMAN CARDIAC SYSTEM	3
1.2 ECG SIGNAL AND ITS COMPONENTS	5
1.3 ECG SIGNAL GENERATION AND ACQUISITION	8
1.4 ECG NOISES	10
1.5 EXPERIMENTAL ECG DATABASE	13
1.6 SOFTWARE BASED HIGH LEVEL DESIGN TOOLS.....	15
1.6.1 MATLAB	16
1.6.2 Xilinx System Generator Tool.....	16
1.6.3 Simulink	17
1.7 PERFORMANCE PARAMETERS	17
1.8 MOTIVATION	19
1.9 RESEARCH GAPS	20
1.10 RESEARCH OBJECTIVES	20
1.11 THESIS ORGANIZATION	21
CHAPTER 2	
LITERATURE REVIEW	24
2.1 QRS DETECTION ALGORITHM.....	24
2.1.1 Derivative based slant for QRS detection	26
2.1.2 Wavelet Based Approach for QRS detection	27

2.1.3 Other Approach for QRS detection.....	27
2.2 CARDIO-VASCULAR DISEASES	28
2.2.1 Abnormalities in P, QRS, T waves	28
2.2.2 Abnormalities resides in the Cardiac Rhythm	32
2.3 ECG SIGNAL PRE-PROCESSING USING DIGITAL FILTERS	33
2.4 DIGITAL FILTER DESIGN BASED ON FPGA	35
2.5 HRV BASED CLASSIFICATION	41

CHAPTER 3

RESOURCE EFFICIENT FPGA BASED DENOISING MODULE.....	48
3.1 INTRODUCTION.....	49
3.1.1 FPGA Technology	52
3.1.2 Zynq- 7000 Zedboard Architecture.....	54
3.1.3 Design Flow of Xilinx FPGA	55
3.1.4 Design Flow for FPGA based DSP.....	56
3.2 DIGITAL FILTERING TECHNIQUES	57
3.3 PROPOSED METHODOLOGY	59
3.3.1 Two-tier ECG Denoising Architecture.....	62
3.3.2 Three-tier ECG Denoising Architecture.....	63
3.4 RESULTS & DISCUSSION.....	64
3.4.1 Two-Tier ECG Denoising Block	64
3.4.2 Three-tier ECG Denoising Block.....	67
3.5 COMPARISON OF PROPOSED ARCHITECTURES WITH EXISTING LITERATURE	72
3.6 CONCLUSION	73

CHAPTER 4

FPGA BASED POWER EFFICIENT WEARABLE ECG MODULE.....	76
4.1 INTRODUCTION.....	76
4.1.1 Types of Power Dissipation in FPGA	78
4.1.2 Power Contributing Factors in FPGA	80
4.2 PROPOSED METHODOLOGY	82
4.2.1 Collateral Architecture	84

4.2.2 Sequence Architecture.....	86
4.3 RESULTS AND DISCUSSION	88
4.3.1 Collateral ECG Denoising Architecture.....	89
4.3.2 Sequence ECG Denoising Architecture	91
4.4 VALIDATION OF RESULTS.....	93
4.5 COMPARISON OF PROPOSED ARCHITECTURES WITH EXISTING LITERATURE	95
4.6 CONCLUSION	96

CHAPTER 5

MULTISTAGE HEART RATE VARIABILITY CLASSIFICATION SYSTEM.....99

5.1 INTRODUCTION.....	99
5.1.1 Heart Rate Variability	100
5.2 PROPOSED METHODOLOGY	101
5.2.1 HRV Classification by employing Time-domain features.....	111
5.2.2 HRV Classification by employing CAD-FSC system	111
5.2.3 HRV Classification by employing MSHVC system.....	113
5.3 RESULTS & DISCUSSION.....	114
5.3.1 HRV Classification by employing Time-domain features	114
5.3.2 HRV Classification by employing CAD-FSC.....	118
5.3.3 HRV Classification by employing MSHVC	125
5.4 COMPARISON OF PROPOSED METHODOLOGIES WITH RECENT LITERATURE	134
5.5 CONCLUSION	135

CHAPTER 6

CONCLUSION AND FUTURE SCOPE137

6.1 CONCLUSION	137
6.2 FUTURE SCOPE.....	140
LIST OF PUBLICATIONS.....	143
REFERENCES	146
APPENDICES	163

DECLARATION BY THE SCHOLAR

I hereby declare that the work contained in the Ph.D thesis entitled “**A Low Power Wearable ECG Module for Heart Rate Variability Classification System**” submitted at **Jaypee University of Information Technology, Wagnaghat, India** is an authentic record of my work carried out under the supervision of **Dr. Shruti Jain & Dr. Harsh Sohal**. I have not submitted this work elsewhere for any other degree or diploma. I am fully responsible for the contents of my Ph.D. thesis.



Kirti

Enrollment No.: 176006

Department of Electronics and Communication Engineering

Jaypee University of Information Technology,

Wagnaghat, Solan, H.P-173234

Date: 23-11-2020



JAYPEE UNIVERSITY OF INFORMATION TECHNOLOGY

(Established by H.P. State Legislative vide Act No. 14 of 2002)
P.O. Wagnaghat, Teh. Kandaghat, Distt. Solan - 173234 (H.P.) INDIA

Website: www.juit.ac.in

Phone No. (91) 01792-257999

Fax: +91-01792-245362

SUPERVISOR'S CERTIFICATE

This is to certify that the work reported in the Ph.D. thesis entitled “**A Low Power Wearable ECG Module For Heart Rate Variability Classification System**”, submitted by **Kirti** at **Jaypee University of Information Technology, Wagnaghat, India**, is a bonafide record of her original work carried out under my supervision. This work has not been submitted elsewhere for any other degree or diploma.

Dr. Shruti Jain

Associate Professor

Department of ECE

Jaypee University of Information

Technology, Wagnaghat

H.P, India

Dr. Harsh Sohal

Assistant Professor (Senior Grade)

Department of ECE

Jaypee University of Information

Technology, Wagnaghat

H.P, India

ACKNOWLEDGEMENT

*First of all, I owe and dedicate everything to the **Almighty GOD** for the strength, wisdom and perseverance that he had bestowed upon me during this research project, and indeed, throughout my life. A major research project like this can never be achieved by the only person's effort. The contribution of number of people in different aspects have made this happen. I extend my sincere gratitude to everyone who stood by me during the entire course of my Ph.D. work.*

*I would like to express my special appreciations and sincere thanks to my supervisors **Dr. Shruti Jain & Dr. Harsh Sohal** for sharing their truthful and illuminating views on a number of issues related to my topic of research and encouraging my research and allowing me to grow as a research scientist. They provided inspiring guidance for successful completion of my research work. I rate this as my privilege to work under their supervision. Your advice on both researches as well as on my career has been priceless. I have been blessed with your continuous moral support, invaluable inputs and suggestions when I needed the most.*

I gratefully acknowledge Jaypee University of Information Technology for offering me to perform this research successfully, for providing necessary facilities and support. I owe my gratitude to the Vice-chancellor Prof. (Dr.) Vinod Kumar for his optimism and humble nature that has always been an inspiration for me. A special thanks to the Director & Academic Head Prof. (Dr.) Samir Dev Gupta for imparting quality based education with ethics and values as its bedrock.

*My heartfelt appreciation to **Prof. M. J. Nigam**, Ex. Head of Department of Electronics and Communication & **Dr. Rajiv Kumar** present. Head of Department of Electronics and Communication for their co-operation, support and constant encouragement.*

I am also thankful to DPMC members for their guidance and valuable suggestions throughout my research work. I wish to convey my sincere thanks to all the faculty members of Department of Electronics and Communication Engineering, for their help and

*guidance at the various stages of this study. I am grateful to all the members of technical and non-technical staff especially for their valuable contributions special thanks to **Mr. Mohan Lal & Mr. Pramod Kumar Sir** for their unconditional support.*

*Last but not least, I want to thank my parents and brother for their encouragement, moral support, personal attention and care. I can't forget the pain that my parents have taken throughout my research work. It is only because of the support of my father **Mr. Manoj Kumar Tripathi**, love and blessings that I could overcome all frustrations and failures. I would like to thank my **grandmother, all family members and relatives** for their unconditional support, both financially and emotionally throughout my Ph.D. They always stood by my decision and provided me all the resources even in difficult times to help me achieve my goals and realize my dreams. Most of all I owe my gratitude towards my parent-in-laws and Husband **Mr. Pranav Kaushal** for their extraordinary belief, love and providing me the space for completing this research work.*

*I am also thankful to my senior colleagues **Dr. Prabhat Thakur, Dr. Ashima Kukkar & Dr. Jyotsna Dogra** for their moral support. Besides, I can never ever forget my colleagues and friends **Charu Bhardwaj, Urvashi Shrama, Pooja Sharma, Mahima Poonia , Amit Sharma & Ekta Thakur** who have helped me in numerous ways. I cherish the years spent in the Department of Electronics and Communication Engineering, JUIT, Wagnaghat.*

I am indebted to all those people who have made this dissertation possible and because of whom this research experience and wonderful journey shall remain everlasting and cherished forever in my sweet memories.

All may not be mentioned, but no one is forgotten.

Thanks to all of you!

Kirti

LIST OF ABBREVIATIONS AND ACRONYMS

ANOVA	Analysis of Variance
ASIC	Application Specific Integrated Circuit
AV Node	Atrio- Ventricular Node
BLW	Baseline Wander
BPF	Band-pass Filter
CHF	Congestive Heart Failure
CLB	Configuration Logic Blocks
CVD	Cardiovascular Disease
DER	Detection Error Rate
DSP	Digital Signal Processor
DWT	Discrete Wavelet Transform
ECG	Electrocardiogram
EMG	Electromyography
FFT	Fast Fourier Transform
FIR	Finite Impulse Response
FPGA	Field-programmable Gate Array
HDL	Hardware Descriptive Language
HR	Heart Rate
HRV	Heart Rate Variability
I/O	Input/ Output
IIR	Infinite Impulse Response
kNN	k Nearest Neighbor
LUT	Look Up Table
MCU	Micro-controller Unit
MIT-BIH	Massachusetts Institute of Technology-Beth Israel Hospital
NN	Neural Network
PLI	Power Line Interference
PPV	Positive Predictive Value
RAM	Random Access Memory

SA Node	Sinoatrial Node
SNR	Signal to Noise Ratio
SOC	System On Chip
SVM	Support Vector Machine
VHDL	VHSIC Hardware Description Language
WT	Wavelet Transform
XSG	Xilinx System Generator

LIST OF FIGURES

Figure No.	Title	Page No.
1.1	Distribution of Primary CVDs and other causes	2
1.2	Human Cardiac System	4
1.3	ECG signal waveform & its components	6
1.4	Einthoven's Triangle	9
1.5	Placement of 12 –lead ECG	10
1.6	Pie-chart of the dataset source used	13
2.1	Block Diagram of Cardio – Vascular Disease	29
3.1	Portable ECG Equipment	48
3.2	Comparison of different processing units	49
3.3	General FPGA architecture	53
3.4	Overview of Zedboard architecture	54
3.5	FPGA design flow	55
3.6	FPGA/DSP design flow	56
3.7	Different window functions	59
3.8	Methodology of ECG pre-processing block	59
3.9	Steps to follow the digital filter design and specification	60
3.10	Effect of word length on the frequency response (a) 8-bit (b) 16-bit	61
3.11	Proposed methodology for two-tier ECG denoising architecture	62
3.12	Proposed Methodology for three-tier ECG denosing architecture	63
3.13	Simulink model for the realization of architecture 1	64
3.14	Scope results (a) Input ECG signal (b) Electromyography Noise Removal (c) Base Line Wander Removal	65

3.15	RTL schematic of low pass and high pass filter	66
3.16	Proposed architecture for pre-processor design	68
3.17	Basic constituent of FIR window function (a) Anti-symmetric (b) Symmetric	69
3.18	Scope view outcomes (a) Raw input ECG signal (b) Electromyography Noise Removal (c) Power Line Interference Removal (d) Base Line Wander Removal	70
3.19	RTL schematic of proposed ECG denoising block 2	71
4.1	Power contributing Factors in FPGA	80
4.2	Proposed methodology for ECG denoising block	83
4.3	Collateral ECG Denoising block	85
4.4	Sequence ECG Denoising block	86
4.5	FPGA Board(a) Virtex (b) Kintex(c) Zedboard	87
4.6	RTL schematic of ECG denoising block and its core structure	92
4.7	An Expert system for ECG denoising block	97
5.1	ECG waveform generation from various stimuli	100
5.2	Proposed methodology for HRV classification	102
5.3	Beat to Beat variation of $R-R$ intervals (Tachogram)	105
5.4	PSD for $R-R$ interval	106
5.5	Proposed Methodology of HRV Feature processing	111
5.6	Proposed CAD-FSC Methodology	112
5.7	Proposed methodology for the classification of Heart diseases	113
5.8	Histogram Plot (a) meanRR (b) maxRR (c) minRR (d) maxminRR (e) SDNN (f) HR	114
5.9	Q-Q Plot (a) meanRR (b) maxRR (c) minRR (d) maxminRR (e) SDNN (f) HR	115

5.10	Box Plot(<i>a</i>) meanRR (<i>b</i>) maxRR (<i>c</i>) minRR (<i>d</i>) maxminRR (<i>e</i>) SDNN (<i>f</i>) HR	115
5.11	Feature selection criteria based upon the <i>p</i> -value	119
5.12	Percentage improvement for accuracy and AUC by utilizing Time- domain	123
5.13	Percentage improvement for accuracy and AUC by utilizing Frequency-domain	123
5.14	Percentage enhancement for accuracy and AUC by utilizing Time- domain and Frequency-domain	124
5.15	Percentage Improvement for accuracy and AUC during 2- stage classification.	131
5.16	Percentage Improvement for accuracy and AUC during 3-stage classification	132
5.17	Percentage improvement during MSHVC classification	133
6.1	An expert system for low power wearable ECG module	139

LIST OF TABLES

Table No.	Title	Page No.
1.1	ECG Database Description	14
1.2	Confusion Matrix for the Diagnostic Test	18
2.1	Comparison of various QRS Detection Algorithms	25
2.2	Stages of MI	30
2.3	Explanation of disparity in ECG signal due to LBBB and RBBB	31
2.4	Primary abnormalities of cardiac rhythm	32
2.5	Secondary abnormalities of cardiac rhythm	33
3.1	Comparison of HPF and LPF for various types of Windowing techniques	67
3.2	Resource utilization and On-Chip power consumption of proposed 3-tier pre-processor design using window functions	72
3.3	Comparison with recent literature	73
4.1	Resource utilization and On-Chip power of Collateral denoising block	90
4.2	Resource utilization and On-Chip power of Sequence denoising block	91
4.3	Validation of results by employing wavelet transform	95
4.4	Comparison of Proposed architecture with recent literature	96
5.1	HRV Feature Description	103

5.2	z & p value of HRV parameters	116
5.3	Correlation of HRV features	116
5.4	Comparison of normal ECG and arrhythmic ECG	117
5.5	Performance measure of classification system utilizing time domain parameters before & after HRV statistical analysis	120
5.6	Performance measure of classification system using frequency domain features before and after using statistical analysis	121
5.7	Performance measure of classification system using time domain and frequency domain before a after employing statistical analysis	122
5.8	Comparison of HRV measures by ANOVA test	125
5.9	List of experiments performed for MSHRV system	126
5.10	Performance measure of classification system for two stage classification before HRV statistical analysis	126
5.11	Performance measure of classification system for two stage classification after HRV statistical analysis	127
5.12	Performance measure of classification system for 3-stage classification before HRV statistical analysis	128
5.13	Performance measure of classification system for three stage classification after HRV statistical analysis	129
5.14	Comparison with existing literature	134

ABSTRACT

The electrocardiogram (ECG) technology has emerged as one of the significant and easily available diagnostic techniques in the clinical cardiovascular domain to detect the diseases related to the heart and monitoring the electrical activity of the heart. The primary use of the ECG is to detect several cardiovascular diseases (CVD) namely myocardial infarction, Arrhythmia, Atrial Fibrillation & Ventricular Hypertrophy, etc. In recent time the research is going on automatic heartbeat detection, miniaturization of low power ECG processing wearable module & wireless patient's information transformation with IoT and MEMS-based chip design and integration. It is possible by the personalized heartbeat classification of a patient and accumulation of medical data with the integration of high-performance computing devices by using a reliable processing unit.

ECG signal attained is corrupted with several mechanical & electrical noise namely Power Line Interference (PLI), Baseline Wander (BLW), electrode movement/ electromyography (EMG), motion artifacts. For accurate analysis, the clinician requires a noiseless ECG signal. The Infinite Impulse Response (IIR) and Finite Impulse Response (FIR) filtering techniques help to remove the noise of the ECG signal. The FIR filters are chosen due to their linear response & hardware implementable nature. The FIR filters require large computational complexity for general purpose multiplier during the implementation, which limits its speed and demands more power & resources. This issue has been partially resolved by employing a Field Programmable Gate Arrays (FPGA) processing unit. The re-programmability, high speed, low power consumption & low execution time employ FPGA as an efficient processing unit in the area of biomedical applications designing. In this research, the most advanced & popular board namely Zynq-

7000 zedboard is utilized to design the wearable ECG denoising module for the multistage classification system.

The pre-processing of bio-signal is a very important step before the analysis as it affects the quality of the data & the decision making capability of clinicians. It also plays an important role in the performance of the bio-signal classification system. An optimized design for a resource-efficient digital filter is implemented on FPGA to denoise the ECG signal.

The different types of window filtering techniques are employed to test & validate the denoising ECG signal. The ECG samples obtained from the online platform of the MIT-BIH database is corrupted with various types of low & high-frequency noise. These noises are eradicated by employing digital filters in the MATLAB environment. A high-performance optimal order digital filter design is designed & implemented on an efficient modified hamming window. The modified window provides a better frequency response in comparison to other classical window functions. The proposed window function is modeled into Simulink using the Xilinx System Generator (XSG). The proposed Simulink model has been transferred to the Verilog Hardware Description Language using XSG. The high-performance ECG system chip design & its verification is done on an FPGA board. The proposed digital filter design is simulated & synthesized in Xilinx VIVADO on the FPGA development board. To make the FPGA an ideal fit and viable alternative for ECG diagnosis, a symmetrical structure design is proposed to make it more resourceful by optimizing the hardware components to accommodate it in a small chip area.

To attain the optimized results in terms of resource utilization and power consumption, various combinations of window filtering design (Kaiser, Bartlett, Blackmann, Hamming, Rectangular, and Hanning) for low pass and high pass filter is applied. To low power and resource utilization validates by an exhaustive comparison has been done among diverse windows functions that comprise of symmetric and anti-symmetric designs. The symmetric window function architecture has been chosen because it eliminates all three types of noises simultaneously and provides high performance in terms of resource utilization. The proposed architecture consumes 0.86 % of LUT, 4.52% of slice register & 7.72% of DSPs but it consumes 510 mW on-chip power; which is very high. The proposed architecture can attain minimum resources to remove ECG noises simultaneously but failed to lower the

power consumption. The selected architecture is employed in the stationary ECG module in which power consumption is not an important criterion.

The low power consumption is a vital criterion for wearable and handheld ECG devices. A robust collateral & sequence XSG architectures to attain low power criterion by employing modified hamming window function are suggested. Among collateral and sequence architecture; the sequence architecture provides better results as it acquires only 0.86% of slice LUTs, 5.13% slice registers, and only 8.18% of DSP for the proposed window function. The chosen architecture has consumed only 0.138W of on-chip power, which is suitable for portable ECG devices. The validation of the result has also been done by employing DWT based denoising using five wavelet functions (haar, daubechies, coiflet, symlet and biorthogonal). Among them, the Haar wavelet function utilizes 33% fewer resources as compared to the window function but in terms of power utilization, it consumes 122 mW more power than the proposed window function, which is not appropriate for the wearable ECG denoising module. The sequence architecture performs exceptionally for wearable ECG denoising blocks. This XSG architecture assists to design an overall expert system for the classification of several CVDs. In the classification of HRV based CVDs several HRV features are obtained by computing tachogram & PSD of R-R interval.

A multistage classification system contributes noteworthy applications on heart rate variability (HRV) based machine learning algorithms in medical diagnosis. HRV analysis has tremendous applications of mortality prediction due to various cardiac diseases. Machine learning algorithms offer optimized solutions in various medical domains like data mining for disease diagnosis, patient data management, patient data clustering, and classification for decision making, etc. The major intent of this thesis is the early stage prediction of Arrhythmia & Atrial Fibrillation by using HRV features & a machine learning approach. As in recent times, CVDs have become a growing social issue in India and across the world, therefore, its incidences, various risk factors, and prevention strategies have been presented in this research work. Three methodologies namely time-domain classification, a Computer-aided diagnostic system for feature-based classification (CAD-FSC) & Multistage HRV classification (MSHVC) have been proposed. Several HRV features in various domains (time, frequency & geometric) have been extracted from the pre-processed ECG signal. A total of 21 features are extracted for each subject. The

statistical analysis helps to select these significant features from the group of HRV features by eliminating redundant and irrelevant features. Only a few attributes signify a prominent effect on the classification accuracy and by utilizing these features three methodologies are proposed to develop an algorithm for better classification. A maximum of 82%, 97%, and 99% of overall accuracy is obtained by time-domain methodology, CAD-FSC system, and MSHVC system respectively. The proposed MSHVC system provides 98.55 % sensitivity to classify the CVDs accurately. The current work provides a robust system as compared to that of other published studies.

The Classification of HRV features is essential for the automatic detection of CVD cardiovascular disease. With the recent development of low-power wearable ECG devices, it becomes more viable to employ ECG for HRV based classification in daily life. The progress in embedded system design & technology unlocked the capability of wearable ECG expert system. This thesis work also introduced a low power expert system developed for HRV based multi-stage classification. The ECG expert system incorporates the sequence ECG denoising architecture for the pre-processing block & ANN classifier for the categorization of arrhythmia, atrial fibrillation & normal sinus rhythm. The wearable ECG expert device allows simple and rapid ECG monitoring of patients with suspected CVDs.

CHAPTER 1

INTRODUCTION

CHAPTER 1

INTRODUCTION

Cardiovascular diseases have merged as one of the leading causes of mortality in the world. The study conducted by the Indian Council of Medical Research (ICMR) presents that twenty-five percent of deaths due to cardiac diseases appear in the age group of 25-69 years.

The various Cardio-Vascular diseases (CVDs) such as heart attack, acute ischemia, myocardial infarction, etc. have emerged as one of the leading causes of death [1]. CVDs account for approximately 49% of sudden death and app. 51% of other types of cancers and injuries as illustrated in Figure 1.1. Stroke and acute ischemia accountable for more than 80% of deaths in India [3].

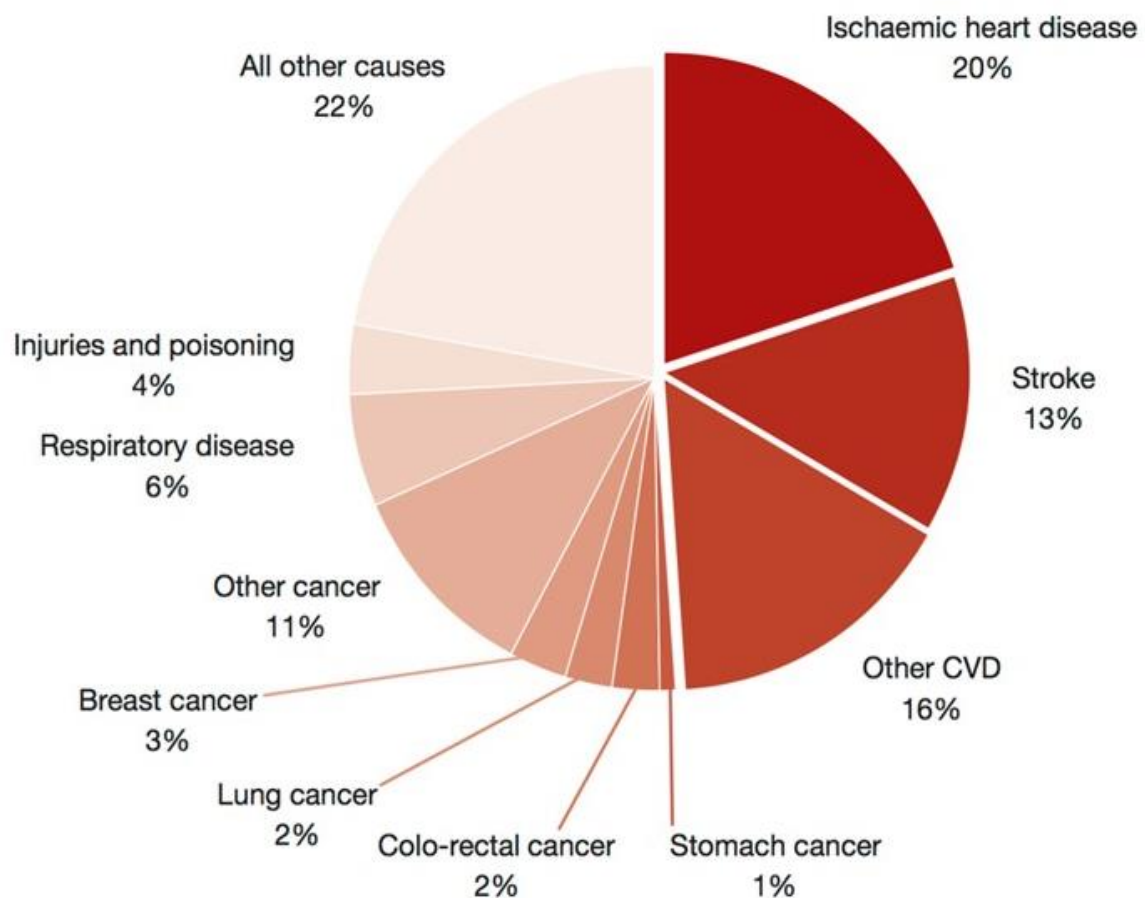


Figure 1.1: Distribution of Primary CVDs and other causes [2]

1.1 HUMAN CARDIAC SYSTEM

The cardiac muscles comprising about three hundred billion muscle cells are termed cardiac pacemaker cells and myocardiocytes. The myocardiocytes along with skeletal and nervous cells are labeled as excitable cells. These cells possess electrical properties of action potential and resting potential. An electrical potential difference is generated within the internal membrane and external membrane of the myocardiocytes.

The internal environment generally termed as cytosol has more concentration of K^+ ions in comparison to Ca^{2+} , Na^+ , and Cl^- ions. Whereas the external environment labeled as extracellular fluid has a low concentration of Na^+ in comparison to the Ca^{2+} , K^+ , and Cl^- concentrations. A cardiac action potential is generated due to the concentration difference within the internal and external membrane of the cardiac cells. In the Sino-Atrial (SA) node, Purkinje fibers, Bundle of His, and Atrio-Ventricular (AV) node of heart pacemakers cells are located. The pacemaker cells have the prominent feature of automaticity that makes a difference from the myocardiocytes.

An individual task is performed by the pacemaker cell for the generation of electrical impulses, which help to build an action potential in the myocardiocytes. This action helps to keep the heart beating. The heart rate of an individual is determined by the period of one action potential.

The cardiac system of an individual constitutes of various parts and the heart is situated in the center of the cardiac system. The circulation of the blood in the entire body is done by the cardiac system. Figure 1.2 represents the illustrative diagram of the human cardiac system. The heart is divided into two parts: left and right, which is further separated into two chambers termed as atrium (upper chamber) and ventricle (lower chamber). The

atrium receives the deoxygenated blood from the lungs and ventricles transmit the blood to the whole body.

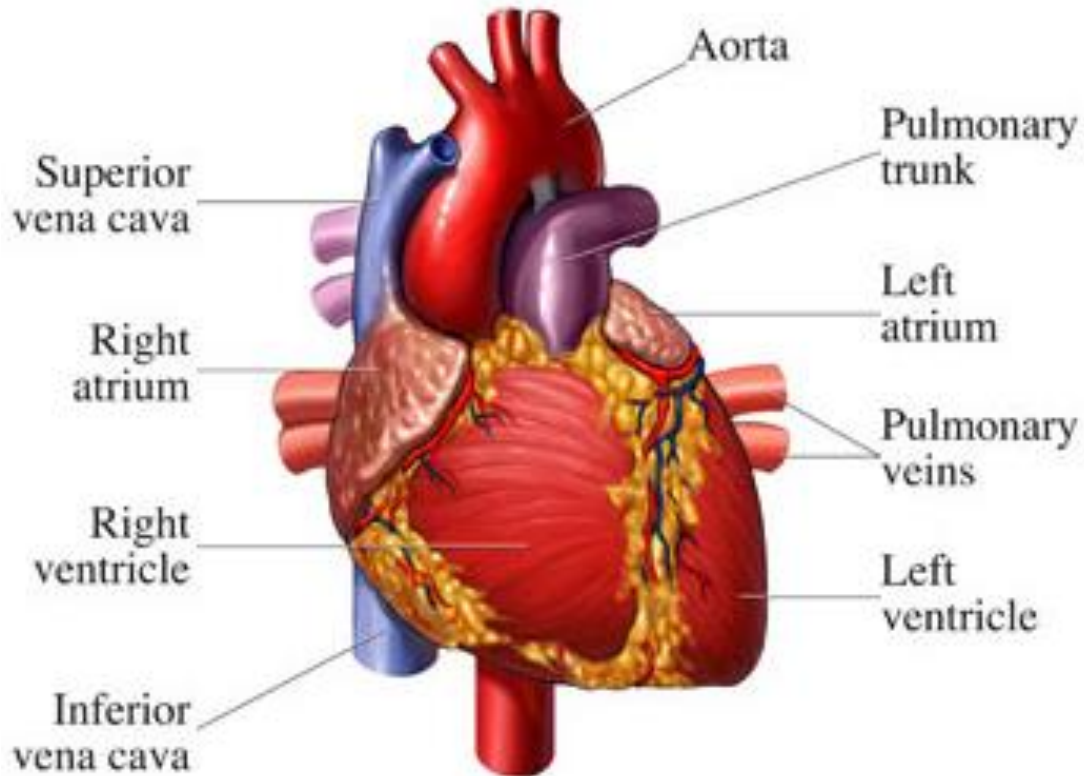


Figure 1.2: Human Cardiac System [5]

A non-conducting tissue namely fibrous helps to provide electrical isolation within the atrium and ventricle [5]. The isolation from the right atrium to the right ventricle and left atrium to the left ventricle is provided by the tricuspid valve and mitral valve respectively.

The right part of inferior and superior venacava collects the de-oxygenated blood from the entire body. The flow of blood is moving towards the right ventricle using a tricuspid valve and further pulmonary atria assist the flow of blood toward the lungs. The oxygenated blood is taken from the lungs via pulmonary atria towards the left atrium and the mitral valve facilitates the blood to transfer to the left ventricle. Then the oxygenated blood from the left ventricle is transferred to the entire body via the aorta. Throughout this cardiac procedure, Na^+ ions diffused through the cardiac cell membrane. Due to this, an

action potential generally termed as depolarization is generated within the internal and external cell membrane [7]. Also, the diffusion of K^+ ions from the internal to external cardiac cell membrane leads to repolarization. If the potential difference within the membrane is greater than the threshold value of the heart's primary pacemaker, that it generates an electrical pulse. This electrical pulse constructs a series of waveforms with the help of electrodes and leads situated on the patient's body.

When the trajectory of this pulse is drawn then it provides a graphical view of the electrical activity of the cardiac system, generally termed as Electrocardiogram (ECG). It is one of the primary diagnostic methods for the early diagnosis of CVDs. A typical ECG signal consists of components like waves, segments, and intervals. The morphology and amplitude of every component comprise vast medical information. In the biomedical signal processing community, the description of every component & automatic detection emerged as one of the challenging tasks.

1.2 ECG SIGNAL AND ITS COMPONENTS

A train of electrical impulses passed through the heart and sensed by the electrodes & leads attached to the human's body in the form of a waveform labeled as ECG. The repolarization and depolarization process of diverse muscle tissue constructs each part of the ECG waveform when an electrical impulse passes.

The repolarization and depolarization of the muscle tissue present in the atrium and ventricle provide a graphical representation in terms of *P-Q-R-S-T* segments and waves in an ECG as represented in Figure 1.3.

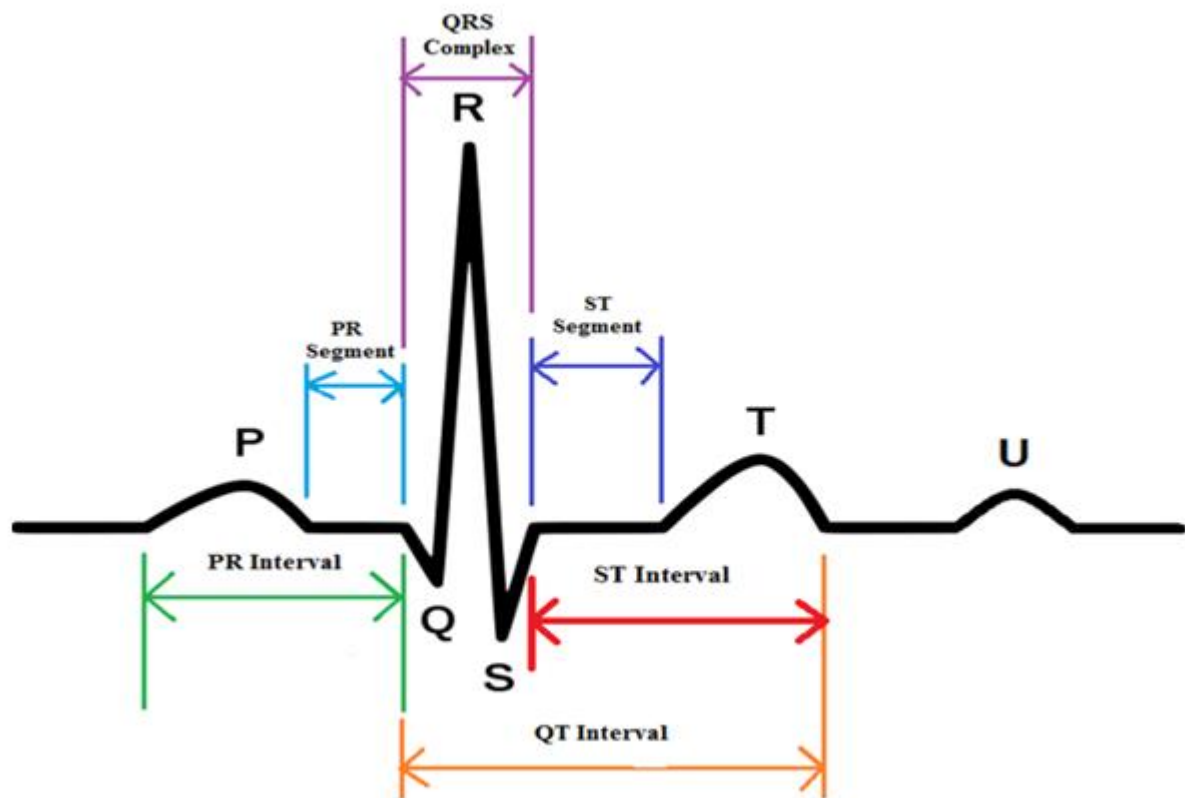


Figure 1.3: ECG signal waveform & its components [8]

The typical amplitude of an ECG signal is 0.2 mV and the useful frequency range lies between 0.5 to 100 Hz. When an electric impulse passes from the right atrium to the left atrium, there is a contraction that leads to the generation of a *P*-wave. Thereafter, the electrical impulse reaches AV node that causes ventricular contraction. The *Q-R-S* complex is produced as a result of this contraction process. The *T* wave generation & depolarization of ventricles is due to the electrical impulse which is passed through the bundle of His, bundle branches (left and right), and Purkinje fiber.

- i.* *P* wave: The depolarization of the atria which begins before the contraction of the atrium is illustrated by *P* wave. The interval of the *P* wave lies between 60ms to 110 ms.
- ii.* *QRS* Duration- The information about the duration of ventricular depolarization is given by *QRS* duration. The high amplitude *R* peaks are produced due to the high conduction velocity of an electrical impulse. The reason behind the increased conduction velocity is the more muscle mass of ventricles as compared to the atrium. In the beat detection procedures *R*- peak is generally the most common

standard. It is easily differentiable from the noise due to its high amplitude. The ventricle provides more to the QRS wave due to the high left muscle mass. The time interval of the QRS wave normally lies within 60 to 100ms.

- iii. T wave:* The T wave represents ventricular repolarization which is also commonly stated as ventricular recovery. The extent of the T-wave is less than 5mm with the shape being sharply or bluntly rounded. The period of the T wave is between 0.10-0.25 seconds. Alarming diseases such as hyperkalemia are generally associated with the T-wave anomalies, hence when dealing with peaks (eg. Low amplitudes) denoising of ECG signals becomes essential. Thus when conducting an ECG via a wearable ECG module, denoising eliminates the mixing/overlapping of noise peaks along with the informative peaks of an ECG waveform.
- iv. PR Interval:* The length of the period measured between the beginning of P wave and QRS complex is defined by PR interval. The atrio-ventricular (AV) node delay corresponds to this interval. The heart rate is controlled by the AV node which is activated by the node delay. The normal duration of PR interval is between 0.12 to 0.20 seconds and any abnormality in this provides initial diagnostics of certain cardiac arrhythmias.
- v. ST Segment:* The QRS complex is followed by the ST segment, where both the ventricles become completely depolarized. The depression or elevation of the ST segment is important during diagnostics as it reveals conditions such as ventricular ischemia or hypoxia. The time frame for this segment is around 0.43 seconds.
- vi. QT Interval:* The total time frame of depolarization and repolarization of signals is reflected by the QT interval. This is also defined as the time taken by the heart to complete one refill action, i.e., contracting and refilling blood before the beginning of the next contraction. This duration doesn't last more than 440ms.
- vii. R-R Interval:* The period between QRS complexes is termed as R-R interval. Nowadays the instantaneous heart rate calculation by wearable ECG sensors is provided by the R-R intervals where the normal range of pulse is 60-100

beats/minute. The atrial rhythm is examined by P-P interval, whereas the R-R interval inspects the ventricular rhythm. In case both these intervals are equal throughout the ECG then the heart is healthy, and if there are unrhythmic beats, it is an early sign of heart problem [10].

- viii. *U Wave*: The U wave follows the T wave of ventriculation repolarization and is rarely visible due to its small size. The U waves are expected to represent the repolarization of Purkinje fibers.

1.3 ECG SIGNAL GENERATION AND ACQUISITION

To gauge the electric impulses in the heart, a set-up comprising of electrodes and leads is connected to the human body from an ECG machine. The electrodes carry electrons while the ions carry the body current. Adding electrolytic gel on the metal electrode helps in creating an electrode-electrolyte interface. This interface measures the current in the body.

There is a change in magnitude and orientation of the dipole and the field produced by it, as per the electrical movement of the heart at a given stage. The dipole movement can be used to represent the dipole field of the heart, as an alternative to field plot drawing. The dipole movement being a vector is directed from negative to the positive charge.

In a single cardiac cycle, there are three main variations which are shown in the cardiac vector, namely:

- (a) Atrial Depolarization
- (b) Ventricular Depolarization
- (c) Ventricular Repolarization

The difference in magnitude, duration, and direction in all the above result in the formation of an ECG waveform. The pairing of two electrodes is called lead and space in two leads is called a lead vector. To generate a maximum voltage in a lead, the cardiac vector direction is defined by the lead vector. The most obvious way to record the ECG is between the Right Arm (RA) and the Left Arm (LA) although another two combinations

using the Left Leg (LL) are also used clinically (RA–LL and LA–LL). An equilateral triangle is formed by the three-lead position, which is known as Einthoven's triangle as represented in Figure 1.4.

The clinical ECG comprises three limb leads, six chest leads and three augmented leads. The augmented leads in the front plane (aVR, aVF, and aVL) are derived from the limb lead electrodes. The 12 leads are stemmed to the same electrodes, but the heart activity is viewed from different angles.

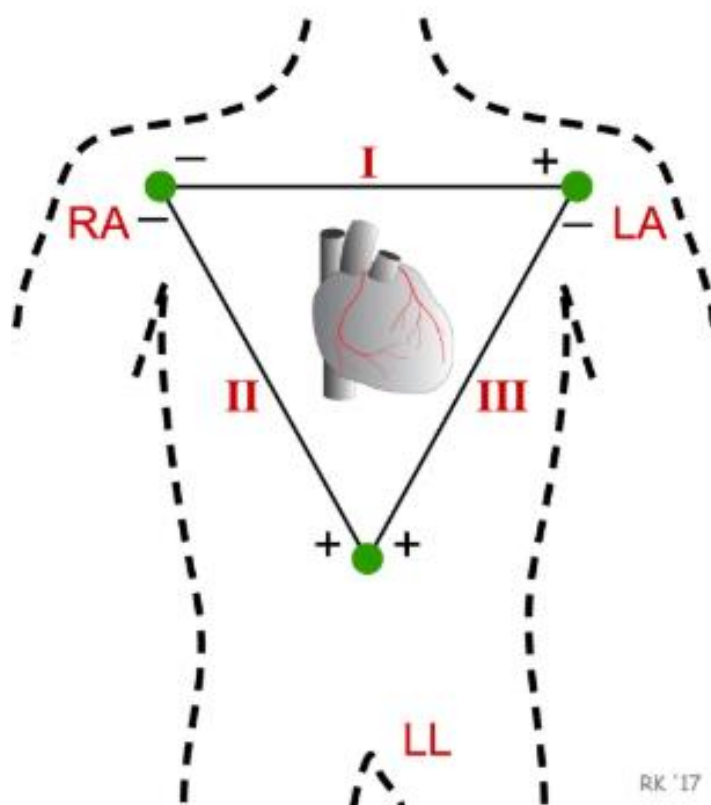


Figure 1.4: Einthoven's Triangle [7]

The augmented and transverse leads are based on the signals obtained from multiple electrodes. They are termed as unipolar leads since the potential on one electrode is taken concerning an equivalent reference electrode. The reference electrode is selected by averaging out the signals at two or more electrodes. This whole setup is coined as the Wilson Central Terminal. The 12 lead ECG setup has leads in the frontal as well as the transverse plane, as shown in Figure 1.5.

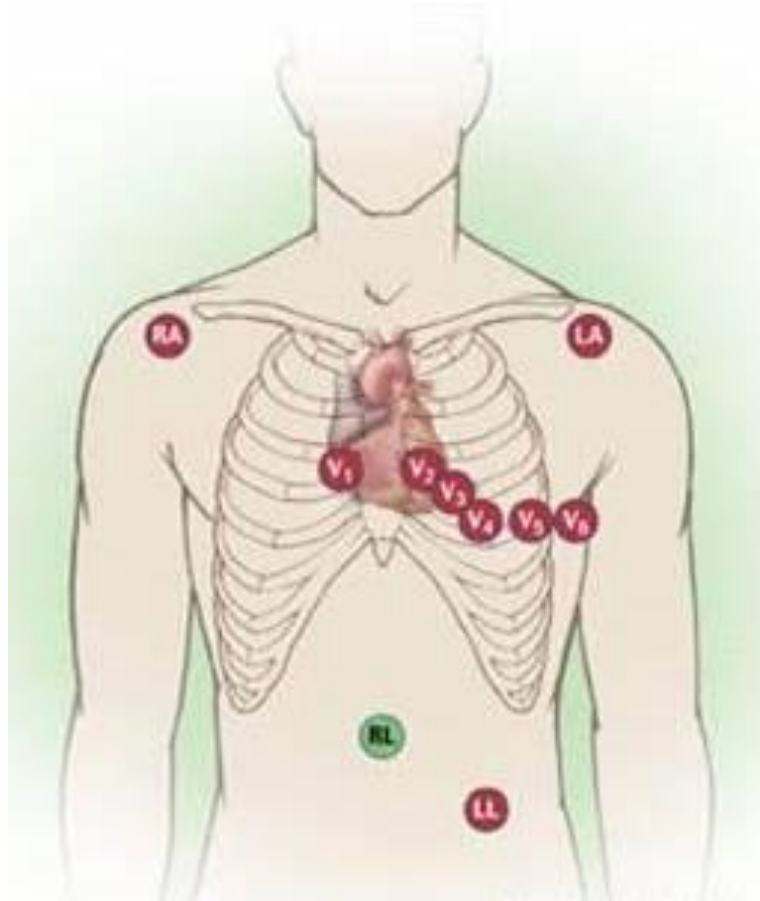


Figure 1.5: Placement of 12 –lead ECG [9]

1.4 ECG NOISES

The noises from various resources contaminated the ECG signals and often degrade the signal significantly. To get a comprehensive picture of the electrophysiology of heart diseases and myocardial ischemic changes, there is a necessity for a clean ECG signal. The low and high-frequency noise components in an ECG signal must be filtered before any further analysis. Several internal and external sources give rise to artifactual signals.

- i. *Power Line Interference (PLI)*: The interfering voltage in the ECG from power line interference has a frequency of 50/60 Hz. The loop in the patient's cable creates alternating current fields and its stray effect causes the interference. The ECG waveform may become completely imprecise due to PLI in case the machine is not grounded properly. The power lines also have some electromagnetic interference which may result in poor quality tracing. Heavy electrical appliances/equipment draw heavy power, such as elevators, X-rays, Air Conditioners, etc., induce the interfering voltage of 50/60 Hz in the

input circuits of the ECG machine. Switching action influences the ECG trace as the electrical power system induces a rapid pulse into the circuit.

- ii. *Electrode Contact Noise:* This noise is a short-lived delay which is a result of the loss of contact between the skin and electrode, which disengages the system from the subject. This disengagement could be permanent or irregular depending upon when a loose electrode is brought in or out of contact with the skin due to the movements and vibrations. As the ECG signal is capacitively coupled to the system the switching action at the measurements system input can result in large artifacts. The 60 Hz interference might be significant when the amplifier input is disconnected. The electrode contact noise could be patterned as a rapid baseline transition appearing arbitrarily and disintegrates to the baseline exponentially with a component of 60 Hz being superimposed. This switching action may occur once or several times in succession.
- iii. *Motion Artifacts:* These are short-lived baseline changes resulting in the electrode-skin impedance with electrode motion. The ECG signal amplifier grasps various sources of impedance as there are variations in the occurrence of the impedance. Therefore, as the electrode position is changed, the source impedance changes, which results in the variation of the amplifier input voltage. The most common source of motion artifacts is presumed to be the vibration or movement of the subject. The baseline disturbances caused by motion artifacts create a shape assumed to be a biphasic signal comparable to one cycle of the sine wave.
- iv. *Muscle Contraction:* The artifactual millivolt-level potential is generated due to muscle contraction. The contraction may be presumed to be a transient burst of zero-mean band-limited Gaussian noise. The distribution's variance could be calculated by using the variance and duration of the bursts. A peak-to-peak ECG amplitude having a standard deviation of 10%, the frequency content of dc to 1000Hz, and a duration of 50 ms are the typical parameters of the muscle contraction.
- v. *Baseline Drift:* The addition of a sinusoidal component at a frequency of respiration to the ECG signal represents the drift of the baseline with respiration. There is a variation of around 15% in the amplitude of the ECG signal with respiration. This amplitude

modulation of ECG with the help of this sinusoidal component could be used to reproduce the variation.

- vi. *Instrumentation Noise*: The QRS detection algorithm is not sufficient to correct the artifacts generated by electronic devices in the instrumentation system. No information on the ECG can reach the detector as the input amplifier has saturated. In such a situation, an alert should be sounded to the ECG operator to take a remedial step.
- vii. *Electrosurgical Noise*: These noises have frequencies in the range of 100Khz to 1MHz which could be represented by large amplitude sinusoidal and can destroy the ECG signal. The duration, amplitude, and the aliased frequency should preferably be variable. Usually, this noise has an amplitude of 200% of peak-to-peak to ECG amplitude.

A significant variation in the physiological activity of the heart has been observed due to the effect of ECG noises. It has been observed that the ECG noises create a prominent variation in the physiological activity of the heart. The clinicians may falsely diagnose the subject with Cardiovascular Disease (CVD) due to these disturbances. It has been well acknowledged that ECG noises have a significant influence on cardiovascular physiology. The oxygenated blood is supplied through myocytes or valves by the heart to the whole body under various processes, and CVDs are caused due to any disturbance in any of the processes [15]. Such diseases cause a significant variation in the normal values of ECG features. CVDs are divided into two parts in this thesis,

- (a) Abnormalities in *P*, *QRS*, T wave
- (b) Abnormalities of cardiac rhythm

This research work targeted three types of CVD abnormalities in the cardiac rhythm section namely sinus rhythm, super ventricular tachycardia, and escape rhythm. The Sinus Rhythm has a normal heart rate (HR) of 60-100 bpm and is manifested in the ECG by slow and rapid HR. A Super Ventricular Tachycardia disorder in the heart raises the pulse to more than 100 bpm even when the patient is not in active mode (exercise) and may cause Arrhythmia. An escape rhythm is generated when the heart rate is controlled by AV node or His-Purkinje fibers other than its primary source. This discontinuous generation of escape rhythms leads to Atrial Fibrillation Disease.

1.5 EXPERIMENTAL ECG DATABASE

In this research work, three real databases of ECG have been used namely MIT-BIH Normal Sinus Rhythm Database (NSR), MIT-BIH Arrhythmia database (AR), MIT-BIH Atrial Fibrillation database (AF). An online platform is used to obtain a standard MIT/BIH database for this research work. The database comprises of the 24-hour length of ECG of patients having different age and gender. The experimental database contains a total number of 64 ECG waveforms having different values of HR. The sampling frequency of NSR is 128 Hz, AR has 360 Hz and AF has 250 Hz.

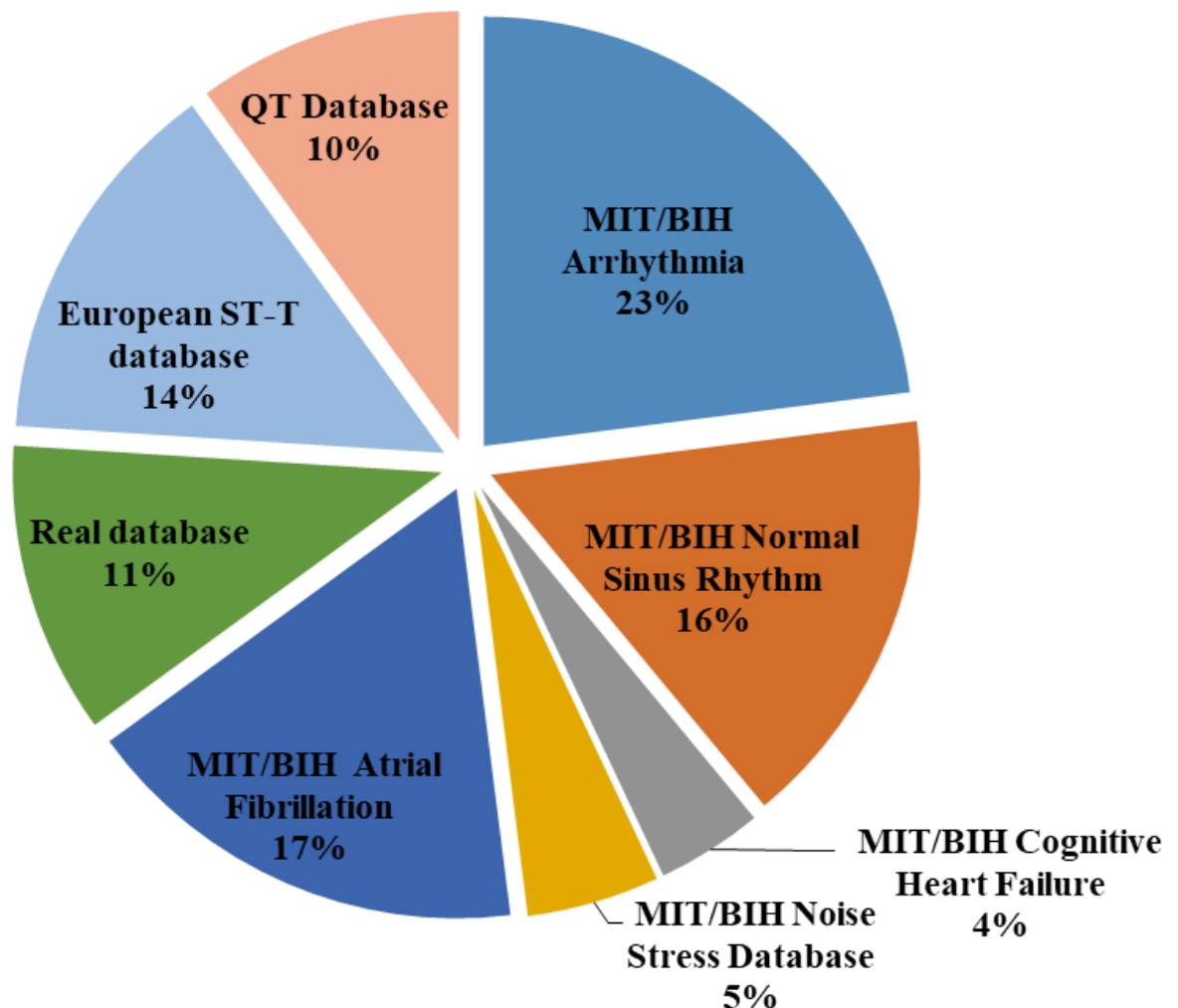


Figure 1.6: Pie-chart of the dataset source used

There are various MIT/BIH datasets are available in online and offline mode namely the Noise Stress database, Cognitive Heart Failure dataset. In literature, various researchers have also utilized the QT database and European ST-T database as shown in Figure 1.6.

1.5.1 MIT-BIH NSR

This database refers to the Arrhythmia Laboratory of Beth Israel Hospital located in Boston (changed to Beth Israel Deaconess Medical Center). The dataset includes 18 long-term ECG recordings of the subjects, including 13 women in the age group 20 – 50 years and 5 men in the age group 26 – 45 years, and none of them were found to have any significant arrhythmias.

In this thesis, 61 ECG waveforms from three datasets are considered for experimentation. Table 1.1 illustrates the description of the ECG database used in the experiment.

Table 1.1: ECG Database Description

Database Description	No. of ECG Database with outliers	No. of ECG Database without outliers	Class Description
MIT/BIH NSR	18	18	60bpm < HR < 100bpm
MIT/BIH AR	21	20	60bpm > HR > 100bpm
MIT/BIH AF	25	23	HR > 100 bpm
<i>HR : Heart Rate</i>		<i>bpm : beats per minute</i>	

1.5.2 MIT-BIH AR

One of the foremost contributors in co-operative work from Beth Israel Hospital Laboratory of Boston & MIT laboratory is the MIT-BIH Arrhythmia Database. The main content of this Arrhythmia Database is the standard material for evaluating arrhythmia and was introduced in the year 1980 [13]. The database has a dataset studied by the BIH Arrhythmia Laboratory, consisting of 47 subjects having 48 half hours of two-channel ECG recording [14]. The digitized ECG signal samples have been collected at a frequency of 360 samples per second with 11-bit resolution over a 10-mV range.

1.5.3 MIT-BIH AF

One of the most popular real databases used in different research work is Atrial Fibrillation [14]. It is used as a reference to validate the delineation algorithm, an automated ECG component. The database contains two-channel real ECG signals collected from different subjects. There are 25 human subjects with atrial fibrillation (mostly paroxysmal) whose long-term ECG recordings are collected in the database. The two-channel ECG is represented only by the rhythm (.atr) and unaudited beat for the 23 records. The individual recordings are each 10 hours in duration and contain two ECG signals each sampled at 250 samples per second with 12-bit resolution over a range of ± 10 millivolts. The original analog recordings were made using ambulatory ECG recorders at Boston's Beth Israel Hospital (now the Beth Israel Deaconess Medical Center) with a typical recording bandwidth of approximately 0.1 Hz to 40 Hz.

1.6 SOFTWARE BASED HIGH LEVEL DESIGN TOOLS

FPGAs are still not extensively accepted in DSP applications, despite its advantages, due to the absence of software-based design flow, such as C language. There is no requirement of hardware description language (HDL) knowledge or an FPGA architecture for such languages. Traditionally, it has been quite a task for the DSP programmers to do implementations on hardware, moreover, it is not easy to search for FPGA solutions. With the incorporation of C – based Design Flow, one has a plethora of options to reduce design flow problems and these reflect the traditional DSP design flow, thus been adopted by programmers on a larger scale. Software-based designs are processed into hardware languages automatically with the help of such devices, but there are a lot of limitations in the existing code writings to make such a transformation seamless & continuous. A perfect example of such a limitation is a repetitive task still cannot be converted to hardware using this process. This section tries to provide a high-level overview of these devices

1.6.1 MATLAB

MATLAB is an algorithm development tool and a high-level technical language that is applicable in many areas such as control design, signal processing, and much more. The traditional programming languages such as C, C++ are very slow when compared to using Matlab software. There are special-purpose functions in MATLAB which can be availed by the add to toolbox call out separately [16]. Such extensions and enhancements of MATLAB extend its competencies to address specific problems in explicit application areas.

MATLAB is a high-level language that comprises a combination of data structures, control level descriptions, object-oriented programming, and the input/output. There is an ample number of libraries available in MATLAB, and these include a large collection of computational algorithms that range from very basic functions (arithmetic) to complex ones (Fourier Transforms). In this research work, to import the Xilinx Blockset Library, we have used the Simulink add-on tool of MATLAB.

1.6.2 Xilinx System Generator Tool

Xilinx provides a tool called System Generator for DSP design which helps in FPGA design with the help of using MathWorks model-based design environment. The Xilinx specific blocks make it possible to capture designs in the DSP-Simulink modeling environment [17]. The DSP functions along with instructions and algorithms form a highly parameterized library, called Xilinx-Simulink blocks. The Xilinx DSP block set comprises over 90 DSP building blocks for simulation. The module comprises common DSP building blocks, e.g. additives & registers. Xilinx IP core generator module comprises complex DSP building blocks, e.g. filters & FFTs, and provides optimal results for the chosen device.

The product consequently changes over the significant level framework DSP block diagram to RTL. With the help of using ISE tools, the outcome can be blended with the Xilinx FPGA innovation. FPGA programming document is created with the natural execution of FPGA steps including synthesis, place, and route[18].

System Generator offers a system integration platform to design DSPs over FPGAs, allowing the C / C++ components of RTL, Simulink, MATLAB, and DSP systems to be in a single simulation and execution environment together. The blockchain technology is

supported by the System Generator Blackbox which not only permits to import of RTL into Simulink and but also Co-duplicate. The inclusion of a Microblaze embedded processor which helps in the running of C/ C ++ programs is supported by the System Generator tool. DSP Building Blocks are provided in the Xilinx DSP Blockset for Simulink.

1.6.3 Simulink

The dynamic systems modeling, simulation, and analysis are done by a tool from MATLAB called Simulink. The Xilinx System Generator which has been explained above runs as a part of Simulink. Xilinx block-sets comprise the elements of the system generator and appear in the Simulink Library Browser. The Simulink model-based design methodology creates a base for the functioning of the system generator. The Simulink block-set is generally used to create the executable specifications. Such specifications can be created in the absence of any hardware specification and an impermanent point of numerical accuracy. The system generator is used for specifying the hardware execution details for a specific Xilinx device, post defining the operational and basic data flow issues. The Xilinx DSP block set is used by the system generator for Simulink and then it creates highly optimized netlists for DSP building blocks by automatically using the Xilinx Core Generator. All the downstream tools can be run by a system generator for bitstream production for FPGA programming [19]. An alternative testbench for the use of simulators can be created using test vectors extracted from the Simulink environment.

1.7 PERFORMANCE PARAMETERS

Diagnostic tests are one of the most common ways in biomedical studies to determine the occurrence or absence of any disease in study subjects. This research includes testing for the presence or absence of CVDs. The validation of a diagnostic test that establishes the true status of the subject is done by comparing the test results against a gold standard. Test validation is an assessment method that determines whether a test is competent for a particular use and through it; the ability of the test may be assessed on how good the test is at identifying subjects with and without a CVD or condition as represented in Table 1.2.

Table 1.2: Confusion Matrix for the Diagnostic Test

Result of Diagnostic Tests	Result of Gold Standard Test	
	Disease Present	Disease Absent
Test Positive	True Positive (x)	False Positive (y)
Test Negative	False Negative (z)	True Negative (w)

Accuracy, sensitivity, specificity, and positive predictive value (PPV) are the four primary objectives that measure the validation of any test performance [20]. A diagnostic test under ideal conditions would identify subjects with or without disease with 100% accuracy.

The total number of correctively classified subjects to the total number of subjects classified is known as Classification accuracy as shown in Eq. (1.9).

$$Accuracy = \frac{x+w}{x+y+z+w} \quad (1.9)$$

To quantify the diagnostic accuracy of a test the basic measures include sensitivity and specificity. The ability of a test to correctly identify those with a disease (true positive rate) is called sensitivity. It is the probability of a positive test given that the patient has the disease as expressed in Eq. (1.10).

$$Sensitivity = \frac{x}{x+z} \quad (1.10)$$

The ability of a test to correctly identify subjects without a condition is called Specificity. It is the probability of a negative test given that the patient does not have the disease as shown in Eq. (1.11).

$$Specificity = \frac{w}{y+w} \quad (1.11)$$

Standard methods for proportions can be used to calculate the confidence intervals for sensitivity and specificity as both are proportions.

The PPV is related to sensitivity and specificity via disease prevalence and is the basic measure of diagnostic accuracy. The PPV is the probability that the disease is present in each subject given a positive test result and is defined by Eq. (1.12).

$$PPV = \frac{y+z}{x+y+z+w} \quad (1.12)$$

1.8 MOTIVATION

In today's world, everyone is busy in their work and life is running at a tremendous pace. Taking care of one's health has become a daunting task due to this fast-paced world. Talking about heart rate monitoring, in the late 20th century, the manual entries of the cardiac activity started to go digital to create automatic monitoring systems. These systems became popular in the space of sports early on and were used by a variety of performers across different areas and segments of the sports world. This eventually gave rise to modern-day wearables, which not only monitor but also record a person's physical activity daily, even when one is sleeping. Large players in the cardiovascular segment kept this as a basis for bringing electrocardiography (ECG) technology from big machines in the hospitals and emergency centers to non-invasive wearable ECG modules that give real-time analytics (report) of any abnormalities, if any, found in the heart. These reports may suggest an early diagnosis of a possible cardiac arrest, arrhythmia, or heart failure which could in turn alert people in advance. These reports may be correct but as the individuals wear ECG modules daily there is a high probability that external noises might contaminate the signals received by the sensors, which would result in some definitive error during the beat detection process. The noises in such cases may be mainly man-made due to the movement of limbs during routine activities, wireless signal transmission, baseline movement which would eventually result in dilution in the ECG information quality received. Considering all the worst situations and making sure there are at least false limitations, the denoising and the data-cleaning component of the QRS detection algorithm must be fool-proof To ensure the real-time tracking of the heart rate, the algorithm must be able to differentiate the variability in heart rate under normal and various cardiac abnormalities. In this research, the algorithm was already coded and tested for accuracy in software using MATLAB, after which the code was converted to a Simulink model to test the algorithm on the hardware. The software processes run ideally in virtual environments which is easier to deal. For the real-time effective analysis, the XSG environment provides reliable hardware interfaces & confirms that every part of the algorithm works in the same manner as it does in software.

1.9 RESEARCH GAPS

The exhaustive study of the popular and recent literature assists the researchers to discover some of the research gaps.

i. Resource Optimization in wearable ECG module

An investigation for obtaining sufficient diagnostic quality of ECG recording

ii. Design of low power ECG pre-processing module

ECG Denoising employing different functions for power optimization

A novel architecture for ECG pre-processing

iii. Beat Detection and Classification Algorithm

Acquiring prominent features for Arrhythmia and Atrial Fibrillation based on HRV

Decreasing the False Positive Rate for the classification of Arrhythmia and Atrial Fibrillation

Based on the research gaps, different objectives were framed for obtaining the low resource utilization, low power consumption, and multi-stage classification system for the detection of NSR, AR, and AF by employing different types of bio-signal processing techniques.

1.10 RESEARCH OBJECTIVES

In context to the information perceived from the literature, the author realizes that in Biomedical Signal Processing the design of an automatic ECG monitoring system is popular research work. To attain these objectives, the author has proposed a methodology for a power-efficient ECG system. Various moderations in the pre-processing and post-processing ECG system have been proposed to improvise the performance of the module.

The primary focus of this research work is to design a *QRS* detection algorithm having higher sensitivity and PPV. The developed algorithm should require low resources of basic characteristics of real-time monitoring system such as LUTs, registers and DSPs, and low power. Heart rate can easily be computed when the corresponding R-peaks of an ECG signal are detected. Thus, the authors have to design an efficient algorithm that can authentically determine the heart rate from the ECG signal.

Objective I

Design and Implementation of ECG Denoising Module for Optimal Resources

Objective II

The Robust Hardware Design of Low Power Module for Clinically Significant ECG

Objective III

Development of Multi-Stage Classification System for Heart Rate Variability

1.11 THESIS ORGANIZATION

This thesis consists of six chapters inclusive of this chapter. The remaining thesis orientation is as under:

Chapter 2: Literature Survey

This chapter describes the total literature survey used in this work. The author has taken into consideration multiple literature reviews to get enough information about ECG wave signal processing. The literature review is divided into four sections where first part consists of detecting *QRS* complex, the second one consists of types of CVDs that affect the ECG waveform, classification of the selected heart disease using statistical analysis constitute the third part, and the last discussion about how hardware implementation of wearable ECG pre-processing modules on FPGA is done.

Chapter 3: Design and Implementation of ECG Denoising Module for Optimal Resources

In chapter 3 the implementation of the various window-based FIR filter is done and various architectures have been proposed to remove all the types of ECG noises simultaneously. The experimental results have been constituted in terms of LUTs, slice register, and DSPs. The power consumption is computed in terms of On-chip Power (mW) via the FPGA board.

Chapter 4: The Robust Hardware Design of Low Power Module for Clinically Significant ECG

In chapter 3, the authors have not been able to optimize power. To attain low power consumption criteria the authors have proposed novel architecture. This architecture does not compromise the advantages achieved in previous architectures i.e. simultaneous removal of all the ECG noises & resource optimization. The previously established works have been compared with the performance of the proposed work in the result and discussion stage.

Chapter 5: Multi-Stage Classification System for Heart Rate Variability

In chapter 5, HRV feature in different domains has been extracted and most significant features have been selected by employing statistical analysis. Further, to observe the performance of these selected features various classifiers are utilized to classify Arrhythmia, Atrial Fibrillation, and Normal sinus rhythm. In the result and discussion stage, sensitivity, specificity, accuracy PPV and AUC is computed as the performance of the proposed methodology. An analysis has been done between the previously established works and the proposed outcome.

Chapter 6: Conclusion and Future Scope

Here conclusive remarks about the advantages and limitations of this research work have been described. Various application areas have been defined for the current work. The future around this scope has also been highlighted towards the end.

CHAPTER 2

LITERATURE REVIEW

CHAPTER 2

LITERATURE REVIEW

This section covers an extensive analysis of the published study related to the topic of the research with a clear purpose and direction. Keeping in mind the challenges and issues highlighted, related to this topic, a literature review has been carried out from the year 1990-2020. The survey is useful in finding the research gaps & their requirements. In signal processing, biomedical signal processing is an extensive & popular research field nowadays.

The ECG signal analysis becomes a well-known area of research in recent years [22]. Several research studies have been available by different researchers in the field of ECG signal processing. Several research ideas inspire my knowledge to analyze the hardware implementation of signal processing techniques based on ECG. A brief explanation of the published study has been carried out in this research work. The literature survey is divided in four parts: QRS complex detection, selection of CVDs that depends on the QRS complex, filtering techniques for noise elimination & their FPGA implementation, and HRV classification methods are illustrated in modular form.

1.1 QRS DETECTION ALGORITHM

The signal processing of ECG consists of three main phases. These phases are dataset of ECG, Pre-processing, and decision making as shown in Table 2.1. In the first phase, heart signals are preprocessed and evaluated by utilizing historical datasets of ECG.

The algorithm is analyzed to classify the QRS complexes into correctly classified as TP, incorrectly classified (Non-QRS complexes) as FP, and misclassified QRS complexes as FN. The summarization of various QRS detection techniques review is divided into two parts such as performance parameters and used techniques review summarization as described in Table 1. Further, the discussion based on pre-processing and a decision-making rule are mentioned in the first phase. MIT/BIH Arrhythmia dataset based on QT dataset mentioned in [26] is utilized to review the entire literature. *Appendix A* illustrates the Pan-Tompkins algorithm represented by [23].

Table 2.1: Comparison of various QRS Detection Algorithms

Sr. No.	Year	References	Techniques used		Performance Parameters				
			Pre-Processing Stage	Decision Rule Stage	FP	FN	Se (%)	PPV (%)	
1.	1985	[23]	Band Pass Filter	Threshold based logic	507	277	99.75	99.54	
2.	1986	[24]	Linear and Non-Linear Digital Filter	Threshold based logic	248	340	99.69	99.77	
3.	2000	[25]	FIR filter using Kaiser-Bessel Window	Zero crossing Point	187	203	99.81	99.83	
4.	2008	[26]	Hilbert	Based on RMS of segment	836	775	99.29	99.24	
5.	1995	[27]	Wavelet Transform 1995	Zero crossing Point	65	112	99.90	99.94	
6.	2015	[28]	Wavelet Transform	Zero Crossing Local Modulus maximum	89	34	99.94	99.99	
7.	2016	[29]	Undecimate Wavelet Transform	Segment Specific Thresholding	163	273	99.75	99.85	
8.	2008	[30]	Digital Filter	Threshold based Logic	58	166	99.93	99.46	
9.	2016	[31]	Median Filter and SG Filter	RMS of Signal	163	273	99.75	99.85	
10.	2015	[32]	Quadratic Filter	Adaptive Threshold	210	202	99.82	99.81	
11.	2015	[33]	Envelopment Filter	K-mean Clustering	131	71	99.82	99.81	
12.	2014	[34]	Whitening Filter	Adaptive Thresholding	109	210	99.82	99.81	
13.	2017	[35]	Wavelet Transform	Envelopment Filter	165	156	99.86	99.85	
14.	2018	[36]	Matched Filtering	Phase Space Reconstruction	73	140	99.87	99.93	
15.	2018	[37]	Box scoring calculation	Box scoring time-series	610	748	99.32	99.45	
16.	2019	[38]	Band Pass Filter	Variance-Based Detection, Maximum-Likelihood Estimation	164	156	99.86	99.85	
<i>FP: False Positive</i>					<i>FN: False Negative</i>		<i>Se: Sensitivity</i>		<i>PPV: Positive Predictivity</i>

During the left and right ventricles contraction of the heart, a QRS wave is produced. The various QRS complex variations are generated during the depolarization process. It is due to the abnormality of circulatory, structural, and electrical. In literature, various techniques such as Neural Network (NN), Hilbert Transform (HT), Difference Operation Method (DOM), digital filters (DF), Wavelet Transform (WT), Entropy method (EM), derivative methods (DM), etc. have been implemented for the accurate detection of QRS wave. All

these techniques successfully enhanced the ECG waveform characteristics for extracting the relevant information about HR, RR interval, etc. However, various QRS detection techniques are divided into three following categories.

2.1.1 Derivative based slant for QRS detection

Digital filters are utilized to remove the heart signal artifacts whereas slope prominent features are acquired by applying the derivative filters. To detect the QRS waves, the Author of [23] designed a real-time QRS detection method by utilizing the waveform features such as amplitude, slope, and width. In the proposed model, noise is removed by using the Band Pass Filter (BPF), waveform slop is obtained by utilizing 5-point derivation and non-linear amplification is extracted by squaring function. Further, the threshold technique is employed to detect the QRS wave. The proposed model has higher Detection Error Rate (DER) and not capable of detecting the heartbeats properly. Another work by the author of [24] utilized the optimization and digital filtering techniques for improvising the pre-processing phase in a year. The author also designed decision rules based on threshold base logic for increasing the accuracy rate of heartbeat detection. The proposed system successfully increased the detection accuracy but at the cost of time error. To resolve this issue and identify the ECG waveform R peak, the author of [25] proposed the Hilbert Transform method (HTM)by utilizing the first differential signal. The author also utilized the Kaiser-Bessel window (KBW) based FIR filter to remove the artifacts from MIT/BIH Arrhythmia dataset. Further, the zero-crossing technique with the addition of an adaptive threshold technique is employed to evaluate the QRS complexes. To search for the missing peak in the detection task, the author of [26] modified HTM by hybridizing the Hilbert transform with the secondary threshold method. The author also proposed a novel technique to improve the performance of the signal by generating the thresholds automatically with a squaring function. Improved HTM has a high load due to the requirement of Brand Pass Filter on the signals. Further, in the proposed method, the detection of QRS is not robust based on derivative filters. It is also flexible for ECG signal that has varying noisy time.

2.1.2 Wavelet-Based Approach for QRS detection

The author of [27] suggested that the wavelet transformation act as a de-noising method. This method aims to decompose the waves into a frequency and time component. It is also helpful in eradicating the composite noise in valuable data. Further, the zero-crossing technique helps detect the small amplitude QRS wave, due to the low DER. The author also proposed an algorithm for detecting peak detection. The proposed algorithm has two criteria named wavelet transformation (WT) and Entropy Criterion (EC). WT aims to differentiate the signals into two entropies such as low and high. The EC recognized the uncertainty present in the signal. At last, the unwanted low signals are eliminated and the name of the whole process is the EC-WT technique. A new global entropy criterion is added by the author of [28] for enhancing the performance of the approach presented in [27]. Further, a new entropy named multi-time-dependent is introduced by the author of [29] in the approach of [27]. The proposed method utilized the thresholding and Undecimated Wavelet Transform (UWT) techniques for detecting the QRS. The detection rate is improved by the proposed method by utilizing the local entropy method. This method is useful in detecting the abnormality present in the complex structure of QRS.

2.1.3 Other Approach for QRS detection

To achieve faster performance, the author of [30] proposed a new QRS detection method. the proposed method is more reliable and simple than wavelet and derivative-based methods, it is due to the low computation. The proposed QRS detection method used various equations to locate the R peak. These R peaks are later utilized to detect the S and Q peaks. The author also used different preprocessing filters to enhance the QRS complex. Another similar work is done by the author of [31] by using the root mean square method for the detection of beat and Savitzky-Goley filter for denoising. Further, the author of [32] proposed a new algorithm for enhancing the signal to noise ratio (SNR). In this algorithm, a quadratic filter is used for pre-processing and an adaptive threshold is utilized for decision making. A new method is proposed by [3] using the K-mean clustering and two envelopment filter to differentiate between Non-QRS and QRS wave. The proposed method is dependent on the k value and distance metrics types but achieves better results than existing techniques. A new technique is developed by [34] to overcome these dependencies by using an artificial neural network (ANN). In the proposed technique two

filters are used named as the whitening filter (WF) and Squaring and moving average filter (SAMAF). SNR is reduced by using a matched filter along with Radial Basis Function (RBF) based WF. Further, SAMAF has utilized for non-linear transformation beforehand the adaptive threshold process for differentiating QRS from ECG wave. The proposed technique achieved better results but required higher training data in turn computational complexity is increased. To detect the QRS in the online and offline procedure, the author of [35] proposed a new QRS detecting approach. The proposed approach is utilized the thresholding method for forming the envelopes and the Weighted Total Variation (WTV) method for reducing the noise. In the related work, researchers also noticed a new technique based on a vector cardiogram of the heart. The author of the paper [36] proposed a new QRS detecting method. In the proposed method, the phase space reconstruction approach is used to detect the QRS peak, and Matched filtering (MF) is utilized to remove unwanted signals. The proposed method gained a higher accuracy rate as compared to state art methods. A new QRS detection system is proposed by [37] using box scoring time series calculations. Further, the author of [38] developed a QRS detection system by using the maximum likelihood estimation and variance method.

2.2 CARDIO-VASCULAR DISEASES

A survey has been conducted by the authors on different types of CVDs that indicates a significant variation in the normal ECG waveform. Figure 2.1 demonstrates the block diagram of several cardiac abnormalities diseases. These CVDs are separated into two sections: Abnormalities exist in *P*, *QRS*, *T* wave & Abnormalities arise due to the generation of cardiac rhythm [39-42]. This research work is focused on the highlighted CVDs that depend on HR.

2.2.1 Abnormalities in *P*, *QRS*, *T* waves

The irregularities that reside in the *P*, *QRS* and *T* waves represent vital CVD namely Bundle Branch Block (*BBB*), Myocardial Infarction (*MI*) & Ventricular Hypertrophy (*VH*) etc.

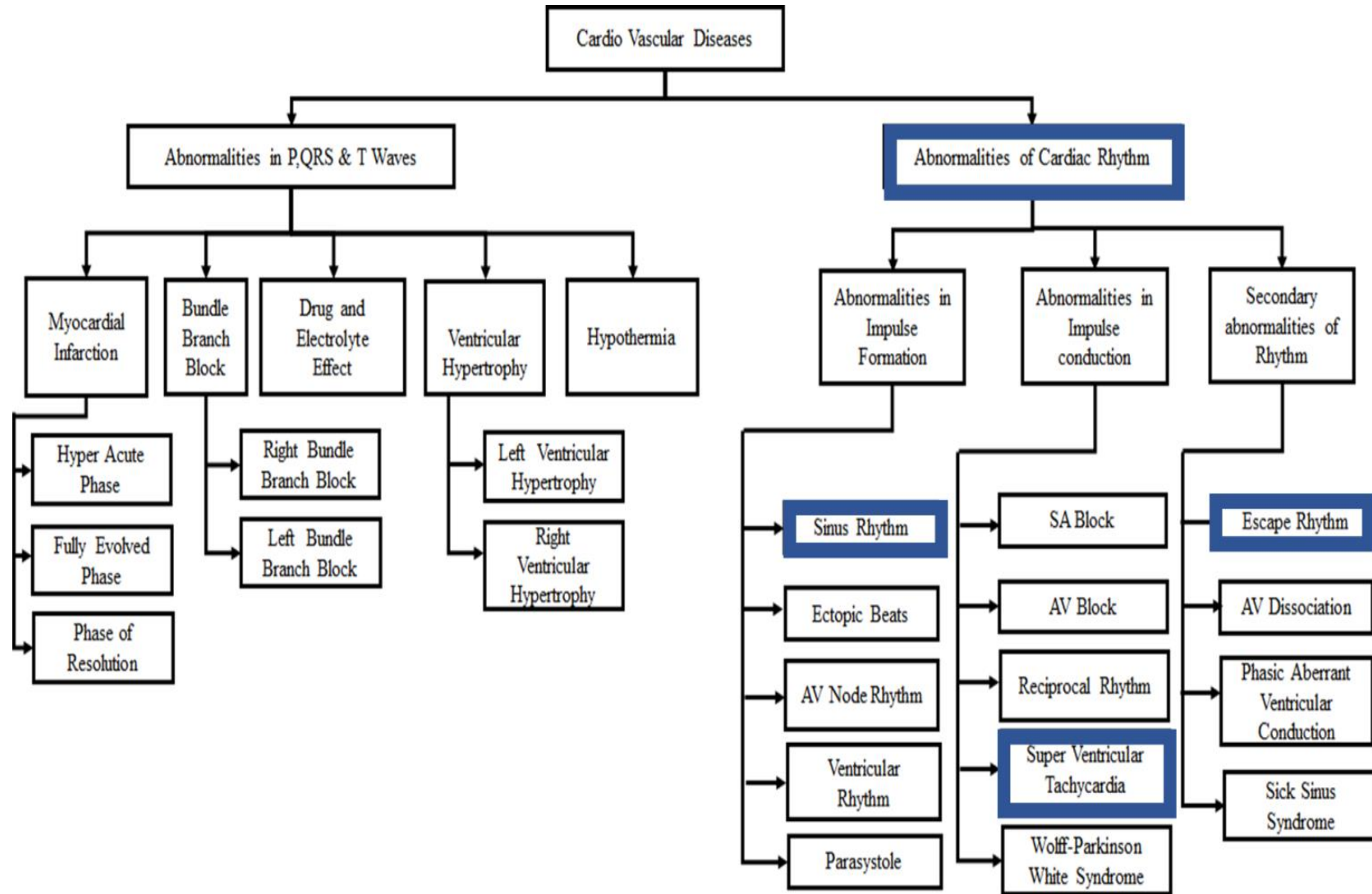


Figure 2.1: Block Diagram of Cardio – Vascular Disease

(a) *MI*: The MI is defined in an ECG waveform by necrosis, injury & ischemia. The procedure of the development of acute MI is separated in three stages namely Hyper Acute stage, Fully Evolved stage, & Phase of Resolution. Table 2.2 defines the diverse stages of MI.

Table 2.2: Stages of MI

Hyper Acute Stage	Fully Evolved Stage	Phase of Resolution
This phase begins within hours after the appearance of MI. It is the most crucial stage to detect the expansion of MI during severe monitoring. In the course of this stage, ventricular fibrillation appears. In ECG waveform this stage is signify by raised slope of ST segment, T & R wave. Severe observance on ECG and attention is very helpful during this phase.	This phase is often named as grown-up stage of acute MI. Necrosis factor of this stage is perceptible in ECG signal due to the presence of deep & wide Q wave or a QRS wave in the leads, looking to the necrotic zone. Myocardial injury is diagnosed by the variation in the ST segment on lead to the superficial injured tissue. The clustering of number of injured tissue leads to the realization of ischemia tissue/dead tissue. It is obvious in the ECG depiction by Q wave, raised ST segment and T-wave also by inverted and symmetrical T wave.	A measurable return to normalcy in the form of normal ST segment, baseline elevation along with T wave is observed after fully evolved stage. However, ST segment & T wave represents coronary insufficiency.

(b) *BBB*: It occurs when there is a delay or block in the electrical conductivity of left & right branches of Bundle of His. The blockage present in the right side of the bundle of His termed as Right Bundle Branch Block (RBBB) & the existence of blockage in the left side of the bundle of His is labeled as Left Bundle Branch Block (LBBB) [43-45]. Table 2.3 represents the essential specifications of the morphological variations in ECG waveform caused by LBBB & RBBB.

Table 2.3: Explanation of disparity in ECG signal due to LBBB and RBBB

LBBB	RBBB
<ul style="list-style-type: none"> • QRS complex period ≥ 120 ms for adults, 100 ms for 4-16 years old & 90 ms for less than 4 year old children. • Wide & peaked R wave in the Lead I, V5 & V6 • Absence of Q wave in any of two leads (I, V5 & V6). • Period of R wave should be greater than 60 ms in V5 & V6 • ST segment and T waves are contrary to each other. 	<ul style="list-style-type: none"> • QRS complex period ≥ 120 ms for adults, 100 ms for 4-16 years old & 90 ms for less than 4 years old children. • The period of S wave must be greater than period of R wave • Absence of Q wave in any of two leads (Lead I, aVL, V5 & V6). • Period of R wave must be greater than 60 ms in any two of these leads (Lead I, aVL, V5 & V6).

(c) *Drug & Electrolyte Effect (DE)*: There have been several drugs associated with the heart & it affects the ECG signal. Two kinds of electrolytes are accountable for the repolarization-depolarization across cardiac cells. The depolarization & repolarization procedures are interfered with by potassium & Calcium concentrations. If disparity happens then numerous problems namely Hyperkalaemia (rise in K concentration level), Hypercalcaemia (rise in Ca level), Hypocalcaemia (fall in Ca concentration level), and Hypokalaemia (fall in K level) arises in ECG signal that is noticeable by small or prolonged QT interval & ST-segment deformation.

(d) *VH*: Any indirect or direct variation in size /mass of ventricles of the heart lead to VH. The expansion of mass in the left ventricle is termed as Left VH (LVH) & the growth of mass on the right side is labeled as Right VH (RVH).

(e) *Hypothermia (HT)*: When the body temperature of an individual falls at a higher rate in comparison to the regular rate. It represents that the person is diagnosed with HT. ECG signal description comprises of *Bradycardia* having symptoms such as *HR* less than 60 bpm, muscle tremor & elongated QT interval [47].

2.2.2 Abnormalities resides in the Cardiac Rhythm

The position of the SA node is located at the wall of the Right Atria of the cardiac system to regulate the HR. The normal sinus rhythms of ECG pursue the consequent path from the SA node to the atrium, which moves from the AV node to the bundle of HIS, bundle branches & Purkinje fibers.

Table 2.4: Primary abnormalities of cardiac rhythm

Disorder		Disease	Abbreviation	Description
Primary Disorder	Disorders of Impulse formation	<i>Sinus Rhythms</i>	<i>SR</i>	These manifest in ECG by slow and rapid HR. SR mainly consist of Sinus Arrhythmia (HR normal), Sinus Tachycardia (HR > 100 bpm), Sinus Bradycardia (HR < 60 bpm).
		<i>Ectopic Atrial Rhythm</i>	<i>EAR</i>	These rhythms are generated due to the impulse originated from atria. EAR disorders consist mostly of Atrial Tachycardia (AT), Atrial Fibrillation (AF), Atrial Flutter (AFL)etc. observed in ECG by perceiving the morphology of P wave.
		<i>A-V nodal Rhythm</i>	<i>AVR</i>	Sinus impulse begins from AV node produces AVR rhythms. It consists of AV Nodal Extrasystoles, AV Nodal Tachycardia etc., noticeable in ECG by monitoring the P-QRS path.
		<i>Ventricular Rhythm</i>	<i>VR</i>	These impulses arise during the sinus impulse formation in ventricles. VR is composed of Ventricular Tachycardia (VT), Ventricular Fibrillation (VF), Ventricular Flutter (VFL) etc. These rhythms can be observed in ECG by perceiving the QRS complex.

Arrhythmia (*AR*) occurs as the sinus rhythm does not pursue the standard path. The *AR* is divided into two kinds of abnormalities: primary & secondary disorders. The primary disorder arises as sinus cardiac impulse forms. The secondary disorders arise during the combination when more than two primary abnormalities occur. Table 2.4 represents

several primary disorders instigated by ventricular rhythms, sinus rhythms, AV Block, SA Block, etc. The Secondary irregularities of cardiac rhythm are tabulated in Table 2.5 [48-53].

(a) *Secondary abnormalities of cardiac rhythm*

Table 2.5: Secondary abnormalities of cardiac rhythm

Disor der	Disease	Abbreviation	Description
Secondary Disorder	<i>Escape Rhythm</i>	<i>ER</i>	When the HR is controlled by AV node or His-Purkinje fibers other than its primary source i.e. SA node then ER is generated. It can be observed in ECG in the form of delayed cardiac cycle length.
	<i>AV Dissociation</i>	<i>AD</i>	It is situated in which atrial activation is independent from ventricular activation causing increased ventricular HR then atrial HR.
	<i>Phasic Aberrant Ventricular Conduction</i>	<i>PAVC</i>	It generally occurs along with SR, EAR, AVR, VR, and PS. It arises due to unequal RR intervals of Bundle Branches and premature impulse formation.
	<i>Sick Sinus Syndrome</i>	<i>SSS</i>	It is an unusual cardiac disease generated due to the malfunction in the natural pacemaker. SSS results in several AR such as Sinus Bradycardia, Sinus Arrest, Conduction disturbances, SAB and Atrial AR.

2.3 ECG SIGNAL PRE-PROCESSING USING DIGITAL FILTERS

To deliver a noise-free ECG for the clinician and increase the accuracy of diagnosis and analysis, several techniques for the ECG pre-processing have been deliberated. The researchers have utilized the online platform for the ECG dataset collection from MIT-BIH. The researcher has utilized several techniques to eliminate high, low-frequency noisy component corrupted in ECG signal in the course of the research.

In [54] a review report has been carried out on high-frequency ECG signal. The useful information of the ECG signal is lies within the frequency range from 0.05-100 Hz. The high-frequency noise component is generally found in the QRS complex. Several researchers have analyzed the QRS complex with the possibility that extra information would deliver information to improvise the diagnostic quality of the ECG.

A mathematical analysis is directed by [55] and it depends on the two sets of information. The objective is proposed by utilizing an adaptable length window that shifts over the ECG signal. The BLW & EMG noise removal designs are evaluated for man-made noisy signals. This technique is appropriate due to its simplicity, speed & to preserve the information from the ECG waveform.

Effective denoising & lossy compression techniques are illustrated in [56] which is designed by employing a modified extended Kalman filter structure (EKF). The performances of the introduced technique are calculated by employing denoising with SNR, compression efficiency, & the weighted diagnostic distortion methods. The denoising system outcome represents SNR enhancement of 10.16 dB that is 1.8 dB more than EKF2. The suggested methodology is applicable for a system that assimilates methods for noise-free storage of ECG data having high output SNR & minimum distortions.

In [57] the authors have studied various techniques for performance evaluation parameters namely SNR & Power Spectral Density (PSD). It has been interpreted that zero-phase filtering is an effective approach for the elimination of BLW. The filter's order is low, thus, the computational load & complexity requirement is very low in comparison to others.

The authors of [58] evaluated theoretically various denoising techniques for noiseless ECG signals. The MATLAB platform is utilized to simulate & evaluate the design. The evaluation of existing studies is compared based on various parameters. Three filters for ECG denoising like Sgolay, Notch, & wavelet filter are employed. Amongst them, Sgolay filter gives better performance as compared to other filters. It provides an enhanced output & low error value of 2.50%. The wavelet filtering & notch filter has an error value of 30.56% & 30.33% respectively. An accuracy of 97.50% is attained by for Sgolay filter.

The window-based FIR & IIR filters to denoise the ECG signal are considered in [59]. The Kaiser window gives a better frequency response & the rectangular window represents the distorted signal.

The authors of [60] implemented various filtration methods such as low pass, bandpass, high pass, & notch filter for the noise-free ECG signal. The Notch filter effectively eliminates PLI using FFT & PSD. It easily smoothed the ECG waveform by employing a moving averaging filter but not able to eliminate BLW noise. Therefore, the combination of BPF with moving average filter is highly effective to clean low & high-frequency noise from ECG.

A 2nd order IIR notch filter is introduced with LMS & DWT method to eliminate PLI noise [61]. The results were evaluated on the MATLAB platform in terms of SNR & MSE. The Daubechies wavelet transform represents the SNR 97.60% in contrast to other IIR, LMS, Haar, Db2 & Db3 wavelet filters.

A filter has been proposed & evaluated to remove PLI noise in [62], it is based Sgolay with a variable filtering window. It effectively eliminates the EMG noise without distorting the useful information from the ECG signal.

2.4 DIGITAL FILTER DESIGN BASED ON FPGA

The enhancement in VLSI Technology & designing digital filters is done on ASIC & FPGA platforms. The scientists & academicians keenly worked towards a method to design & implement the algorithms based on digital filter design. It depends on FPGA because of intrinsic gains of design technology. These filters need many multipliers, adders & registers. It is further appropriate for the hardware implementation of the digital filter. Several studies have been done that relates to implementing digital filter on FPGA platform.

There are many popular processing units are available utilizing by which an ECG processing module that is realizable on various hardware namely DSP, MCU, and FPGA. The complicated computations of digital filters are performed on these processing units.

The processing units facilitate the designing of the filter by performing the complicated computation of adders & multipliers. These factors include re-programmability, execution time, speed, architecture flexibility, complexity, and power consumption. The processing unit based on FPGA is selected due to the notable performance that incorporates low resource & power consumption suitable for wearable and portable applications.

The hardware implementation of the ECG signal processing module comprises of four parts: ECG pre-processing, HRV attribute extraction, HRV statistical analysis & classification. The authors here emphasize firstly the implementation of FPGA based ECG pre-processing module. Data pre-processing is a significant step in the signal processing methodology. It illustrates any sort of process performed on noisy data to set up it for further processing. The basic architecture of the digital filter comprises ADC, Processing unit, and DAC [63]. The raw signal is sampled and digitized using ADC, afterward these digitized values were pre-processed by a processing unit that performs complex numerical calculations of filtering [64, 65]. Thereafter DAC facilitate digitally filtered signal to analog filtered signal.

Noise reduction from the bio-signal is a demanding task & rapidly increasing area. It has a huge number of applications in biomedical signal processing [63]. Several types of high & low-frequency noises contaminate the bio-signal like baseline wander, power line interference, muscle tremor, etc [64]. In comparison to the MCU, DSP based medical equipment and ASIC, FPGA, owing to their reconfigurable property & low cost and low time to market. Much progress in the technology of medical systems gives origin to the monitoring based system on Programmable Logic Devices (PLDs). The software simulation & synthesis aided the prototype design of FPGAs. The increasing design variations via software-based synthesis becoming economical than analogous changes done for hardware models. FPGA is popular in filter's designing, storage, processing & transmission of bio-data. Some popular companies namely Altera, Xilinx, Actel, & Quick logic are developing FPGA boards. VHDL & Verilog HDL are a hardware description language that helps to design a digital logic using FPGA. FPGA delivers peerless device utilization by conserving the system's power & on-chip area [65].

The FPGA-based design provides flexibility and high speed, unlike conventional techniques which are based on microcontrollers, DSP devices, and microprocessors. A VHDL approach to design an optimized filter is done by [66] also it has been compared with the MATLAB FDA toolbox is also taken into account. The adaptive FIR filter is realized by [67] as per ASIC flow with the assistance of MATLAB & Mentor graphic tools. The transposed architecture of the FIR filter is implemented by [68] using VHDL on FPGA. In literature, there are various architectures to realize a multiplier block, that provides low power & delay during bio-signal denoising using FIR filters [69]. The performance of hardware-based digital filter implementation is improved by utilizing FPGA in terms of speed, power, & execution time in contrast to software-based DSP [70]. There are various linear and non-linear analyses to pre-process the biomedical signal like FIR, IIR, wavelet transform, triangular indices, and Poincare plots, etc.

Nowadays, many innovative approaches for the ECG pre-processing stage have emerged. Out of them, the major research is carried on the wavelet transform (WT) [71]. The Fourier Transform (FT) helps to determine the frequency present in a given signal. But during the case of non-stationary signals like ECG, FT does not know at what time the frequencies are present. So, to conquer this challenge WT is utilized as it transforms the input signal into another form that signifies the signal in a more valuable form by convolving the input signal with a function termed as a wavelet. This wavelet function is moved at different locations, squeezed and stretched on the input signal. The wavelet function is utilized as a mathematical microscope at different stages of magnification. WT emerged as one of the widely used techniques to pre-process the biomedical indicators such as Electrocardiogram (ECG), Cough signal analysis, Electroencephalogram (EEG), Phonocardiogram (PCG), etc.

A threshold-based technique is presented for employing Wavelet Transforms (WT) for denoising. As for cough signal analysis, a multi-resolution implementation is provided by WT. The techniques based on WT utilizes soft thresholding has been introduced [72]. A hard thresholding method by employing a Discrete Wavelet Transform (DWT) is proposed as compared to a soft thresholding technique due to its effectiveness over cough signal analysis.

An intelligent system based on PCG is presented, in which signal filtering is done by using DWT. To denoise the Phonocardiogram signal the authors of [73] utilize the DWT for the removal of the noisy signal.

A soft threshold-based WT is proposed for the non-stationary environment in which the elimination of some wavelet coefficient is done for obtaining a noiseless signal [74]. This research work also expressed the drawbacks of some popular algorithms namely Adaptive Impulse Correlated Filter (ACF), Time Sequence Adaptive Filter (TSAF), Least Mean Square (LMS) adaptive method, Signal Input Adaptive Filter, and on a non-stationary signal like ECG. The authors introduced a wiener filter based on WT to eradicate high-frequency noise from the signal by altering the coefficients of WT based on the projected noise level [75]. The wavelet filter with hybrid thresholding is also introduced in the literature. To eliminate the PLI noise from the ECG signal; symlet wavelet of order 8 and decomposition level up to 6 is suggested by using the wavelet shrinkage technique of Empirical Bayes posterior median filter [76]. A novel approach is introduced to denoise the ECG by adaptive bionic WT termed as Bionic Wavelet Transform (BWT). High sensitivity, non-linearity, and frequency selectivity are some of the advantages of BWT. It also can reconstruct the signal by inverse transform and concentrated energy distribution. A denoising technique based on DWT is introduced and results are compared from the existing techniques based on SNR. It illustrates that WT provides better results than other techniques [77].

The author of [78] implemented field-programmable gate arrays (FPGAs) based on digital filter algorithms. This algorithm is used for processing the digital chips or digital filtering chips in audio applications, for a higher sampling rate in ASIC. Proposed FPGAs have higher sampling rates from the existing DSP chips, higher flexibility than other existing approaches, and low cost for moderate volume applications rather than ASIC.

The fundamental programming technologies and historical programmable logic devised development is surveyed and reviewed by the author of [79]. The author also described the basic concepts from the research on architectures. These concepts are 1) performance speed of the final device, power consumption, and area efficiency is affected by FPGA architecture. 2) Future prospective of FPGA is also enhanced by collaborating the key fundamentals of up-to-date commercial FPGA architecture. The author also mentioned the

various problems in complex architectures of FPGA and explained the important difference in the utilization of technologies. The further author observed that FPGA has various characteristics that made it different from rest architectures.

In paper [80], the work suggested that to filter the various high-frequency noises and coupled noises of 50 Hz, a digital filter is used with a low pass FIR structure. The inferences are of Filter signals related to the Short Time Fourier transform are drawn by medical experts. The module that is implemented on FPGA is tested using the recorded ECG signals. Xilinx Integrated Software Environment (XISE) and Modelsim Xilinx Edition (MXE) are utilized for synthesis and simulation. Additionally, results are evaluated by using the Xilinx Chipscope tool (XCT) and logic is run on FPGA with the development board of Xilinx Spartan-3 Family FPGA. EGC monitor system is utilized for collecting, playback, and store the wire transmission that is assimilated into the FPGA chip for the development cost, design cycle, development of analog circuits, and research is reduced. Authors have also suggested that filters have good value for application. FPGAs are widely used in the application of signal processing due to fast time-to-market, parallelism, tractability, and high speed. Digital filter plays a significant role in digital signal processing. The lower order frequency selection of digital filter is widely used in modern signal processing systems as compared to IIR digital and FIR filters. The software programming languages are different from hardware programming languages like Verilog. It is due to the dependencies of signal and time propagation. In literature, IIR filters are utilized in the processing of digital signals alongside the advantage of programmable digital processors. However, the complex computation of higher filter order affected the flexibility, speed, and cost of digital signal processing. Therefore, the employment of IIR filters (2nd order) on XC2S150 processor FPGA architecture is suitable and appropriate as it increased the speed. Due to this reason, researchers implemented a lot of multipliers hardware on FPGA, but this process affected the limitation of programmable digital processors. This approach enhanced the performance as compared to the structures of a common filter in respect of power consumption, speed of operation, and cost. The proposed approach can also be applied to the processing of any digital signal in real-time effectively.

Author of [81] simulated and developed an IIR filter by utilizing the Simulink environment and Generator software of Xilinx System. The proposed filters are

implemented using the MATLAB platform on FPGA. The author observed that quantization and overflow effects are useful for stability in the process of filter designing with the given specifications. It is observed from the experiment that the filters implemented on FPGA enhanced the computational speed as compared to a conventional DSP processor. Further, FPGA has the capability of parallel processing that enhanced the operation speed in the designing and implementation of cautioned and digital filters and also protect the filters from overflow errors and quantization effects.

The implementation of FPGA and cost of FIR filter is analyzed by the author of [82] based on different windowing techniques. The proposed filter is implemented using MATLAB 7.6. The number of adder circuits and the multiplier is very crucial in the chip area, increasing speed and reducing cost, in the process of implementation. The performance of the windowing technologies is compared with existing technologies using several multipliers and adders. The experimental results revealed that Hanning & Blackman window functions provide improved results in contrast to Bartlett, Rectangular & Hamming techniques. Further, the Equiripple window method improved the performance by achieving a 28.97% and 29.08% reduction rate in multiplier and adder respectively as compared to Kaiser. The equiripple window method also provided a cost-effective solution for the applications of DSP.

The author of [83] presented the study of adaptive power line interference canceller (APLIC) & its implementation on noisy ECG signals. The author also implemented an APLIC on FPGA by using the Least mean-square (LMS) method and proposed Notch filters for power line interference. In the study, it is suggested that notch filters do not provide better performance in the condition of the unstable power line frequency. A misalliance between power line frequency and suppression band decreased the PLI. Thus, APLIC is valuable & the LMS method is generally utilized on adaptive filtering due to the advantage of modular systolic architectures (MSA). The combination of LMS and MSA increased the operation speed and reduced the area. The author also implemented the APIC on digital signal processors and general-purpose microcontrollers. It is observed that this process has sequential execution and low processing speed. Therefore, APLIC is designed with a software program. An alternative solution is also proposed by implementing the APLIC with FPGA due to the ability of parallel employment of ECG signal processing

approaches without affecting the processing speed. This solution also provided the monitoring and control features for ECG process monitoring.

To remove wander that changes the low-frequency segment like S-T segment that has the heart attack information of ECG signal, author of [84] invented a high pass filtering. Different filter design methods such as various windowing techniques, least-square, and equiripple are compared utilizing SNR in MATLAB. Further, the mismatch degree between filtered and noisy ECG is found by analyzing the correlation coefficient. The author also implemented an FIR platform FPGA platform with Kaiser Window for eradicating the baseline wandering. The proposed filter achieved better results, required less time, less power consumption, and fewer hardware resources as compared to other design methods.

In paper [85], the author examined the optimal implementation with the performance based on the cost of various IIR filters that are useful in real-time application. FDA tool is used to analyzed and designed the low IIR filters. The cost of implementation is analyzed following input samples, multiplier, filter order, and adder. The simulation results presented that the Elliptical IIR filter provides benefits over their substantially of system latency and complexity of hardware or lower computational.

To filter the ECG signal noise, the author of [86] utilized the low pass FIR filters. The author also researched finding the flexible implementation option, increased speed, portable, and reduced the hardware cost. Further, to reduce the resources of hardware in designing the hardware author utilized the FIR serial architecture technique. Before filtering, filter output is compared with ECG signals by plotting the signal in frequency and time domain using MATLAB. According to the above literature survey, FPGA has various advantages of throughput but at the higher cost of hardware.

2.5 HRV BASED CLASSIFICATION

The primary source of HRV is the dynamic interface within the multiple physiological actions that regulate the variable HR. HRV is influenced by several physiological activities namely the vasomotor system, central nervous system, etc. Several medical reports scrutinize a broad review of CVDs as per HRV.

The control of HRV is performed by the crucial part of the brain termed as ANS. It monitors the HR functioning, breathing, digestion & blood pressure. The employment of HRV provides information regarding the mental-physical health via monitoring the lifestyle of an individual [87, 88]. HRV features assists the doctor to observe emotion, stress sleep, thought, physical activity & feelings constraints on patients. Low HRV illustrates weak cardiac health which specifies anxiety, heart stroke, & high blood pressure, whereas high HRV illustrates healthy cardiac health. HRV features are computed in the time, geometrical & frequency domain [89].

HRV provides information about mental & physical strength [90]. The author of [91] obtained the HRV features from different domains & duration. Several statistical analyses were utilized for the comparison in between sets namely t -test, f -test & ANOVA, etc. The contrast between the two groups of CVD was directed to follow the t -test & f -test. The contrast of more than two groups of CVDs leads to utilizing the ANOVA test [92]. The Type-I introduced if more than two group CVDs is employed during t -test & f -test. The frequency & time domain HRV features are obtained for the evaluation of the stress test. A comparison has been made based on different stress levels [93]. The estimation between meditative & and non-meditative situations of an individual by employing ANOVA test [94].

The procedure of classification is done by the popular & widely utilized machine learning algorithms that aid the doctors in precise identification. The supervised & unsupervised are the classes of machine learning. A lot of machine learning approaches namely Support Vector Machines (SVM), Decision Trees (DT), k-Nearest Neighbor (kNN), & various neural network approaches are employed to extract the information from the features. The authors of [95] proposed a programmed predictive model based on short term HRV to categorize the existence of mental pressure in the course of viva-voce. The evaluation of the vulnerability of falling of hypertensive patients by using short-term HRV is done by [96]. This model attained 68.9% & 79.3% classification accuracy for 10 minutes & 15-min correspondingly. In [97] academicians have employed a kNN classifier to categorize normal sinus rhythm & Congestive Heart Failure (CHF). A parallel study has been carried out by [98] that utilizes HRV features on the ECG dataset [98]. There has

been a challenge in the selection of centroids in kNN by assigning the weight with the centroids & labeled as weighted kNN.

To classify heart diseases based on HRV analysis numerous studies have been already completed [100-101]. Classification based on HRV analysis provides optimistic results at various levels of classification. Automatic computer-based machine learning algorithms reduce the manual error arising during medical analysis and diagnosis [102]. Mental health, schizophrenia, anxiety, arrhythmia, congestive heart failure, and atrial fibrillation are the main categories of diseases, which can be accurately analyzed by HRV [103-105]. Nine features from various domains are extracted on short-term HRV using SVM [106]. The extraction of non-linear parameters of HRV is done in [107] using SVM to categorize normal patients and congestive heart failure patients. He achieved 94.4% accuracy on 2-hour time-length and 96.7% accuracy by applying non-standard features of HRV. The proposal of using an ensemble classifier is less reliable as compared to other classifiers due to the varying nature of the training dataset [108]. Authors of [109] introduced Incremental ANOVA and Functional Networks-Feature Selection (IAFN-FS) techniques to deal with the complex nature of already existing methods such as decision trees and naive Bayes with better accuracy.

A prediction based technique by HRV analysis is presented and obtained 68.9% & 79.3% classification overall accuracy used for 10 min & 15-min respectively [110]. Authors in [111] obtained a low accuracy of 57% during short-term HRV signal established on footprint analysis. To classify Paroxysmal Atrial Fibrillation (PAF) genetic algorithm is utilized to attain better accuracy [3]. kNN classifier using short term HRV is employed by [112] to classify the HRV feature of 54 normal and 29 abnormal subjects of congestive heart failure. The same classifier is also presented by [113] using non-standard HRV parameters on the MIT/BIH database. To overcome the problem of selection of centroids in kNN classifier researchers of [114] associates the weights along with them. Also, by using four HRV features for 1000 RR-intervals a significant accuracy has been obtained [115].

During the review of QRS detection algorithms, it has been inferred that wavelet transforms for the pre-processing stage and zero-crossing local modulus maximum gives

better sensitivity and positive predictive value as compared to the recent literature. Also, after the successful detection of QRS, the authors can easily calculate the Heart Rate. Various types of cardio-vascular diseases depend on Heart rate variability.

Subsequently after studying several types of CVDs differentiated based on their origin in the heart and how it can be observed in an ECG waveform. It has been inferred that various types of CVDs alter the heart rhythm or heart rate. In this thesis, the authors have been selected Arrhythmia and Atrial fibrillation disease that marks a significant effect on ECG waveform and HR. Also. The online databases of these diseases are easily available on Physionet. HR is the primary constituent to extract features for HRV. Based on this concept, the authors have extracted different types of features and try to classify arrhythmia, atrial fibrillation, and normal sinus rhythm by employing renowned classifiers.

It has been perceived that in comparison to DSP and micro-controller, FPGA performs better in terms of resource utilization and power consumption for wearable and portable ECG module. In this work, emphasis on the implementation of the ECG pre-processing module on FPGA is done. Many academicians and researchers have employed FIR filter due to its less hardware computational complexity and linear phase. Further, to enhance the performance of the ECG denoising, a few authors have also utilized wavelet transform. The authors have chosen the latest FPGA board i.e. Zynq-7000 for its evaluation.

During the literature survey of various machine learning algorithms employing HRV; it has been inferred that nowadays Artificial Neural Network (ANN) is a popular topic in the literature. Previously, enormous work has been done on ANN to classify various types of heart diseases using HRV analysis. Several authors have evaluated the results from ANNs with existed classifiers and conclude ANN gives better accuracy than the other binary classifier. It has been observed that the performance of the classification accuracy gets improved after feature selection or employing statistical analysis. Because it removes the redundant and irrelevant features from the feature set and selects only that parameter which

gives additional useful information than others. In this research work, the authors have employed the SVM, kNN, and ANN methods for the classification of NSR, AR, and AF ECG signals. These concluding remarks motivate the author to formulate the research gaps & objectives for this research work.

The exhaustive study of the popular and recent literature assists the researchers to discover some of the research gaps.

iv. Resource Optimization in wearable ECG module

An investigation for obtaining sufficient diagnostic quality of ECG recording

v. Design of low power ECG pre-processing module

ECG Denoising employing different functions for power optimization

A novel architecture for ECG pre-processing

vi. Beat Detection and Classification Algorithm

Acquiring prominent features for Arrhythmia and Atrial Fibrillation based on HRV

Decreasing the False Positive Rate for the classification of Arrhythmia and Atrial Fibrillation

Based on the research gaps, different objectives were framed for obtaining the low resource utilization, low power consumption, and multi-stage classification system for the detection of NSR, AR, and AF by employing different types of bio-signal processing techniques.

In context to the information perceived from the literature, the author realizes that in Biomedical Signal Processing the design of an automatic ECG monitoring system is popular research work. To attain these objectives, the author has proposed a methodology for a power-efficient ECG system. Various moderations in the pre-processing and post-processing ECG system have been proposed to improvise the performance of the module.

The primary focus of this research work is to design a *QRS* detection algorithm having higher sensitivity and PPV. The developed algorithm should require low resources of basic characteristics of real-time monitoring system such as LUTs, registers and DSPs, and low power. Heart rate can easily be computed when the corresponding R-peaks of an

ECG signal are detected. Thus, the authors have to design an efficient algorithm that can authentically determine the heart rate from the ECG signal.

Objective I

Design and Implementation of ECG Denoising Module for Optimal Resources

Objective II

The Robust Hardware Design of Low Power Module for Clinically Significant ECG

Objective III

Development of Multi-Stage Classification System for Heart Rate Variability

CHAPTER 3

RESOURCE EFFICIENT FPGA

BASED DENOISING MODULE

CHAPTER 3

RESOURCE EFFICIENT FPGA BASED DENOISING MODULE

In the present scenario, CVDs are the widespread problem that occurs in most each becomes the are one of the most common problems that occur in the world [116]. There is a need for continuous monitoring of the patient's health. The maximum benefit of the embedded technology is availed by the cardiology department in the medical field by introducing portable and wearable ECG module as shown in Figure 3.1.



Figure 3.1: Portable ECG Equipment

The processing unit's selection for the implementation of the wearable ECG module based on low resources and power is a major challenge. Additionally, a reliable interpretation of the recorded ECGs always remained a key concern to diagnose and treat the patients suffering from CVDs. It is accomplished by attaining adequate diagnostic quality for the analysis of ECG patterns from long-term ECG. These recordings are contaminated with numerous low and high-frequency noises that deteriorate the informatory signal from the ECG [116]. The ECG waveform is usually contaminated with motion artifacts, EMG noise, burst noise, BLW & PLI noise [117]. Among them, EMG, BLW, and PLI are the main types of noise that cause the major distortion in the useful ECG signal.

3.1 INTRODUCTION

The tremendous growth in the embedded systems field has been observed in the past few years, typically in the electronics consumer section. The upward fashion to have quality performance design has led to meeting the stringent system requirements by the researchers as a result of innovative design techniques to meet these objectives. These systems usually perform variants across streaming digital signal processing that involves computer-intensive mathematical computations.

Digital filters have emerged as one of the frequently used devices for the elimination of biomedical noises. The implementation of these software-based digital filter design into hardware design is a rigorous task. The three processing units (MCU, DSP, and FPGA) are taken for the hardware implementation and compared based on re-programmability, power consumption, speed, architecture flexibility as represented in Figure 3.2.

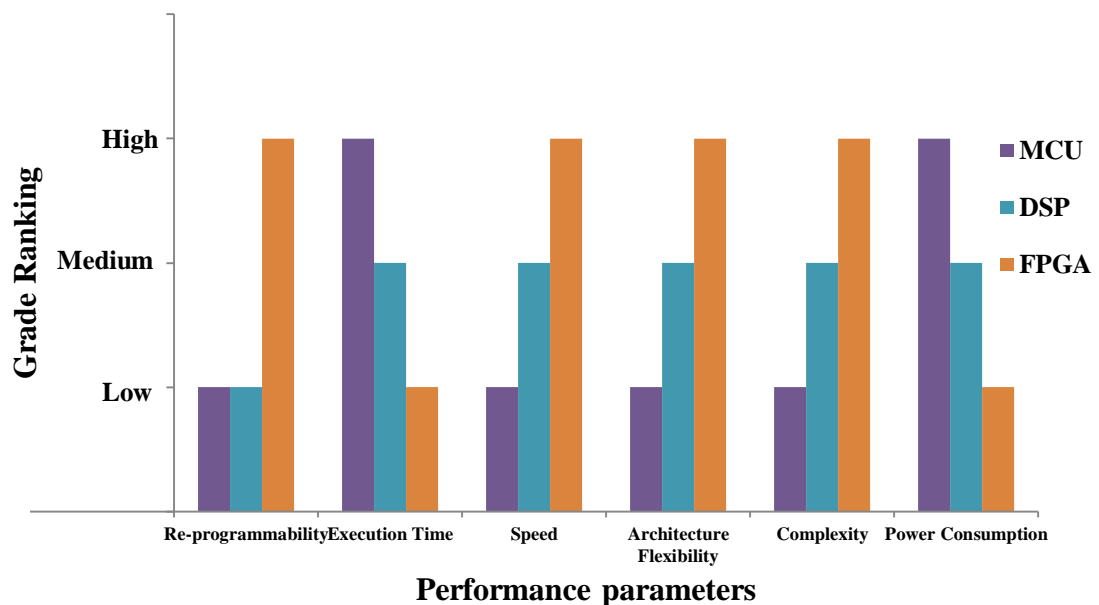


Figure 3.2: Comparison of different processing units

The FPGA has been selected due to its low resource utilization, high speed, ease of architecture flexibility, and power consumption; which is favorable for the portable ECG module. This chapter outlines the FPGA realization of the digital filter design of low power ECG pre-processing module.

With the integration of DSP into several devices, market time & the capability to built late design variations turn out to be imperative. The software provides the freedom to

allow late design alterations but its performance gets compromised in contrast to hardware. Hardware and software execution have their own set of pros and cons [118]. Execution of multiple tasks via hardware could be done in parallel whereas software executes sequentially. On the other hand, it takes a longer time to build an application-specific integrated circuit (ASIC). That's why, FPGA resolution by merging the strengths of hardware design along with software design.

Conventionally, many DSP applications are using digital signal processors mainly due to low cost, lower power consumption, and shorter development time. FPGAs are, however, changing this traditional approach and are being used increasingly in applications where the requirements of the system are not very stringent. In general, this system includes various types of computationally rigorous applications, especially in real-time DSP [118]. There has been rapid progress in fabrication technology due to which the present cohort of FPGA now contains an enormous number of configurable logic blocks (CLBs). These CLBs are making FPGA a feasible platform to implement a broad range of applications. FPGAs have gained attraction for application-specific DSP solutions due to long development time and high non-recurring engineering (NRE) costs for ASIC [119].

DSP is becoming an essential function nowadays. A variety of devices require signal processing with high throughput data nowadays. One of the other kind of DSP algorithms is being used in devices ranging from handheld audio/video devices to satellites. A huge amount of R&D is being done by the engineers to find ways of greater performance and shorter time to market. Arithmetic operations of embedded DSP microprocessors are performed via software. This is a slow approach as these operations are serial but have the advantage of being modified. The FPGA chips have stepped in to solve the problems in the domain where the indication of placing the arithmetic operations in hardware exists for since long but due to extensive upfront time and effort in creating a custom ASIC it never flew off well [120-124]. Using FPGA this problem is being solved as it combines the best of both worlds. FPGAs are even faster than microprocessors, due to its reconfigurable hardware and high performance.

Two major components of FPGA structure are Logic Blocks and On-Chip Memory.

Logic Blocks implement the combinatorial part of the design. Logic blocks consist of storage elements and lookup tables (LUTs)

The majority of applications of DSP are generally performed in terms of the multiplication of data with constant coefficients or an internal feedback mechanism. Almost every processor can perform addition and multiplication, thus they are also capable of performing DSP algorithms. A general-purpose DSP differs from an FPGA only w.r.t. how well the function is performed.

A powerful architecture is offered by FPGAs & a plethora of resources. The FPGA architecture is flexible; as a DSP function is easily able to map directly to the available resources of FPGA. Thus, they proposed tradeoffs between performance & system density. DSP processors are not completely replaced by FPGAs. As far as DSP processors are concerned they still dominate in floating-point arithmetic whereas only fixed-point DSP functions are addressed by the current generation of FPGAs. In general, FPGAs excel in the application areas which are computationally intensive requiring a large number of filter taps, high throughput. Energy-efficient implementation and high performance, persist as a design challenge for digital systems, especially in handy biomedical devices. Optimization at all phases of the design hierarchy is required. Effective designs are needed at the coarse level and effective algorithms facilitate in reducing the overall power utilized at the fine-grained level. The leakage during power consumption, especially in lower geometries, is a prominent factor in total power consumption. In particular, power dissipation in nanoscale systems is due to a significant amount of transistor leakage, which is caused by the scaling of threshold voltage, gate oxide thickness, and channel length [125-127]. Dissipation of dynamic power occurs only when transistors are switching, whereas, in the case of idle transistors, leakage power is consumed [128].

FPGA is a configurable integrated circuit which is configured by the designer to design digital circuits, hence the term "field-programmable". The VHDL & Verilog are two types of hardware description languages that are normally utilized to specify FPGA configuration. FPGAs possess significant advantages in several applications due to its reconfigurability feature and non-recurring engineering (NRE) cost. This is in contradiction to the application-specific integrated circuits (ASICs) where after the chip has been manufactured, no design modification can be done by the designers, in short, they do not have the freedom to play around with the chip design.

FPGAs comprises several configurable logic blocks (CLBs) that facilitates the design flexibility through reprogrammable logic & designable interconnects to club the CLBs.

On-chip memory blocks are also provided, in addition to these basic components. The recent trend in FPGA technology is moving towards creating a complete system on a programmable chip (SOPC) by using the architectural components of coarse-grained level along with DSP blocks, high-speed transceivers, and embedded processors. FPGA innovation deals with flexibility & quick prototyping volumes for a quicker time to advertise. One would then be able to actualize steady changes and repeat on an FPGA plan inside hours instead of weeks. The elevated level of programming instruments diminishes the expectation to learn and adapt and frequently incorporates significant protected innovation (IP) centers for cutting edge control and sign preparing.

There are a few FPGA makers: Reprogrammable (SRAM based/ streak based) FPGA & one time programmable (OTP) FPGA. SRAM-based FPGAs require a memory arrangement that doesn't hold the information when the designer not able to control it. Streak based FPGAs are functions when power on & needn't bother with outside memory and OTP FPGAs are modified, they can't be reconstructed. In the accompanying, a diagram of an FPGA engineering will be introduced, and afterward, the design of the most recent Xilinx FPGA gadget, Zynq-7000 Zed Board, will be canvassed in detail [129].

3.1.1 FPGA Technology

Recent FPGAs deliver the salient attributes that incorporate CLB, look up table (LUT), input/output blocks, etc. The CLBs are the principal rationale assets for executing successive just as combinational circuits. A piece of CLB component is associated with a change lattice to access the general directing grid. The CLB component contains a couple of cuts. These two cuts don't require direct associations with one another. Each cut in a segment has an autonomous convey chain. The on-chip memory gives the storage on FPGA.

The proficient complex function delivers by IP core structures such as transceiver, multiplier, DSP. FPGA also provides the clock management resource that enables frequency synthesis, clock distribution & clock shifting. The I/O block on the FPGA chip provides the interface to the outer world. The embedded processors & routing resources gives the processing power & interconnectivity within logic blocks & hard macros. The general FPGA architecture of 7 series programmable logic is represented in Figure 3.3

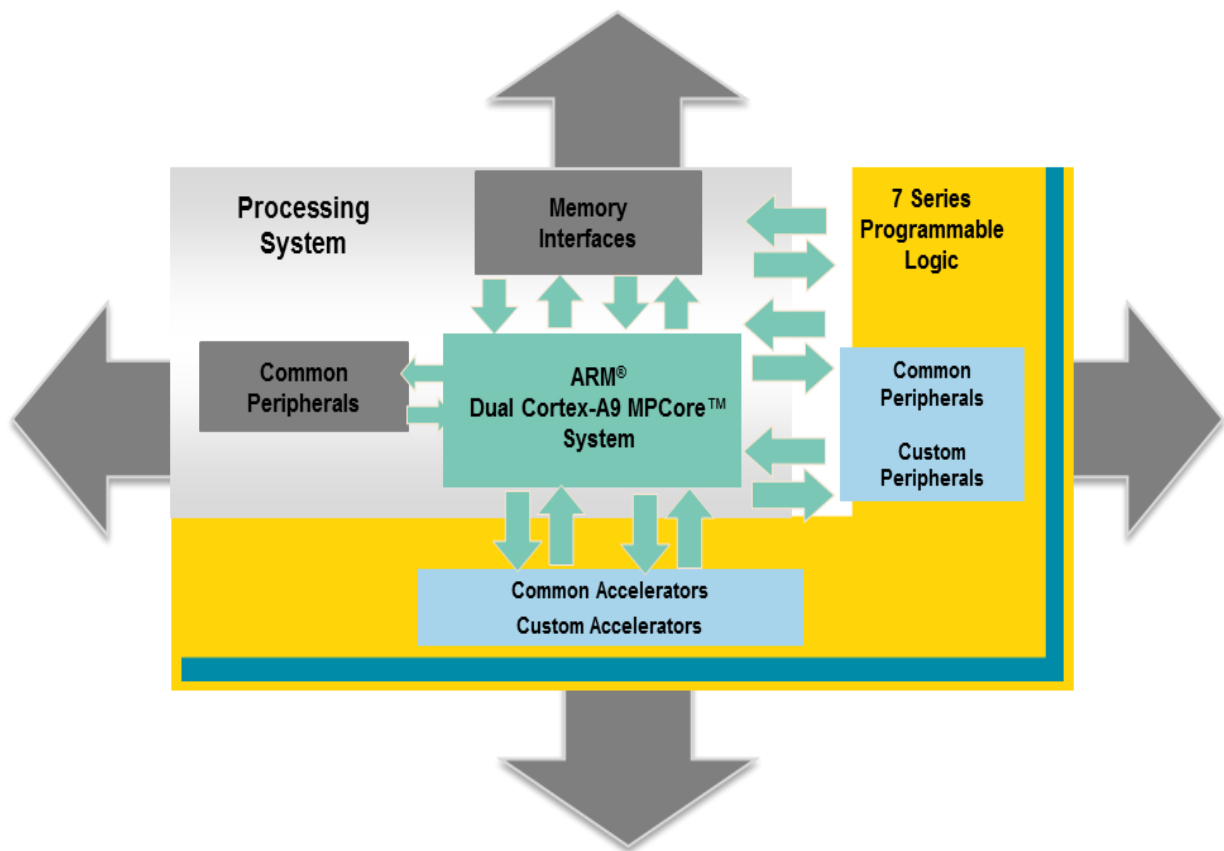


Figure 3.3: General FPGA architecture

It has been inferred from the figure that 7 series programmable logic comprises of peripherals and accelerators and the processing system includes the latest ARM processor.

3.1.2 Zynq-7000 Zedboard Architecture

The Zynq family delivers the latest & powerful features within FPGA families. The scalable platform offers easy migration between series 7 devices as represented in Figure 3.4 [129].

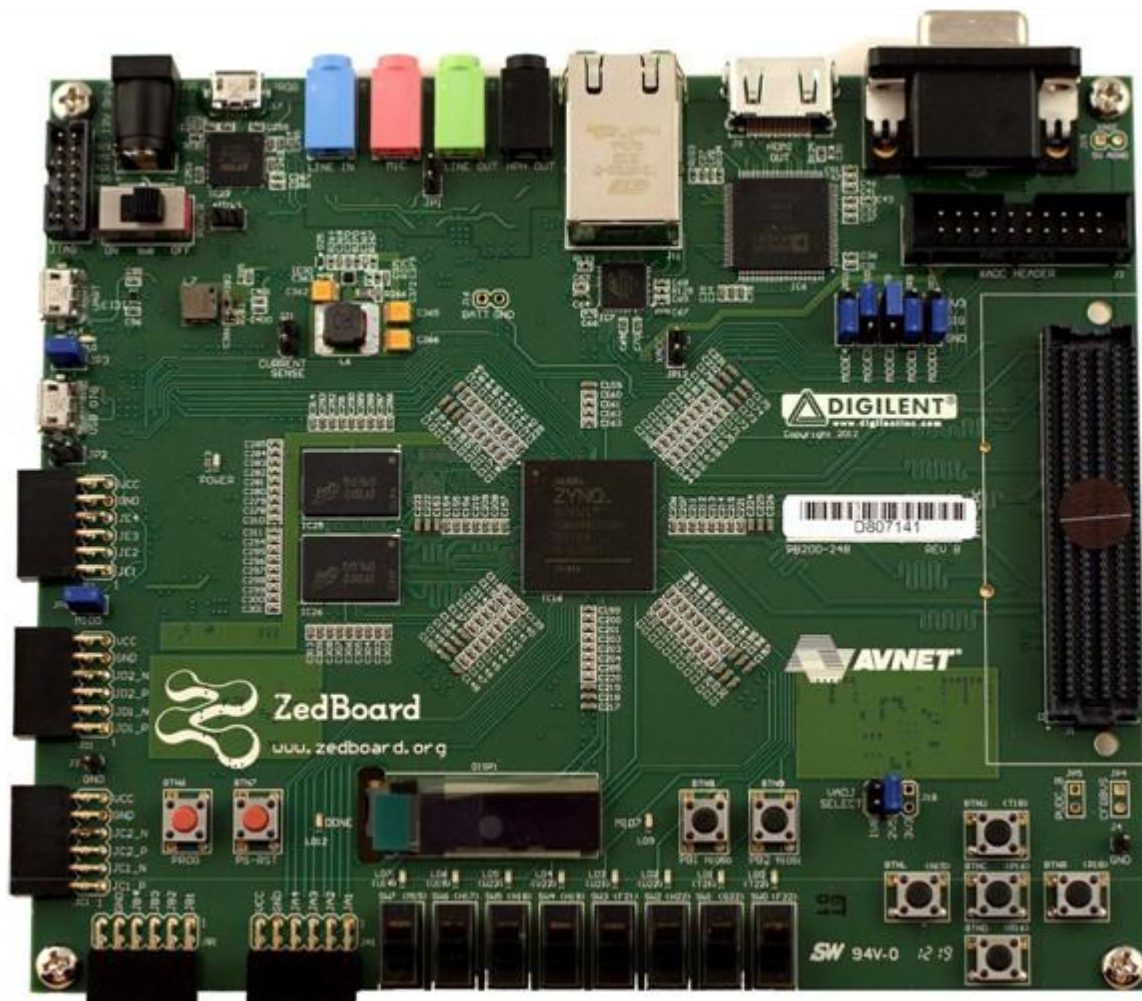


Figure 3.4: Overview of Zedboard architecture [129]

The combination of a dual Coreex processing system (PS) along with 85,000 series-7 programmable logic (PL) cells is targeted for utilization in many applications. The ZedBoard is a combination of on-board peripherals which is an ideal platform for both beginner and experienced designers.

3.1.3 Design Flow of Xilinx FPGA

Figure 3.5 represents the FPGA configuration stream which contains the accompanying advances: useful detail of the framework, plan section in equipment portrayal language, for example, VHDL or Verilog, structure combination, structure usage (spot and course), gadget programming, lastly in-circuit confirmation. Plan confirmation, which incorporates both utilitarian check and timing confirmation, takes place at various focuses during the structure stream. The accompanying depicts what should be finished during each progression.

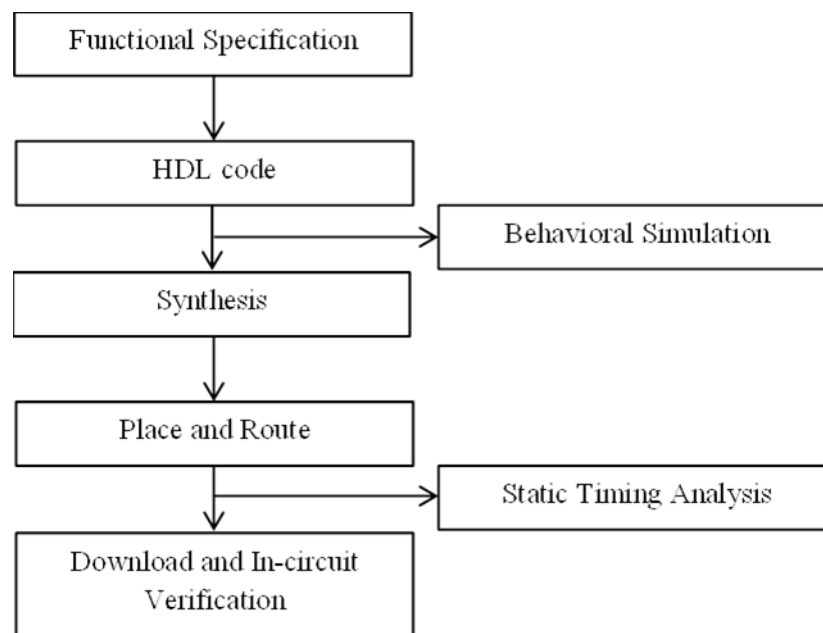


Figure 3.5: Design flow for FPGA implementation

The initial stage includes the examination of structure prerequisites, issue deterioration, plan section, and utilitarian reproduction, where exactness and conduct model is inspected by looking at the yield of the HDL model. In the amalgamation, the HDL detail is changed over to a netlist, which is essentially the entryway level depiction of the plan. At this stage, different streamlining limitations can be applied to the plan. In structure execution, the implicit netlist innovation libraries are mapped onto the particular design of a particular device. This setup information is kept in touch with a different document by a program called bitstream. During time investigation, the product checks whether the predefined programming fulfills the client's predetermined time limits. At this stage, the

first postpone model is utilized to appraise the genuine deferral on the chip in the wake of steering.

3.1.4 Design Flow for FPGA based DSP

The methodology for the hardware implementation of intricate DSP calculations on reusable logic is a defying task. The utmost challenging process in the system design is the identification of the starting point! This method helps us to manage complicated designs efficiently, reduces the time to design, eliminates multiple bases of errors, reduces manpower to accomplish the design, & produces optimal design solutions. The advantages of adopting such a method are different from its development costs.

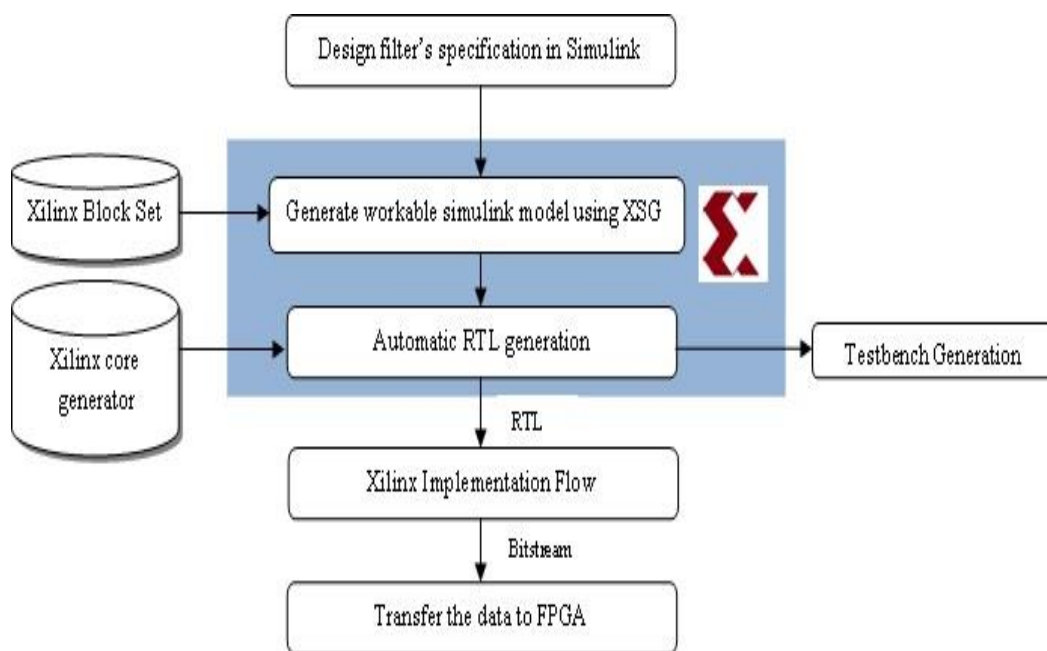


Figure 3.6: FPGA/DSP design flow

The default path to design DSP algorithms achieved by software languages namely C, C++, MATLAB & execute instructions in DSP. FPGAs utilizes hardware interpreter languages to perform such tasks. Turning software-based algorithms into hardware is often an automated process. However, DSP algorithms can be expertly crafted in HDL from scratch. Figure 3.6 represents the flow to design a DSP based solution in FPGA by employing several tools delivered by Xilinx. The MATLAB algorithm is converted into RTL via Simulink modeling. Xilinx presents a DSP library to implement complicated DSP

designs such as filters. Additionally, the XilinxCorgan tool helps to generate complex DSP functions in RTL that perform complex tasks. The automatic conversion of Simulink format to RTL using the System Generator tool is done. However, it is possible to create an RTL based architecture that can be handled using the Xilinx ISE Toolkit. These consecutive stages assist to generate the bitstream needed to configure FPGA.

3.2 DIGITAL FILTERING TECHNIQUES

In digital signal processing applications; digital filters performed an essential part. It helps to perform various tasks of DSP applications, specifically signal filtering, denoising, multimedia compression, biomedical signal & image enhancement, etc. A system that permits preferred signals over unwanted; or to improve or minimizes certain features of the signal; termed as a digital filter. It helps to pass and reject the frequency from a signal according to the pass-band specification. High-pass Filter (HPF), Low-pass Filter (LPF), Band-stop Filter (BSF) & Band-pass Filter (BPF) is the elementary types of filter. According to the impulse, there is two types of filter: IIR & FIR filter.

FIR filter has more advantages over IIR filter in terms of phase, stability, and structure. FIR filters have a linear phase, non-recursive structure, high stability, and variable amplitude-frequency characteristics. The general equation of the FIR filter is expressed by Eq (3.1).

$$y(n) = \sum_{i=0}^N b_i \cdot x(n - i) \quad (3.1)$$

where $y(n)$ represents the output signal

The order of the filter is given by N

b_i is the impulse response at i_{th} time for $0 \leq i \leq N$ of N th order filter

$x(n)$ is the input signal

According to Eq. (3.1), the system's output is calculated based on the filter's coefficients and order of the filter.

Digital FIR filters are effectively utilized in the measurement of electrocardiographic signal processing. ECG signal is contaminated by various kinds of interferences at the specified frequency. At 50/60 Hz, PLI noise is located; below 0.5 Hz BLW noise is present

and above 100 Hz EMG noise is found. To acquire the clinically correct information from the ECG signal one must eliminate these unwanted signals. The intensity of these noises can be varied based on the patient's movement during acquisition, muscle movement rate, and pressure. Due to this clinicians prefer to take ECG from the patient's body; when the muscles are relaxed and make sure the patient should stay still and quiet. Windowing, Frequency sampling, and optimized FIR filter design are widely used techniques for FIR filter designing [130]. Among them, the window method is most frequently utilized for the designing of FIR filters in the recent literature due to its ease of hardware implementation. The easiness of the design procedure makes this technique very popular. The organization of a certain coefficient in a definite array as per the designer requirements generates a window function. A window is a finite array comprising of certain coefficients to fulfill the desired requirements. The design steps for designing a window FIR filter comprises of mainly three parts: Specify the type of filter, compute filter order for a given set of terms and compute the window filter coefficients. The type of filter (LPF, HPF, BPF, BSF, or notch) is selected as per the requirement and their ideal frequency response [131]. For the elimination of High-frequency noise of EMG a low pass filter is used and its ideal frequency response is signified in Eq. (3.2).

$$h[n] = \begin{cases} \frac{\sin[\omega_c(n-M)]}{\pi(n-M)}; & n = M \\ 1 - \left(\frac{\omega_c}{\pi}\right); & n \neq M \end{cases} \quad (3.2)$$

Where $h[n]$ represents the frequency response of the filter, 'M' as the order of the filter, ' ω_c ' as cut-off frequency, and 'n' signifies filter's length. To remove the low-frequency noise of BLW an LPF is utilized and its ideal frequency response is signified in Eq. (3.3).

$$h[n] = \begin{cases} \frac{\sin[\omega_c(n-M)]}{\pi(n-M)}; & n \neq M \\ \frac{\omega_c}{\pi}; & n = M \end{cases} \quad (3.3)$$

For the elimination of high-frequency noise of PLI a low notch or BSF filter is utilized and its ideal frequency response is signified in Eq.(3.4).

$$h[n] = \begin{cases} \frac{\sin[\omega_{c2}(n-M)]}{\pi(n-M)} - \frac{\sin[\omega_{c1}(n-M)]}{\pi(n-M)} ; n = M \\ \frac{\omega_{c2} - \omega_{c1}}{\pi} ; n \neq M \end{cases} \quad (3.4)$$

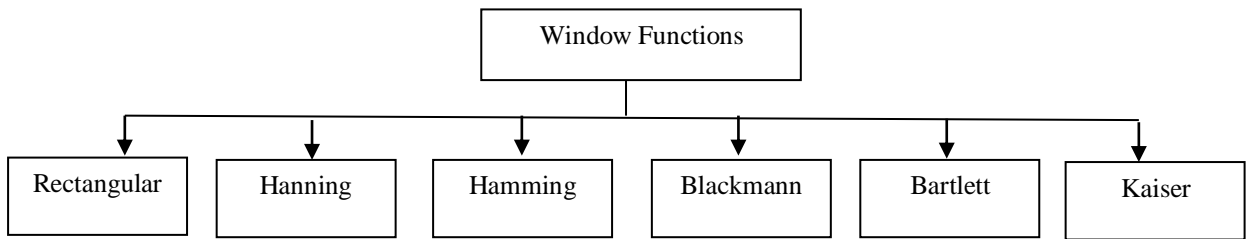


Figure 3.7: Different window functions

The filter's order depends on the type of filter chosen for a given set of specifications. In this chapter, the authors have used a smaller order filter to minimize power and resource utilization. Several classical window functions namely Hanning, Rectangular, Blackmann, Hamming, Kaiser, and Bartlett by which window coefficients are computed. Figure 3.7 signifies the various types of window functions utilized and descriptions about these are given where $w(n)$ defines the window function, 'n' as filter's length, and 'M' termed as an order of the filter. The window function equations and their applications are discussed in *Appendix B*.

3.3 PROPOSED METHODOLOGY

ECG signals obtained can be easily corrupted with various mechanical and electrical noises namely EMG, BLW, and PLI illustrated in Figure 3.8.

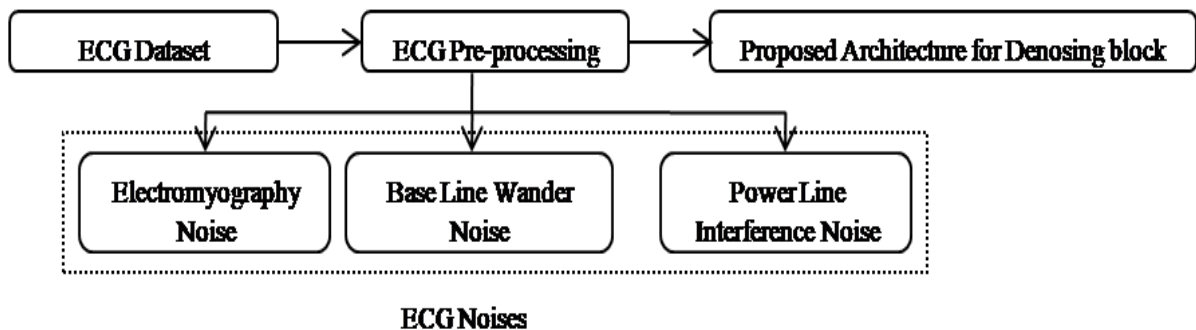


Figure 3.8: Methodology of ECG pre-processing block

This undesirable interruption in the cardiac signal hampers the ECG signal analysis. Therefore, a noiseless ECG signal is the primary requirement for clinicians to diagnose heart-related problems correctly. Digital filter design and its specification are required to implement the filter algorithms for the removal of these artifacts as represented in Figure 3.9. It represents to specify the type of filter require namely LPF, HPF, BPF, and notch filter. Based on the filter's order and its type coefficients are computed. The realization of structuring is selected as per requisite namely Direct FIR filter or Transposed FIR filter. There is a significant effect on the word length has been observed; whether the design requires fixed-point or floating-point representation.

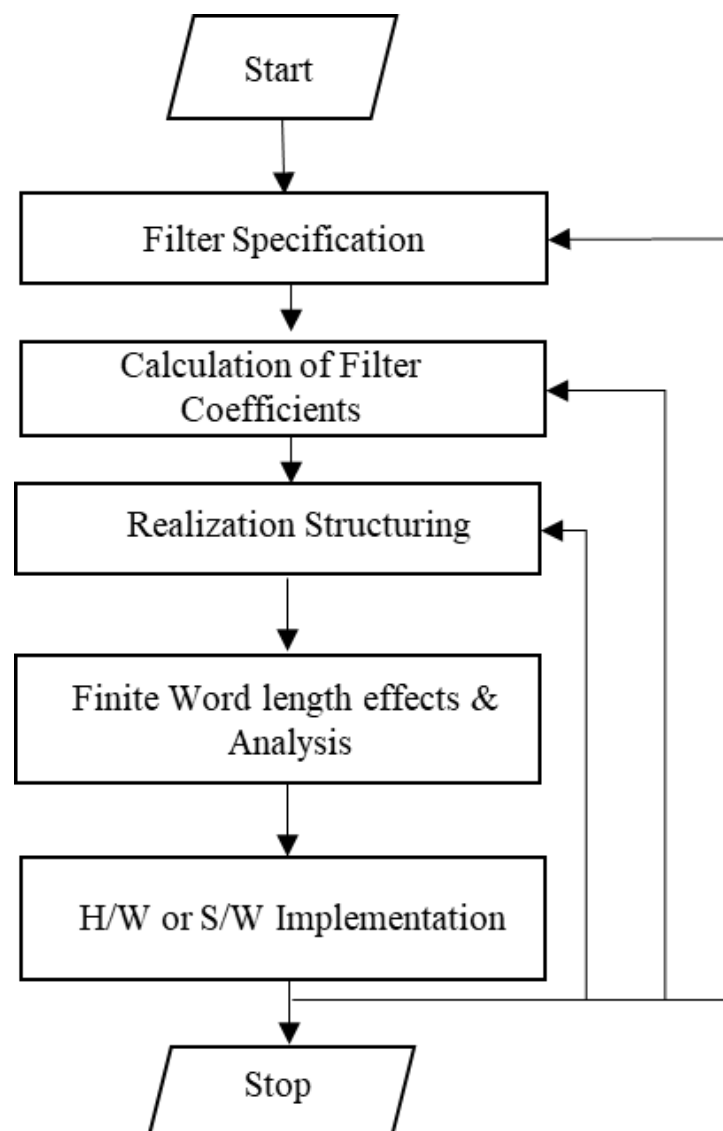


Figure 3.9: Steps to follow the digital filter design and specification

The FPGA implementation of this digital design requires a fixed-point representation. The Fdatool from MATLAB provides an inbuilt function to transform the design from the

floating-point unit to fixed-point unit representation. This representation depends on word length, fractional bit length, and signed/unsigned selection. The effect of word length selection of 8-bit and 16-bit has been shown in Figure 3.10. According to the ECG dataset, the 16-bit word length is preferred over 8-bit because more quantization error arises on the selection of 8-bit word length concerning 16-bit.

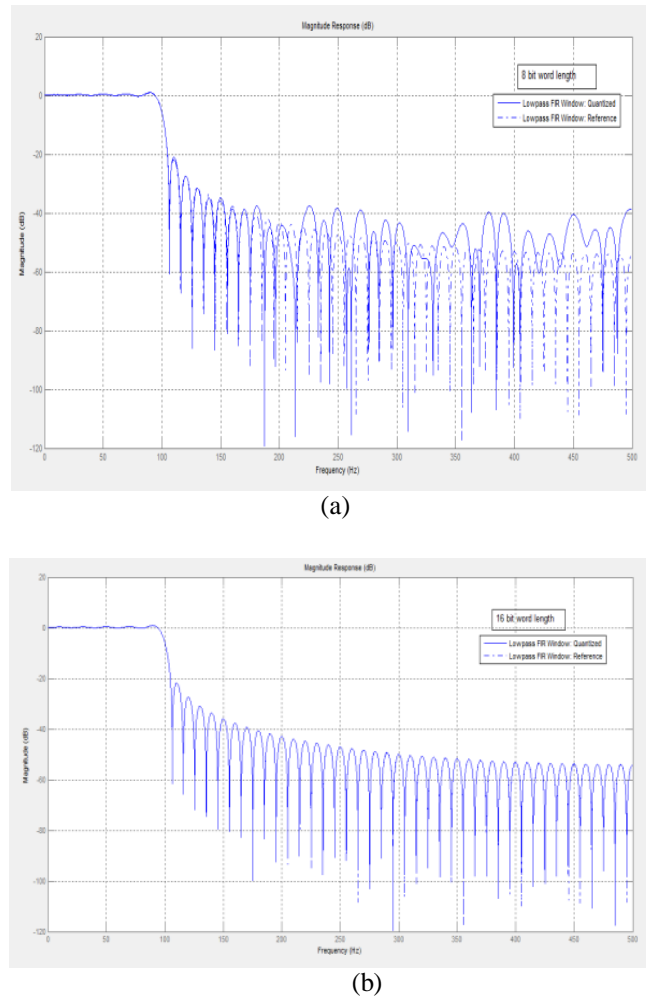


Figure 3.10: Effect of word length on the frequency response (a) 8-bit (b) 16-bit

The 16-bit word length selection leads to implement the digital filter implementation on FPGA. A novel modified hamming window has been proposed by the authors in this research. The standard hamming window function does not provide the appropriate frequency response for the ECG filtering. The authors have proposed a hamming window function which gives better frequency response in comparison with other window methods.

The generalized equation of the Hamming & Hanning window function is:

$$w(n) = \alpha - (1 - \alpha) \cos\left(\frac{2n\pi}{M} - 1\right) \quad (3.4)$$

when $\alpha = 0.5$: Hanning Window Function

$\alpha = 0.54$: Hamming Window Function

The value of ' α ' in the proposed hamming window function equation is taken as 0.74.

$$w(n) = 0.74 - 0.26 \cos\left(\frac{2n\pi}{M} - 1\right) \quad (3.5)$$

The proposed window function design specifications are taken as the order of the filter is 7. The cut-off frequencies (ω_c) of HPF is 0.5 Hz, LPF's 100 Hz, and notch filter's 49.5-50.5 Hz. The proposed window function has been utilized in the methodology due to its low computational complexity and better frequency response. The proposed methodology consists of four steps namely selection of coefficient, proposed architectures, and simulation techniques.

3.3.1 Two-tier ECG Denoising Architecture

The online platform is used for ECG signal acquisition. The proposed methodology represented in Figure 3.11 suggests the two-tier denoising architectures to denoise the ECG signal to investigate the framed research questions. To follow the design flow of XSG, a low-power denoising module for ECG is proposed. The proposed window function design specifications are taken as the order of the filter is 7. The cut-off frequencies (ω_c) of HPF is 0.5 Hz, LPF's 100 Hz, and notch filter's 49.5-50.5 Hz. The proposed window function has been utilized in the methodology due to its low computational complexity and better frequency response.

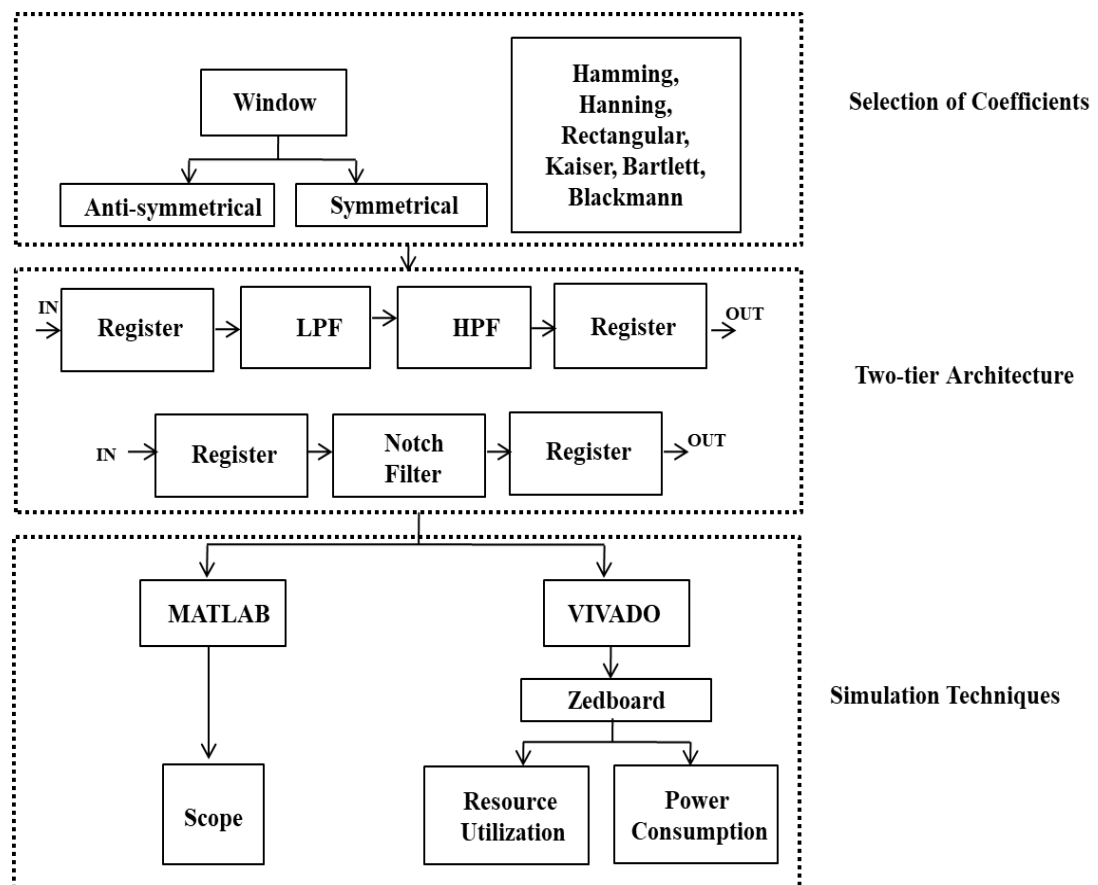


Figure 3.11: Proposed methodology for two-tier ECG denoising architecture

Two designs are introduced in this methodology by using in-built Xilinx blocks. One set of design removed BLW & EMG noise by employing LPF & HPF consecutively. Another set of designs eliminates PLI noise by employing a notch filter. All the classical window functions are compared in terms of resource & power consumption.

3.3.2 Three-tier ECG Denoising Architecture

The three-tier methodology comprises of three digital filters connected consecutively. This block comprises basic components of the FIR filter. The authors have removed all the three ECG noises simultaneously by employing the proposed methodology.

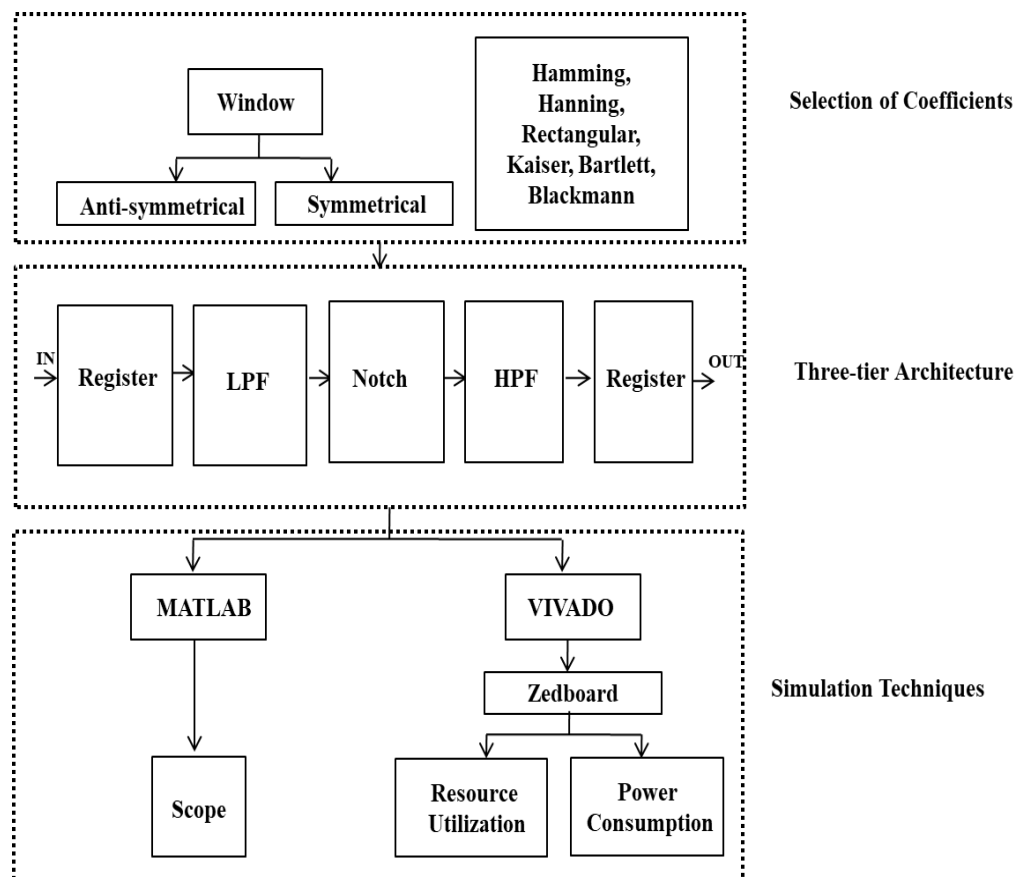


Figure 3.12: Proposed methodology for three-tier ECG denoising architecture

The registers used in the proposed architectures are utilized to store the samples one by one. The three-tier methodology is also compared on all the classical window functions in terms of resource & power utilization. The authors have taken motivation from the existed literature and also considered the practical potentials and conditions at the time of the

investigation. A detailed description and discussion of the findings have been incorporated in the proposed methodology.

3.4 RESULTS & DISCUSSION

This section embodies the two types of proposed architecture: 2-tier ECG denoising block and 3-tier ECG denoising block. Their results are represented in terms of the XSG model, scope results, RTL schematic, and resource and power utilization. The percentage improvement has also been shown in comparison with the existing literature.

3.4.1 Two-Tier ECG Denoising Block

Figure 3.13 (a) suggested the XSG model of serially coupled two digital filters; the first filter is deliberated as an LPF and the second filter as HPF. Figure 3.13 (b) is implemented on the XSG model to eradicate the PLI noise.

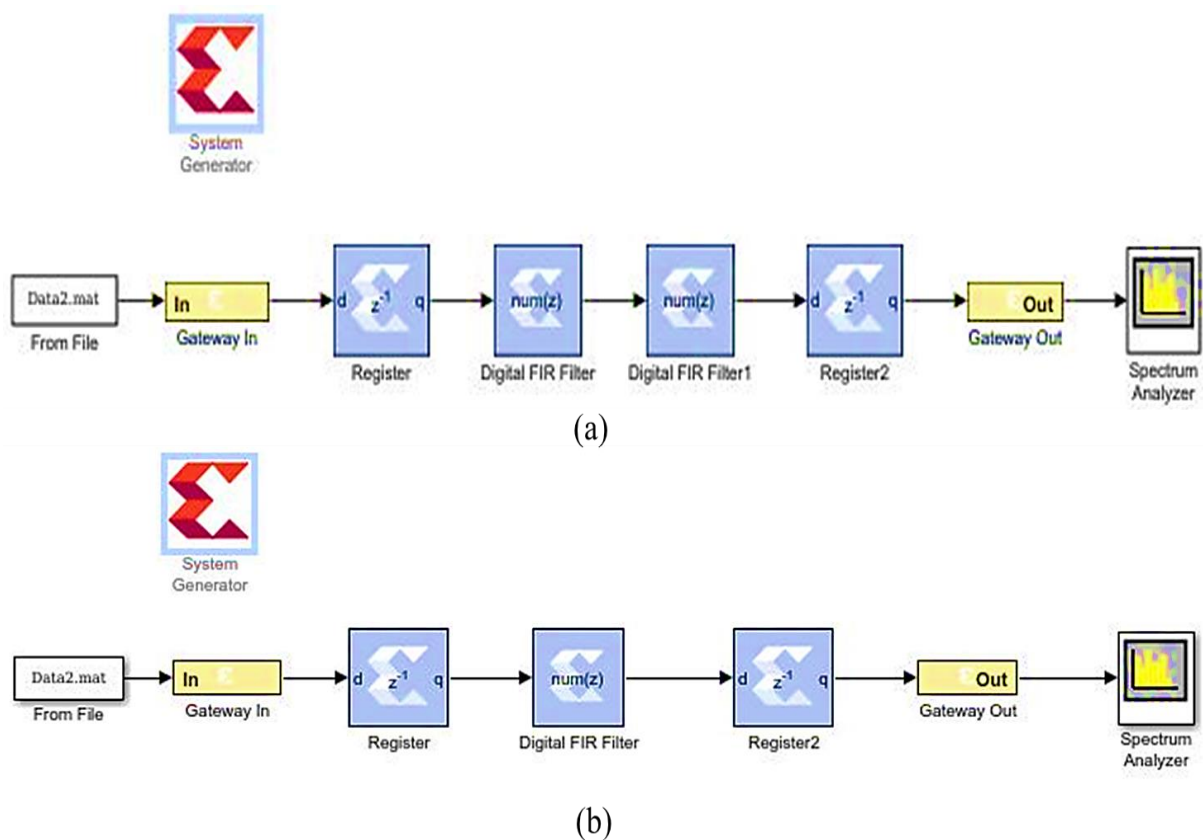


Figure 3.13: Simulink model for the realization of 2-tier architecture (a) LPF & HPF (b) Notch filter

The in-built digital FIR blocks from the Xilinx block set of Simulink is utilized in the structure. The gateway-in and gateway-out blocks are the sources and sink blocks taken from the Xilinx block set; it converts the real values of data into floating and fixed-point numbers.

The ECG input of MIT/BIH was taken from Physionet. The raw ECG signal is corrupted with ECG noises. The simulation is performed on Simulink in which Fig. 3.14(a) signifies 3600 samples of ECG signal of record number '101' for 10 seconds. Fig. 3.14(b) represents the removal of the EMG by applying LPF. Fig. 3.14(c) illustrates the outcome of HPF to eliminate BLW noise.

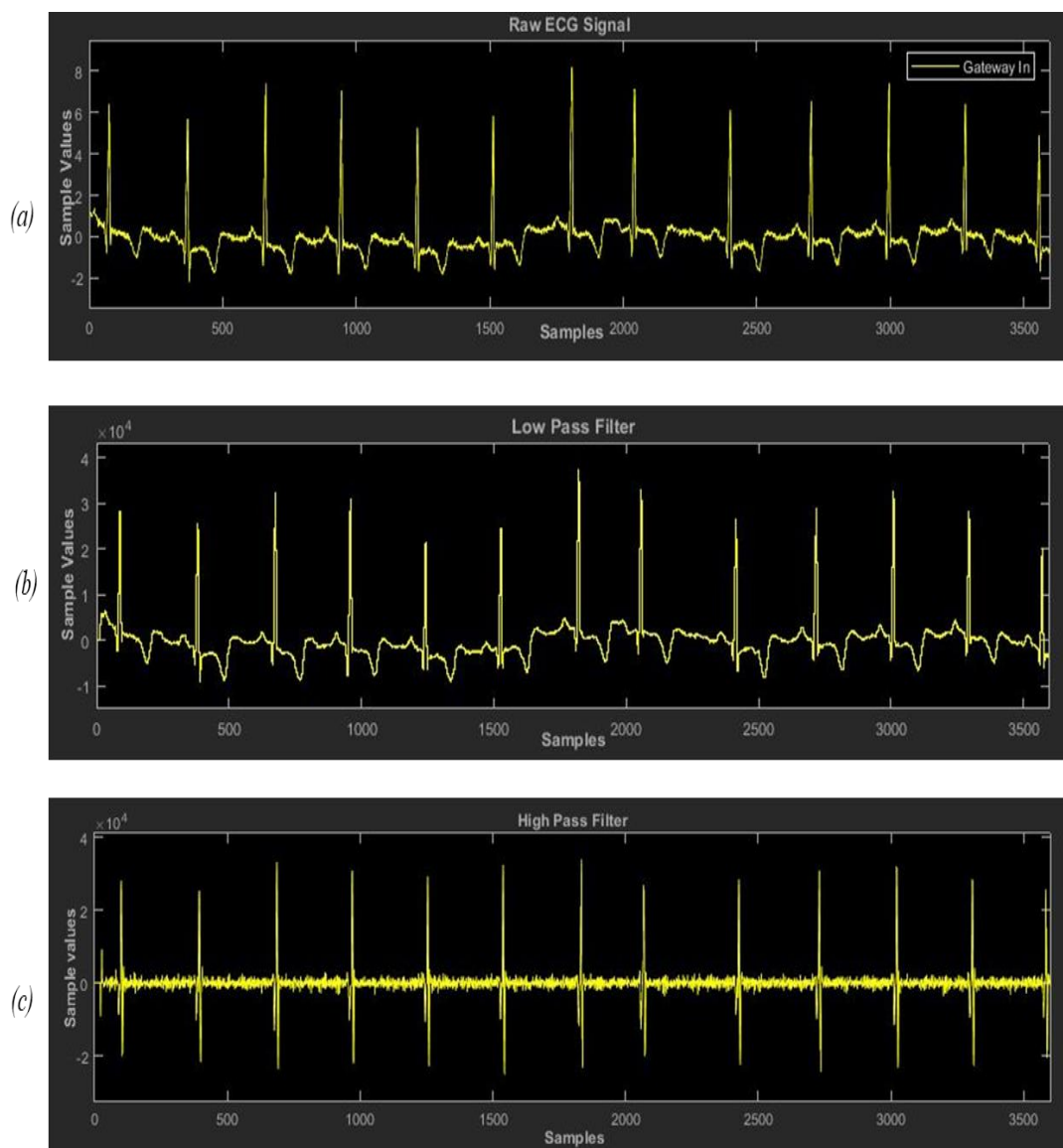


Figure 3.14: Scope results (a) Input ECG signal (b) Electromyography Noise Removal (c) Base Line Wander Removal

The successful simulation at the XSG level is performed to obtain resource & power consumption is calculated. The behavioral simulation waveform and RTL schematic at various abstraction levels on XILINX VIVADO is illustrated in Figure 3.15, abstraction & successful implementation of the Simulink model into RTL schematic using core generator block

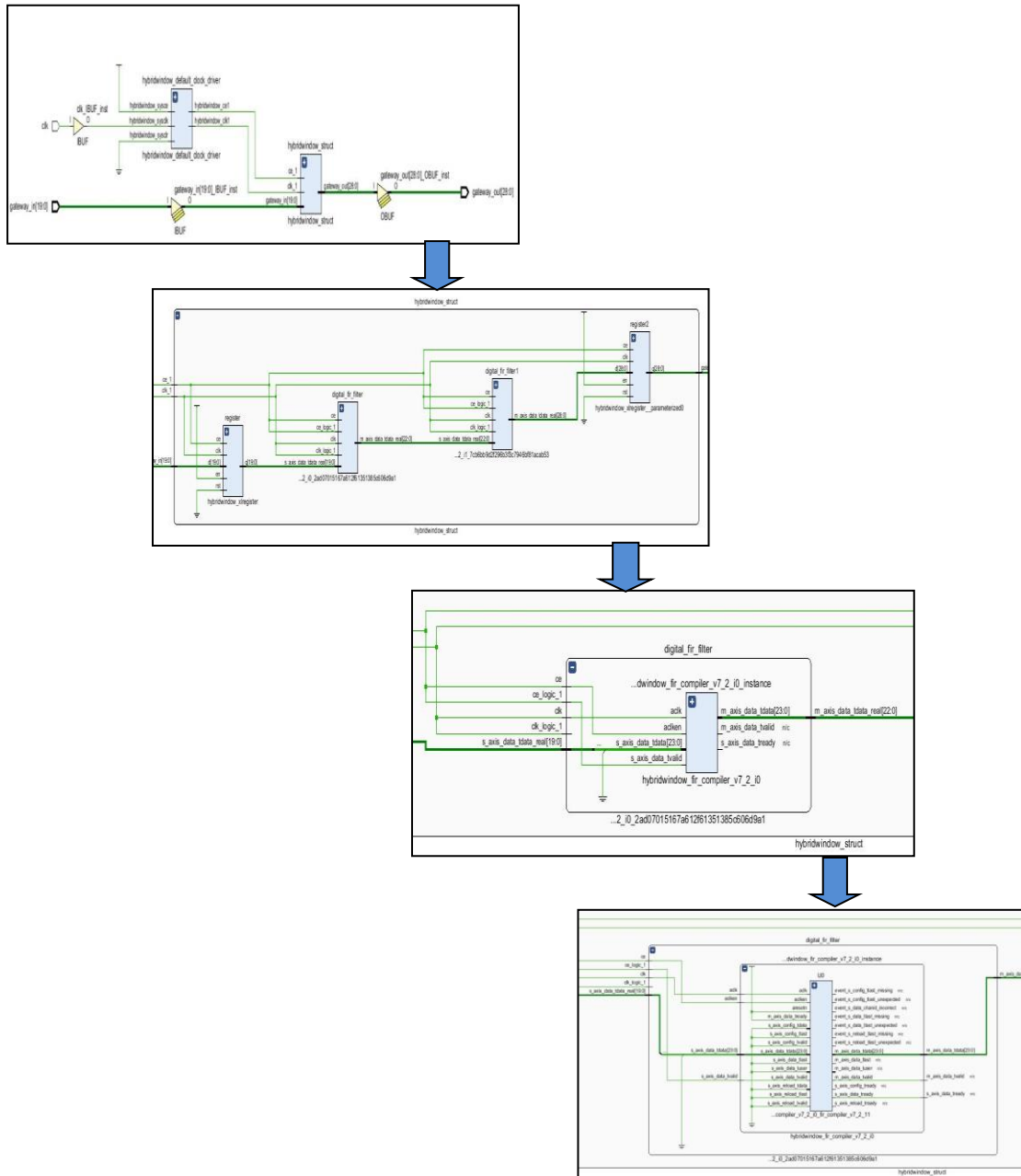


Figure 3.15: RTL schematic of low pass and high pass filter

Table 3.1 tabulated the proposed window technique that consumes 220 LUTs, 391 Registers, and 6 DSPs out of 53200 LUTs, 17400 Registers, and 220 DSPs in contrast with

other windowing techniques. The proposed window function has also consumed only 121 mW of power.

Table 3.1: Comparison Table of HPF and LPF for various types of Windowing techniques

Window Design Methods		Resource Utilization			Power Consumption
Low Pass Filter	High Pass Filter	LUT (53200)	Registers (17400)	DSP (220)	On-Chip Power
Proposed	Proposed	220	391	6	0.121
Hamming	Hamming	220	400	6	0.136
Bartlett	Bartlett	223	399	6	0.128
Kaiser	Kaiser	225	410	6	0.144
Rectangular	Rectangular	247	391	6	0.136
Blackman	Blackman	247	463	7	0.142
Notch Filter	Proposed	105	209	3	0.130
	Hanning	127	273	4	0.135
	Kaiser	117	219	4	0.132
	Hamming	127	273	4	0.135
	Bartlett	105	210	3	0.132
	Blackman	105	209	3	0.132
	Hamming	105	210	3	0.131

In the proposed architecture 1, the researchers have utilized the in-built Xilinx block set of the digital FIR filter. Various types of noises are eliminated by employing the proposed methodology. The Proposed window has been chosen due to low resource utilization. It has utilized only 0.41% of LUT, 2.24% of registers, and 2.72% of DSPs. When the ECG signal is less noisy and only EMG and BLW noise are present then architecture 1 will be employed. To eliminate all the three ECG noises simultaneously Architecture 2 has been proposed.

3.4.2 Three-tier ECG Denoising Block

In the proposed architecture 2, all the low-frequency and high-frequency noise components namely EMG, BLW, and PLI can be removed simultaneously. To realize this architecture various types of window functions have been used the same as architecture 1. Figure 3.16 illustrates three tiers of HPF and LPF block that eliminates the unwanted signal from the biomedical signal (ECG).

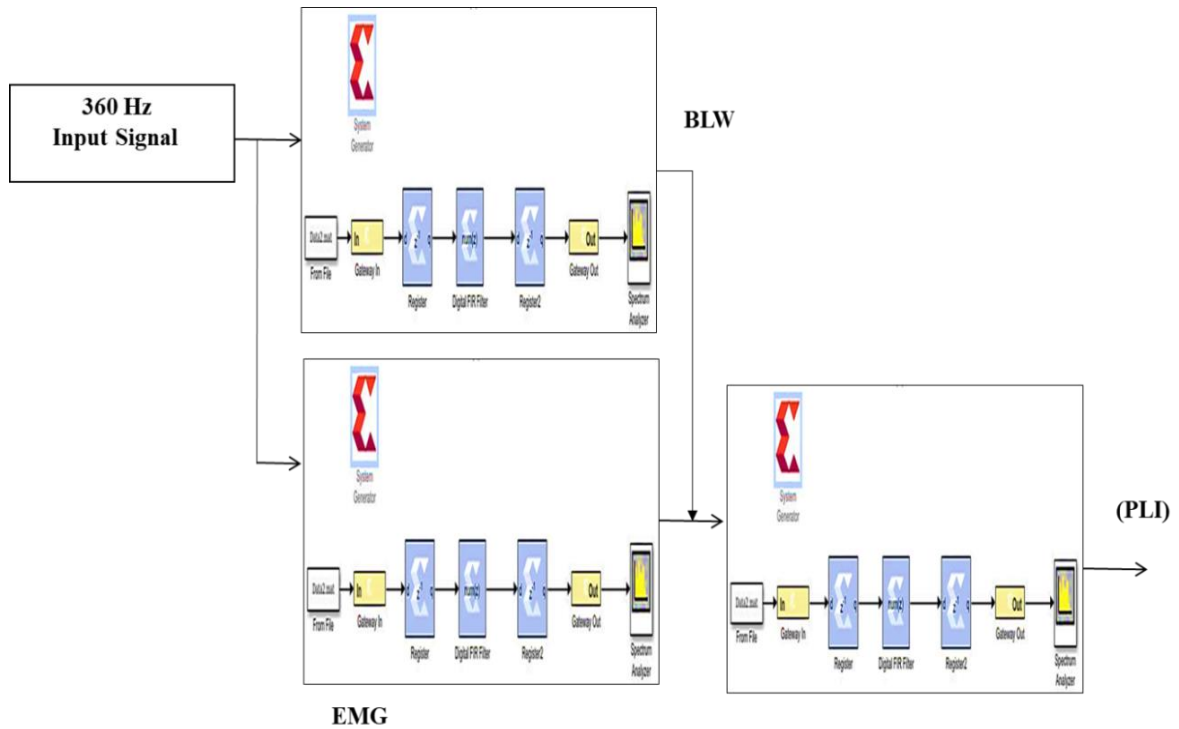
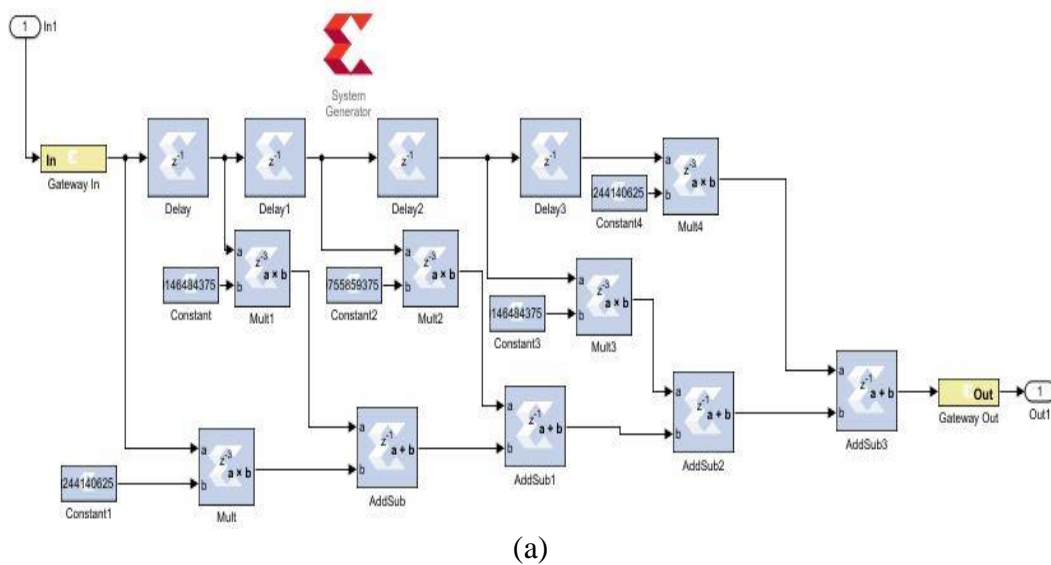
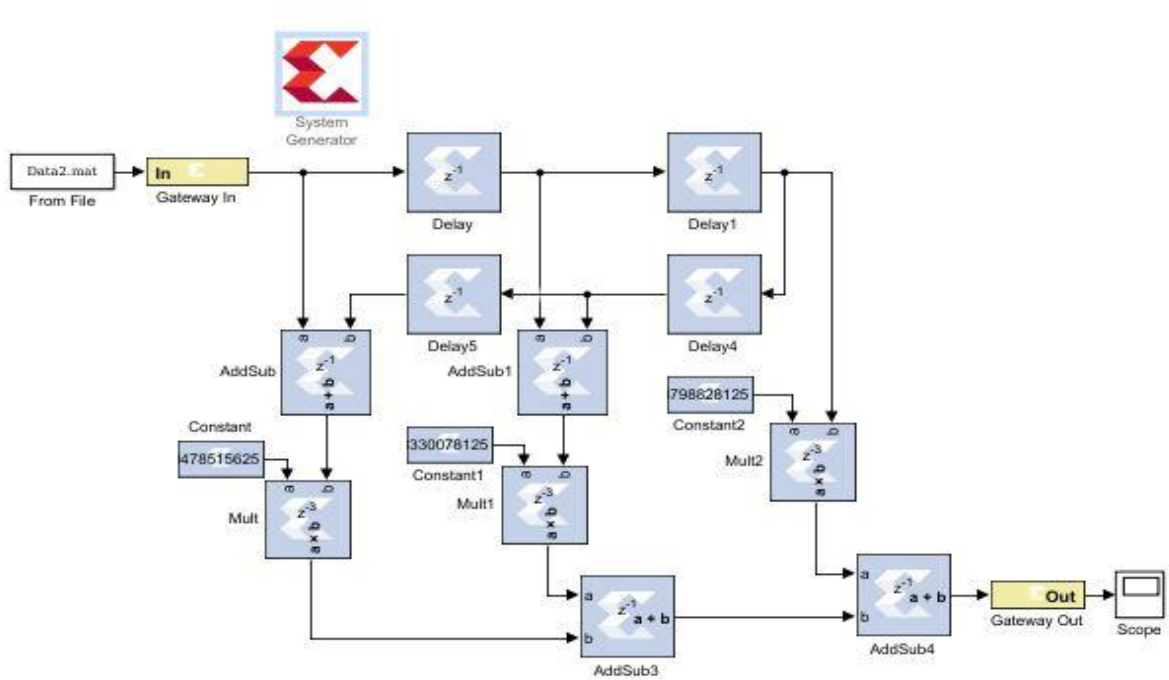


Figure 3.16: Proposed architecture for 3-tier architecture

The time-domain analysis comprises of Finite Impulse Response (FIR) filters consisting of various types of windowing techniques namely Kaiser, Bartlett, Blackmann, Hamming, Rectangular, Hanning, etc. [11]. In this article, analysis has been done by using window techniques. The basic elements of this 3-tier architecture for ECG denoising is comprising of adder, multiplier, and delay element. To observe the performance of the 3-tier architecture the authors have taken symmetric and anti-symmetric structures demonstrated in Figure 3.17.





(b)

Figure 3.17: Basic constituent of FIR window function (a) Anti-symmetric (b) Symmetric

It has been inferred that symmetric architecture has been utilized almost 50% fewer resources and consumes low power as compared to anti-symmetric architecture.

The online ECG database us already been corrupted with ECG noises. The Simulink platform from MATLAB software is utilized for the simulation. Figure 3.18 illustrates the scope block results of Simulink in which Fig. 3.18(a) illustrate Raw ECG signal, Fig. 3.18 (b) shows the elimination of the EMG using LPF. Fig. 3.18 (c) shows the outcome of HPF to eliminate BLW noise in raw ECG signal. Fig 3.18 (d) represents the outcome of BSF having ' f_c ' lies in between 49.5 Hz to 50.5 Hz.

For the successful simulation at the XSG level, the authors computed the resource utilization and power consumption. The consideration of behavioral simulation waveform and RTL schematic at various abstraction levels on XILINX VIVADO is taken. Figure 3.19 shows the RTL schematic of the ECG pre-processing module & it can be seen that the Simulink model is reproduced in the XILINX environment using the available core generator block.

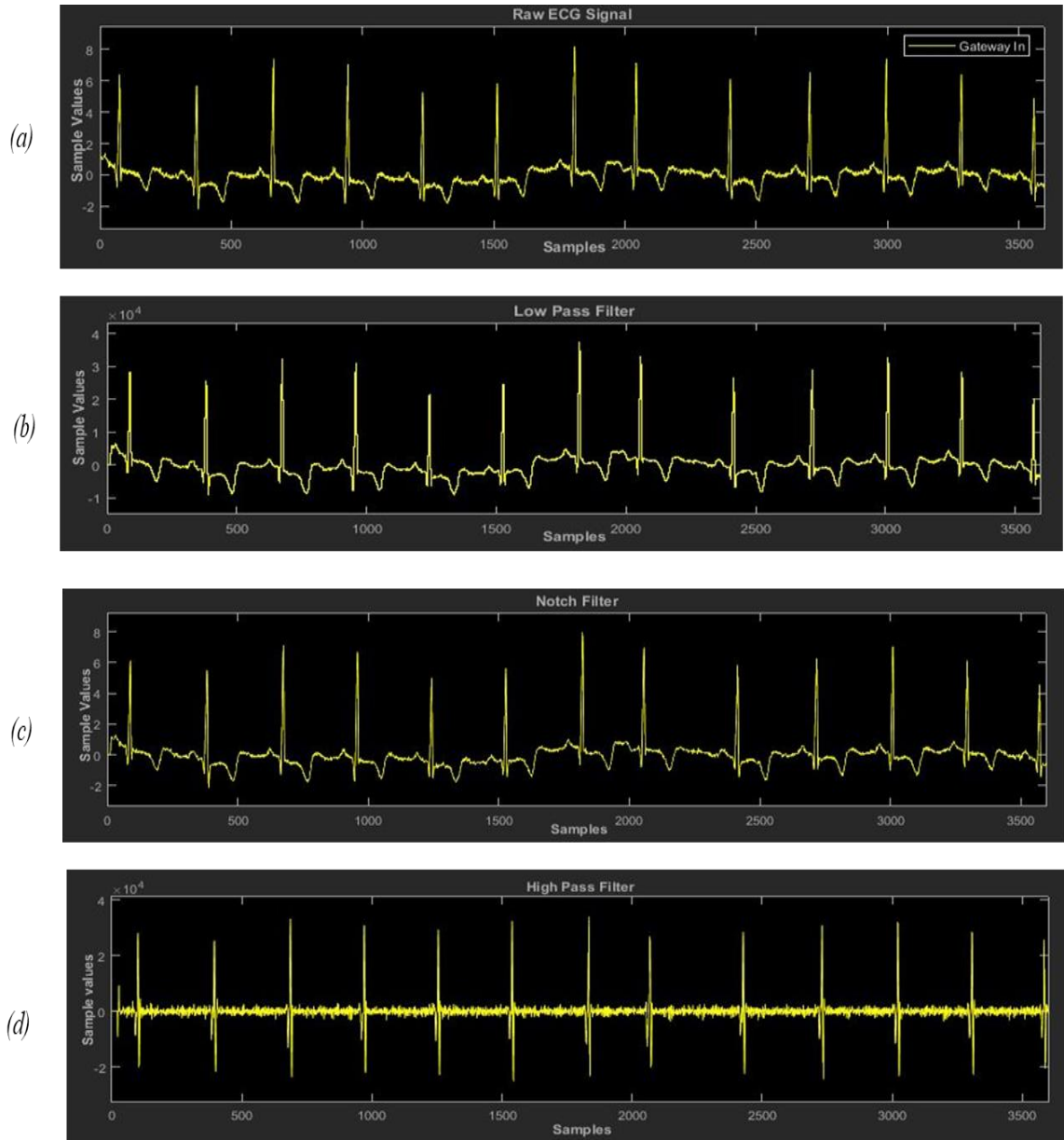


Figure 3.18: Scope view outcomes (a) Raw input ECG signal (b) Electromyography Noise Removal (c) Power Line Interference Removal (d) Base Line Wander Removal

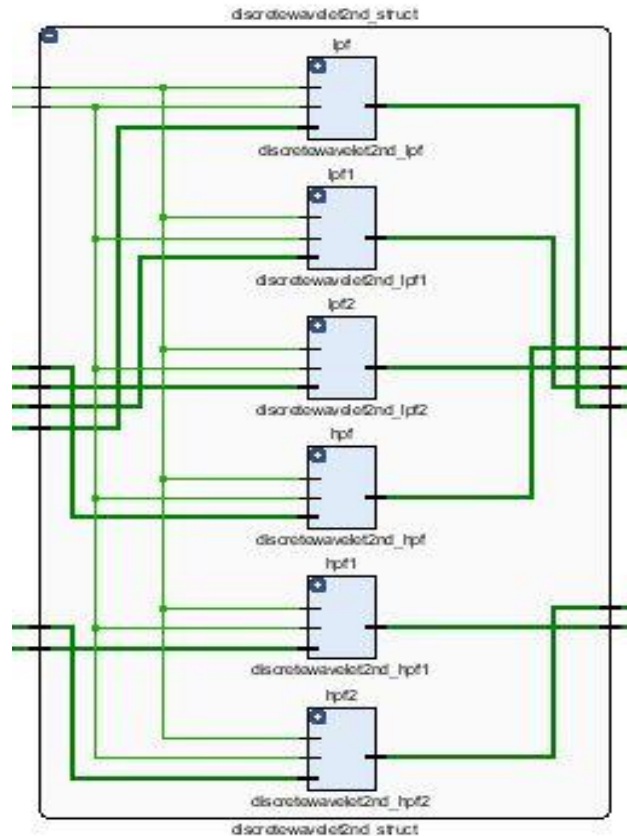


Figure 3.19: RTL schematic of proposed ECG denoising block 2

Table 3.2: Resource utilization and On-Chip power consumption of proposed 3-tier pre-processor design using window functions

Filter's architecture	Resource Utilization			On-chip power (mW)
	Slice LUT (53200)	Slice Registers (17400)	DSP (220)	
Proposed Symmetric Window	460	787	17	510
Kaiser	467	798	18	576
Bartlett	498	795	20	613
Blackmann	569	898	32	723
Hamming	653	919	33	624
Rectangular	781	948	45	667

Resource utilization and on-chip power for various window functions for symmetric and anti-symmetric design are computed based on LUTs, Slice registers, and DSP. It has been observed that symmetric design consumes fewer resources and power as compared to

anti-symmetric design. Among all the window functions proposed window performs better in terms of consumption of resources and power. For anti-symmetric design, the proposed window consumes only 2.33%, 13.2%, and 9.61% of LUT, register, & DSP respectively. It only consumes 384 mW of dynamic power and 110 mW of static power. The symmetric architecture of the proposed window utilizes 0.86%, 4.52%, 7.72% of LUTs, Slice register, and DSPs respectively. Also, it consumes only 354 mW of dynamic power to denoise the raw ECG signal. The implementation of the proposed architecture RTL schematic is transferred on Zedboard by using the VIVADO tool.

3.5 COMPARISON OF PROPOSED ARCHITECTURES WITH EXISTING LITERATURE

Table 3.3 tabulated the comparison of proposed ECG denoising modules with existing literature. The latest FPPA board i.e. Zedboard is aimed to calculate the resources and utilization of power for suggested modules. In the proposed architecture 1, two types of noises are eliminated using inbuilt Xilinx blocks of Simulink. It depletes only 0.61% of SLUTs (Slice Look Up Table), 4.005% of SRs (Slice Register), and 44.54% of DSPs and consuming only 151 mW of power to eliminate BLW and PLI noise. The elimination of all three ECG noises are done by proposing architecture 2; it consumes 0.86% of LUTs, 4.52% of slice registers, 7.72% of DSP at the expense of 510 mW of power. Comparison is done with recent year papers that denoise the ECG signal using XSG modeling and FPGA platform. It has been done based on the technique used, type of noise eliminated, FPGA board utilized as per these specifications resources, and power consumption is computed.

Table 3.3: Comparison of proposed architectures with recent literature

References	Filter design technique	Noises Removed	FPGA	Resource Utilization (%)			Power Consumption (mW)	Percentage Improvement
				LUT	Slice Register	DSP		
Proposed Architecture 1	Proposed	EMG, BLW	ZedBoard (Zynq-7000 AP SoC)	0.61	4.005	4.54	151	3.4 %
Proposed Architecture 2	Proposed	EMG, BLW, PLI	ZedBoard (Zynq-7000 AP SoC)	0.86	4.52	7.72	510	Selected
[132]	Least-square approximation	BLW	Zedboard (Zynq-7000 AP SoC)	0.46	0.44	7.58	142	6.3 %
[71]	Kaiser	EMG	Spartan 3E (XC3S500 e-4fg320)	1.19	1.67	7.32	167	7.13 %
[133]	Kaiser	PLI	Spartan 3E (XC3S500 e-4fg320)	2.1	2.4	9	194	8.2 %

In [132] QRS detection technique is suggested that utilizes the least-square denoising approach to eliminate BLW via Spartan-3A FPGA board. For the consideration of equal comparison, the authors have targeted ZedBoard. In [71] and [133] EMG & PLI noises are removed separately by employing the Kaiser Window using Spartan 3E FPGA board.

3.6 CONCLUSION

In this chapter, two XSG model architectures have been proposed for denoising module to remove the prominent high-frequency and low-frequency noises present in ECG. FIR filters are used to eliminate BLW, EMG, and PLI noises from the useful signal. To achieve the optimized results in terms of resource utilization and power consumption, various combinations of window filtering design (Kaiser, Bartlett, Blackmann, Hamming, Rectangular, and Hanning) for low pass and high pass filter is utilized. The authors have

also proposed second architecture to overcome the limitations of architecture 1. The proposed architectures are implemented on FPGA targeting Zynq- 7000 evaluation and development board. To justify the low power consumption and low resource utilization an exhaustive comparison has been done among diverse windows functions that comprise symmetric and anti-symmetric designs. Amongst them, the symmetric window function from architecture 2 is selected because it eliminates all three types of noises simultaneously to its high performance in terms of resource utilization and power consumption. Based on performance metric architecture 2 provides optimal results and it eliminates all types of ECG noises simultaneously. The proposed architecture finds minimum resources to remove ECG noises simultaneously but failed to lower the power consumption. The selected architecture is employed in the stationary ECG module in which power consumption is not an important criterion.

CHAPTER 4

FPGA BASED POWER EFFICIENT

WEARABLE ECG MODULE

CHAPTER 4

FPGA BASED POWER EFFICIENT WEARABLE ECG MODULE

4.1 INTRODUCTION

In the domain of natural philosophy industries, the principal theme that has emerged over a few years is low power. Dissipation of power has become a critical notion for the performance and space for VLSI Chip style. There are a couple of key challenges as well such as, decreasing consumption of power & its organization on-chip square, which come with shrinking technology [134]. To extend the battery life and cut back package price optimization of power is a critical requirement. In low power VLSI styles, running current & power organization are the key concerns. Integration refers to the interconnection of several electronic components such as transistors, diodes, resistors, etc., on a few square millimeters die produced from a silicon wafer. Interconnection of several electronic components in such a small area yields an Integrated Circuit (IC) which may then be used for a single application or several applications. In the contemporary era of electronic designing, various levels of integration processes are followed from time to time depending upon the number of transistors to be integrated to form an application circuit in IC form. VLSI is the process of fabricating several thousand to one million transistors inside a single IC. From the past two decades, advancements in VLSI expertise have led to the rapid advancement in ECG miniaturized application circuits embedded inside the VLSI IC for continuous monitoring [135]. Thus, miniaturization of the ECG module is the goal of electronic circuit designers in the contemporary era of the medical revolution.

Due to the recent advancements in medical device technology, there has been the birth of monitoring systems based on Programmable Logic Devices (PLDs). Field programmable gate arrays (FPGAs) in spite of being not very new to such devices have attained popularity in the area of rapid prototyping of designs in recent times especially with the assistance of software simulation and synthesis. The formats compatible with FPGA are different than the high-level language description, which is why the software synthesis tool is used to translate them into compatible modes. Cost-effectiveness has

become the price focus for using FPGA as several design changes become easier to do with the help of software synthesis rather than doing them on a hardware prototype. The use of FPGA's is well established and they are widely implemented in the transmission of data using high-speed digital systems for recovery, storage & processing the features. Some of the famous companies manufacturing FPGA in the world are Xilinx, Altera, Actel, and Quick logic. Hardware description languages include languages that are used to FPGA & CPLD based digital logic design by employing Verilog & VHDL. With the capability of the utilization of board space & system power, FPGA provides optimal device utilization, thus reducing the complexity of the system [131].

Considering the expected long life of these miniaturized ECG circuits and the needed compatibility with the other high speed and reliable equipment developed, there is a necessity for developing low power consumption circuit designs with reliable performance to be embedded inside the VLSI IC-based ECG module [137]. Moreover, because of its field-programmable nature, FPGAs are mostly preferred in the design and development of all the futuristic ECG applications so that any required modifications in the existing VLSI based design can easily be implemented in it. Large power consumption generates heat which has to be dissipated with the help of proper cooling techniques. The other factor for low power utilization module is battery life in handheld and portable ECG electronic devices are limited. It is very crucial to design a low dynamic power-consuming ECG denoising architecture. Eventually, these measures will result in prolonged operation time in handheld and portable ECG devices [138].

The design of the problem is already quite complex and designing it for low power adds another dimension to it, thus the existing design has to be optimized for power, performance, and area. The major issues and challenges concerning low power designs are as under:

- (a) Technology Scaling: In technology scaling, there are a few factors that get affected and create issues. They are:
- Supply Voltage reduces by 15%
 - Die size grows by 14% (Moore's Law)
 - Electrical nodes increase by 2X,

- Capacitance per node reduces by 30%
- Frequency Increases by 2X.

To meet these issues relatively there is an increase of active power by 2.7X.

- (b) Leakage power: The high leakage power arises due to counter the demand for power voltage. A low-voltage or low threshold system & circuit design method pursuing 1V supply voltage & utilized low thresholds.
- (c) Low power interconnections: By employing advanced technology, reduced swing & activity facilitate to achieve the low-power interconnects.
- (d) Development of power: It acquires a determined approach & tools for logic synthesis, behavioral synthesis & optimization of the layout.
- (e) Power saving methods: The power-efficient approach is utilized by recycling the energized using the adiabatic switching principle instead of heat dissipation. Also, by assuring some systems where power-speed trade-off occurs

The complete integration of ECG denoising architecture is fabricated on a single printed circuit board with other supporting chips, due to which the FPGA power relates to many aspects [139]. There are various sources of power related to various resources inside FPGAs for achieving high performance by maintaining noise immunity from the EMG, PLI, and BLW noises.

4.1.1 Types of Power Dissipation in FPGA

While designing a particular application, power constraints can be critical. It is a key concern nowadays due to the high demand for low power applications. High computational power is required by most of the new ECG portable applications, thus to have a satisfactory battery life with low-power. Power evaluation should be done early in the process to avoid violations in the power constraints and also to avoid expensive and complicated design changes later on. Power estimation may be utilized for precisely power

trade-off with various other parameters of system design namely performance, area, speed, etc. Incorporation of various techniques could be done to decrease the power utilization in the system [140]. Decreasing the supply-voltage is one of the major causes in the reduction of power dissipation, but at a higher level of design abstraction, various other techniques can also achieve considerable improvement in power dissipation. Parallelism & Pipelining are employed to optimize power at an architectural level, whereas approaches namely decreasing the number of operations executed to reduce the switching capacitances that eventually lead to power consumption. The total required power for each supply source depends on the three components of power [141].

(a) *Device Static Power* – The device static power is defined as the power required for a device to operate for programming. It depends mostly on manufacturing, applied voltage, process properties, and the device junction temperature. The junction temperature is dependent upon the ambient temperature, voltage level and total current supplied. The leak in the transistor holding the device configuration leads to a large portion of this power

(b) *Design Static Power* – Once the device has been configured and is in an idle state an additional power is withdrawn. This power is called design static power which includes static current from I/O terminations, clock managers, and other circuits.

(c) *Design Dynamic Power* - The additional power is withdrawn after the device has been configured and the activity is still going on. The dynamic power depends on voltage level and routing resources used and it changes with time as per the design activity.

4.1.2 Power Contributing Factors in FPGA

In the domain of natural philosophy industries, the principal theme that has emerged over a few years is low power. Dissipation of power has become a critical notion for the performance and space for VLSI Chip style [142]. The power contributing factors in FPGA consists of device power, design power, and environmental power. All these factors create a significant effect on the power consumption by the proposed architecture on FPGA.

(a) Device Power - It relates to the manufacturing and architectural parameters as shown in Figure 4.1. The manufacturing parameter relates to silicon and package technology whereas the architectural parameters relate to the structure, amount, functionality, layout, and routing between the resources inside the FPGA. These choices have a great impact on the static and dynamic power of the device [143].

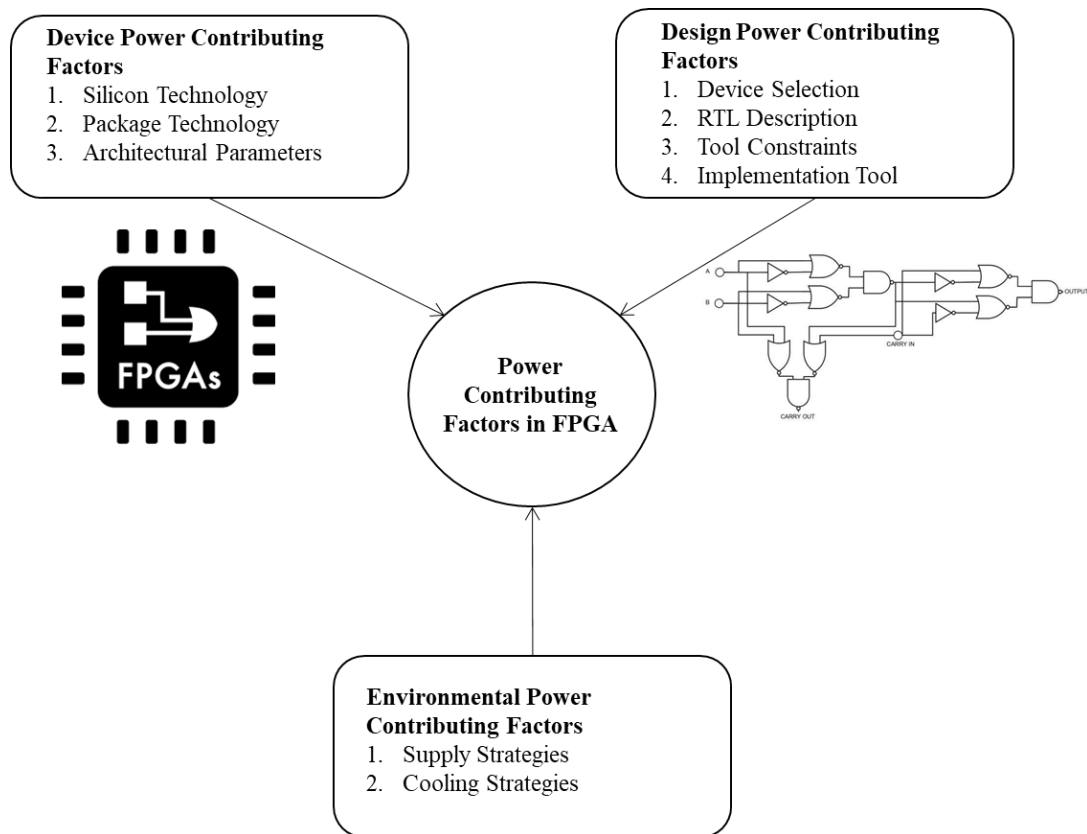


Figure 4.1: Power contributing Factors in FPGA

(b) *Design Power* - The factors related to the power of the design are device selection, RTL description, tool constraints, and implementation tool options. Device selection refers to the selection of the required device family, out of the varieties offered by different vendors. It helps in setting the static power, which is fixed for a particular device family. A good RTL description is to optimize the available resources in the underlying hardware. The knowledge of tool constraints helps in setting the optimization goal. There are various implementation options and algorithms available in the design flow for power [144].

(c) *Environmental Power* - This factor depends upon the supply and cooling strategies. The supply strategy balances the input and output voltage differences. In addition to this, different FPGA families have different voltage and current requirements. The selection of a lower voltage device reduces power. Placing the heat sink over the device and maintaining the ambient temperature, refers to the cooling strategy by transferring the generated heat to the environment by the mentioned process [9].

The low power consumption is another important design goal for the efficient implementation of wearable ECG denoising module. As the size of the battery clocks up more than 50% of the system volume, it leads to system miniaturization along with a prolonged lifetime. Our goal of this chapter is to design a power-efficient design for the ECG denoising module without sacrificing much performance or incurring a larger chip area on FPGA.

In this chapter, the authors are working on the hardware implementation of signal pre-processing techniques that includes the removal of the artifacts from the ECG signal through different types of filtering techniques. At the beginning of this research, the FPGA technology was very new, and it was therefore not well understood whether the analysis of FPGA implementation of ECGs could provide satisfactory clinical information [145]. To

provide clinical usable information from the raw ECGs by employing FPGA is a challenging task during the beginning years of the VLSI industry.

This apprehension was also related to denoise the ECG with minimum resource utilization and power consumption for wearable ECG modules. This research work verifies the design of the digital filter to denoise the bio-signal on FPGA and reduces the risk of misreading and complications during the study of the recorded ECGs. This research work proposed a methodology that aims to optimize the power in ECG denoising architecture.

4.2 PROPOSED METHODOLOGY

The noise reduction in biomedical signals is still a defying job & promptly growing in an area using several approaches for the reduction of noise. The complex QRS signal of it is considered to be very important. Low pass filtering is the most common method used for the removal of these noises. FPGA is used instead of a microcontroller, as it is a cost-effective & reconfigurability feature thus having a quick time to market. A methodology on FPGA-based digital filter design is proposed in this work.

The FPGA established digital filter implementation is superior to classical DSP chips as it has a higher sampling rate & cost-effective. Reduction of noise up to a satisfactory level is done by a digital filter in most cases. An emphasis has been laid down in this chapter by the authors on the hardware implementation of the ECG pre-processing stage and using FPGA to remove unwanted noises from the useful signal, thus helping the clinicians for an accurate diagnosis by utilizing minimum power.

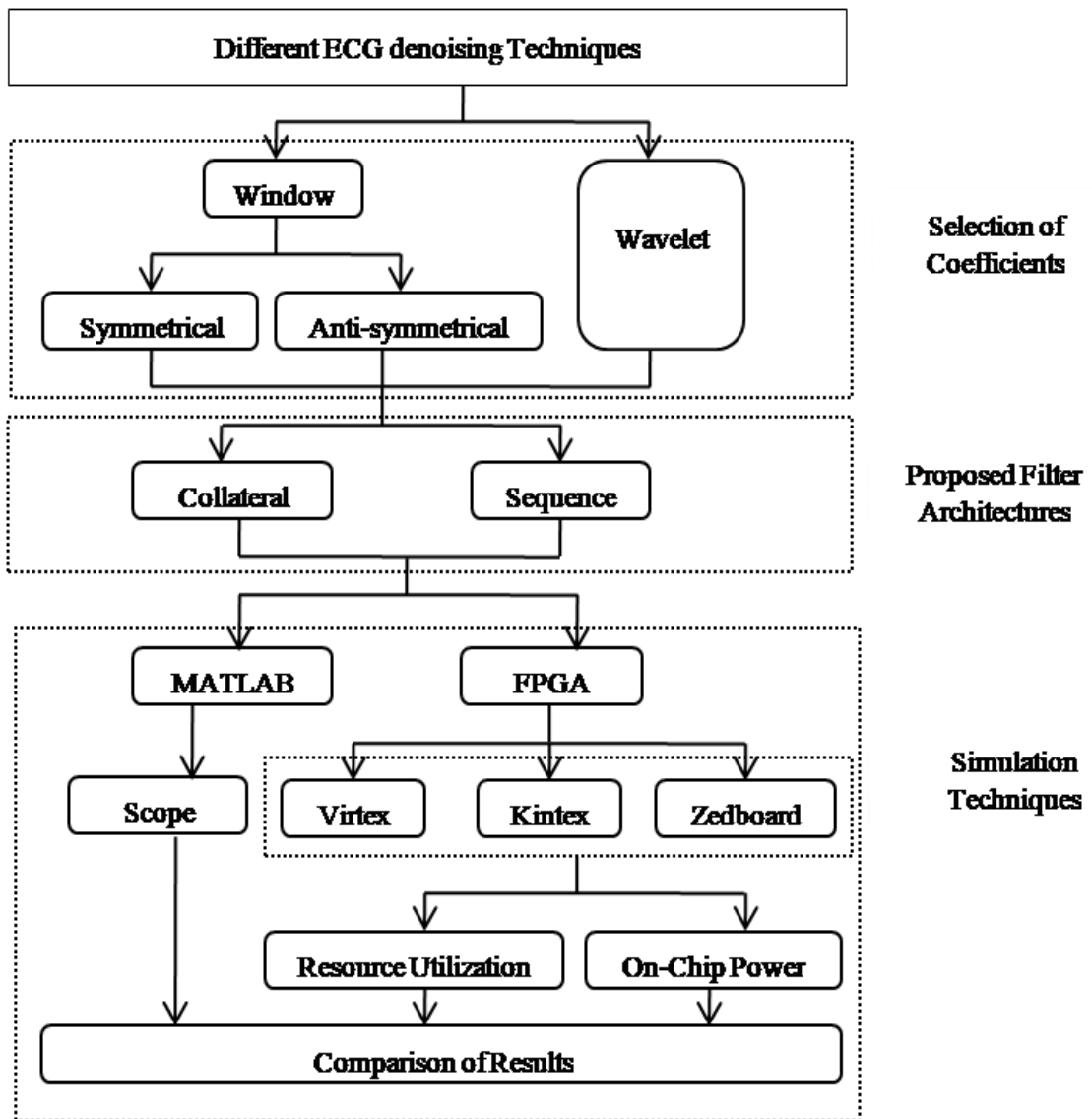


Figure 4.2: Proposed methodology for ECG denoising block

Figure 4.2 signifies the proposed methodology of the implementation of the ECG denoising block by employing different architectures and compare with different FPGA boards. Each signal is referenced from the MIT-BIH database by selecting the target database (MIT-BIH Arrhythmia Database (MITDB)). Pre-processing is done by employing linear function (window) and validated its results using non-linear filters (wavelet) to diminish these undesirable signals.

To perform the pre-processing step the authors have divided this phase into three parts: the selection of the coefficients, filter's architecture, and simulation techniques.

4.2.1 Collateral Architecture

The numbers of filter coefficients are computed based on various windows and wavelet functions. In this work, the authors have considered five types of the window. These functions incorporate Kaiser, Blackman, Bartlett, Hamming, and proposed window functions. The methodology also comprises Haar, Coiflet, Daubechies, and biorthogonal wavelet functions for the validation purpose [17] illustrated in *Appendix C*. The windows function employs the Fourier transform to denoise the ECG from unwanted signals present in the inforamatory signal. But, the Fourier transform only retrieves the global frequency content of a signal.

Figure 4.3 represents the collateral architecture that includes three types of filter particularly HPF, LPF, and notch filter to eliminate EMG, BLW, and PLI respectively. The core structure of the proposed architecture is composed of anti-symmetric and symmetric design. These architectures have utilized the windows coefficients to compute resource and power consumption.

The collateral architecture comprises three filters in a parallel form. The gateway is a Xilinx source block that takes the input from the database and is fed to the filter. The subsystem of the filter constitutes of core elements of filter (adder, multiplier, and delay) in a symmetric form in which proposed window coefficients are fed in the multiplier unit.

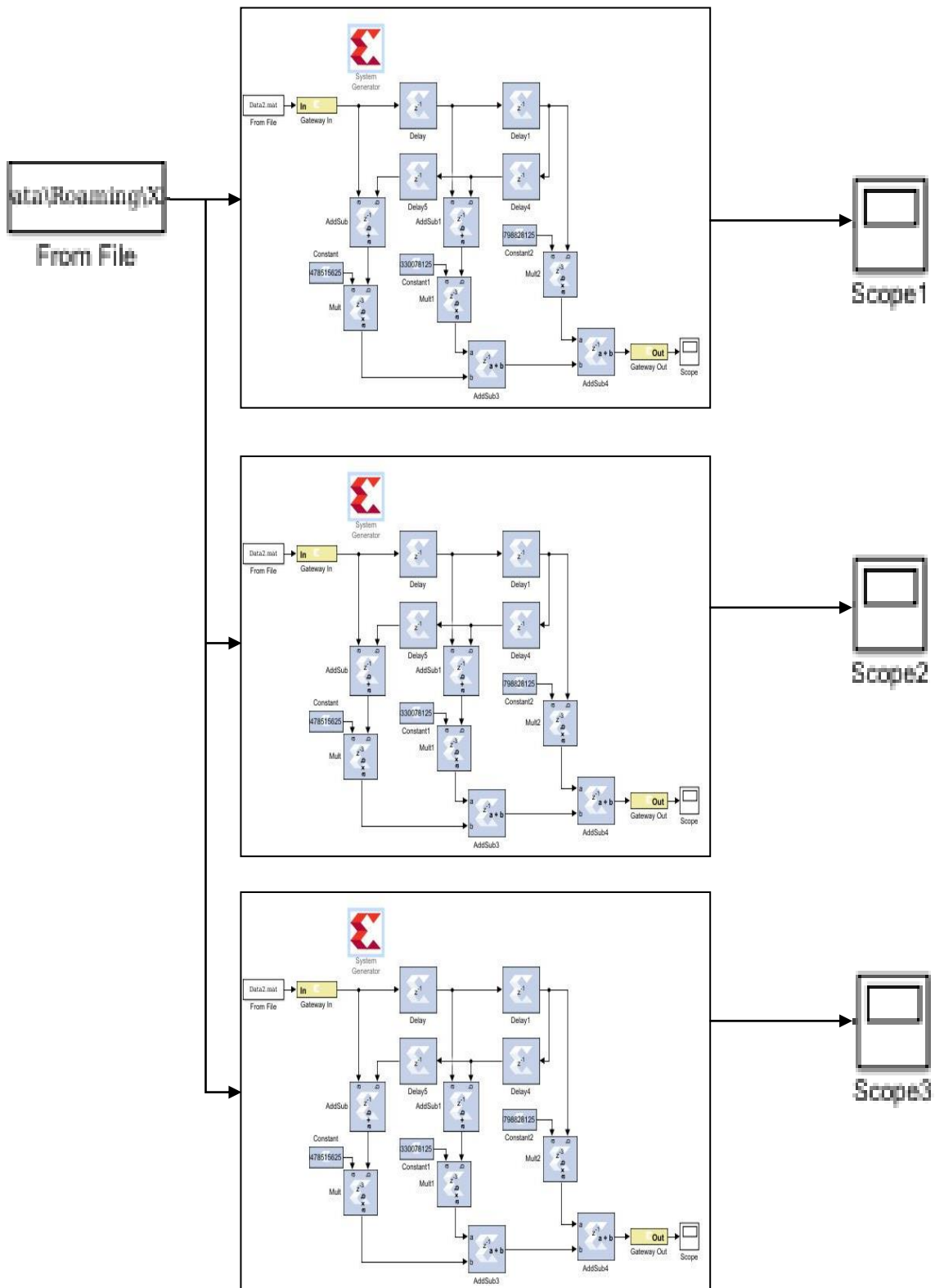


Figure 4.3: Collateral ECG Denoising block

4.2.2 Sequence Architecture

Figure 4.4 represents the sequence architecture that includes three types of filter particularly HPF, LPF and notch filter to eliminate EMG, BLW, and PLI respectively. The core structure of the proposed architecture is composed of anti-symmetric and symmetric design. These architectures have utilized the windows coefficients to compute resource and power consumption. The sequence architecture joins the filters in a serial form to remove the ECG noises simultaneously. ECG database fed through the gateway in source block to the digital filters that help to scrap the unwanted signal from the useful ECG signal. The filtered signal fed to the Xilinx sink block then supplied to VIVADO tool.

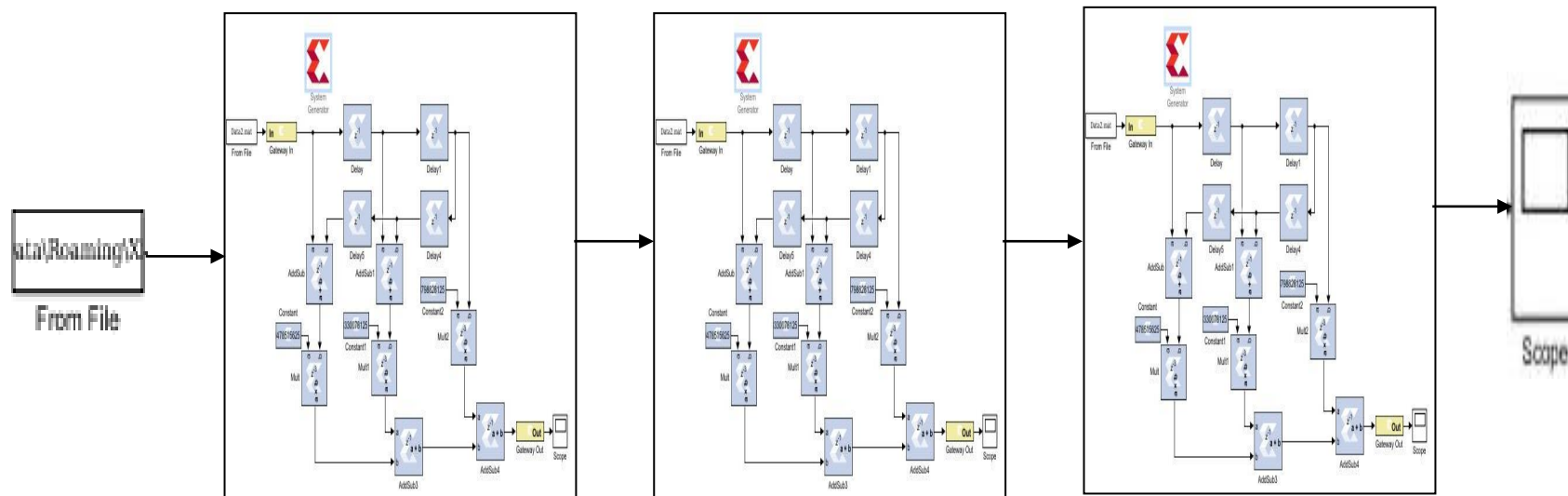


Figure 4.4: Sequence ECG Denoising block

Simulation Techniques

As the complexity of the system increases, the reliability of the system decreases and the hardware platform generally does not guarantee the reliability determined in the meantime between failures (MTBF) calculations. System reliability is largely determined by the level of hardware and software architecture, development and certification processes, and design management. Currently, the main reason many engineers choose FPGAs over DSPs is the need for MIPS (millions of references per second) with the inherent benefits of reliability and stability. MATLAB and VIVADO tool has been used to conduct the simulation of the proposed architecture. Three FPGA boards namely Virtex, Kintex, and Zynq-7000 have been targeted for effective selection as shown in Figure 4.5.

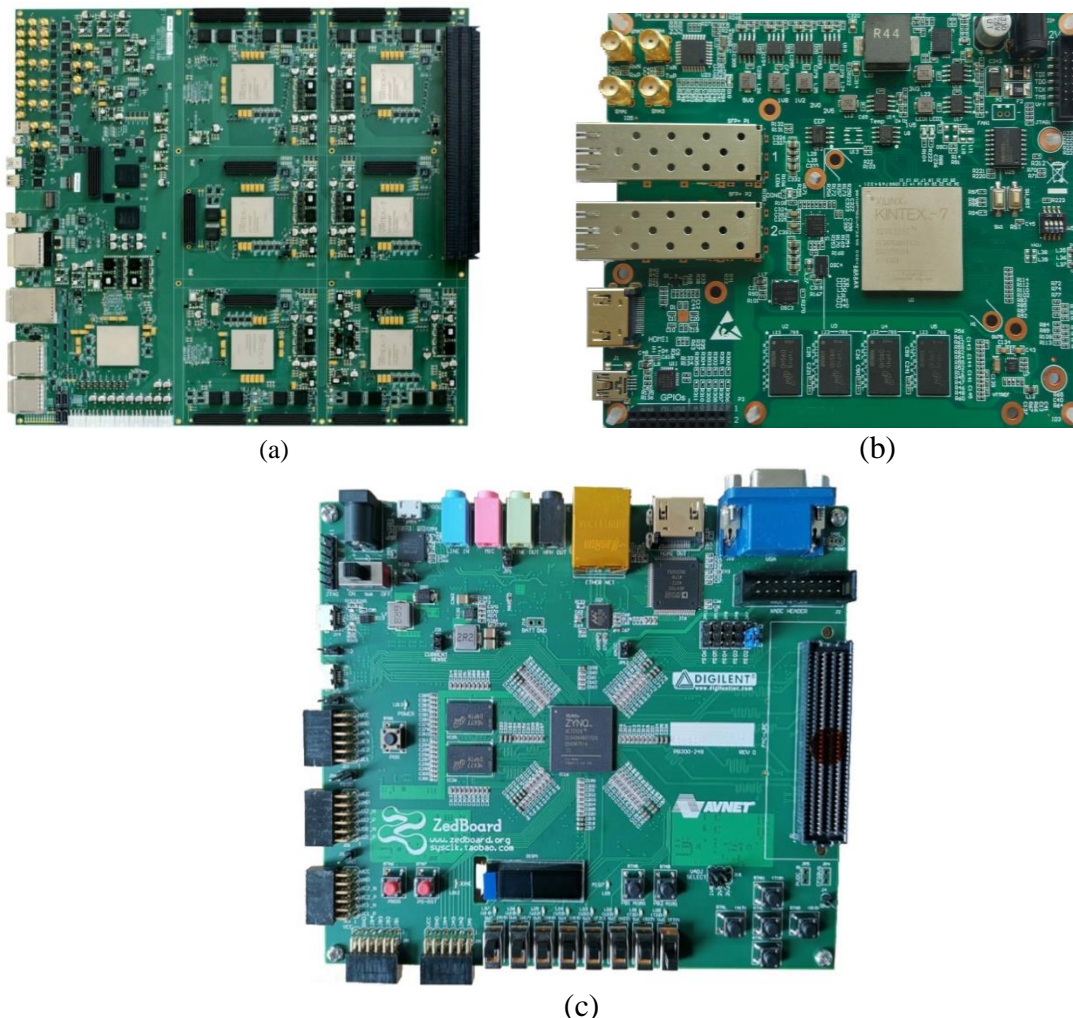


Figure 4.5: FPGA Board(a) Virtex (b) Kintex(c) Zedboard

The Zynq-7000 is essentially a Kintex FPGAs plus the ARM cores. There is no use of ARM cores for small applications; in this case, Kintex board is preferable. The Virtex

board has larger technology as compared to Kintex. When the size is not an important constraint for an application then the Virtex board is utilized. The Zynq®-7000 family is based on the Xilinx SoC architecture having 28 nm Xilinx programmable logic (PL) in a single device. In addition to this PL, it also comprises on-chip memory, external memory, and a rich set of peripheral connectivity interfaces. It yields the minimum on-chip power and uses less resource elements. Xilinx Zynq-7000 programmable SoC (AP SoC) uses ZedBoard, a low-cost development board in comparison with the other two boards. Several extension connectors highlight program logic I/Os and processing systems for easy user access. Zedboard can be used in Linux / Android / RTOS development, General Zynq-7000 SoC prototype video processing, software acceleration, and embedded ARM processing. Designs are captured using the Xilinx specific block set in a DSP-friendly Simulink modeling environment. The Xilinx Simulink Blockset has DSP functions and algorithms and is a highly parameterized library. The Xilinx DSP Blockset for Simulink includes 90 DSP building blocks. These blocks incorporate basic DSP building blocks namely adders, registers & multipliers. These blocks affect the Xilinx IP Core Generator to provide the optimized results for the chosen device. The results obtained from the designed denoising architectures are shown in the next section. The findings are computed in terms of slice LUT, Slice register, DSP, and on-chip power. The comparison has also been made with existing literature and percentage improvement is computed.

4.3 RESULTS AND DISCUSSION

The hardware of digital circuits requires execution because it speeds up the execution from several hours to minutes to seconds. To attain high speed & execution the emphasis should be on hardware implementation. Due to the limited number of logic components & frequency are available. The implementation of a signal processing system on hardware generally ASIC or FPGA are employed. The cost-effectiveness plays a vital role in the extensive employment of FPGA; as it significantly decreases the cost of blocks in comparison to ASIC. FPGA is a better choice instead of ASIC for embedded systems; it is an effective technology for real-time applications. The proposed work deals with two types of software tools: MATLAB and VIVADO. To obtain the resource utilization and power consumption on different FPGA Boards, the authors have employed the VIVADO tool

from XILINX software. The selection of an appropriate tool for hardware designing is a very crucial step as it affects the development time, power consumption, and cost of the research work. Initially, Hardware Description Language (HDL), such as Verilog VHDL as structural or behavioral specifications is targeted for the hardware netlist generation for an FPGA. From the past few years, the focus has been shifted towards higher-level languages than traditional HDLs. Various systems assist in the design, modeling, and simulation of the system. However, all of these systems are still under development and have their limitations. XSG is a DSP design tool from Xilinx that enables Simulink to use the MathWorks model-based design environment for FPGA design [17–18].

The design and implementation of DSP FPGA are done on a distributed system integration platform by XSG which also allows RTL, Simulink, and MATLAB components to club together in a single simulation & execution environment. Window functions are commonly used for digital filter design such as the Finite duration unit pulse response (FIR) filter. The FIR filter design is popularly used nowadays for the measurement and noiseless ECG signal [6]. These filters are utilized to remove the noisy signal from the valuable biomedical signal and its consequence is observed on the input signal that can be defined in the time domain. But, only the time domain technique of ECG signal analysis is not enough to study all the prominent features. Therefore, the filters are also designed in the frequency domain to illustrate the signal in terms of frequency [3]. Zynq-7000 family is chosen for XSG flow & Verilog HDL language is utilized for the netlist generation.

4.3.1 Collateral ECG Denoising Architecture

The whole analysis is performed post-synthesis through which resource utilization and power consumption are calculated. Table 4.1 signifies the utilization of basic units (Slice LUT, Slice register, DSP) for proposed collateral architectures of ECG denoising block using window functions. It also incorporates the anti-symmetric and symmetric architectures for windows function architectures of the core structure. For simulation, the authors have considered three types of FPGA board: Virtex, Kintex, and Zedboard and compared their resource utilization and on-chip power for the proposed architectures.

Table 4.1: Resource & power utilization of Collateral denoising block

Filter Architecture	Selection of Coefficients		Virtex Board				Kintex Board				Zedboard			
			Resource Utilization			On-Chip Power (W)	Resource Utilization			On-Chip Power (W)	Resource Utilization			On-Chip Power (W)
			Slice LUT	Slice Registers	DSP	Total	Slice LUT	Slice Registers	DSP	Total	Slice LUT	Slice Register	DSP	Total
Collateral	Anti-symmetric	Proposed	621	1149	30	2.076	621	1149	30	0.774	621	1149	30	0.142
		Kaiser	621	1149	30	2.079	621	1149	30	0.776	621	1149	30	0.310
		Bartlett	621	1149	30	2.074	621	1149	30	0.772	621	1149	30	0.149
		Blackmann	621	1149	30	2.066	621	1149	30	0.761	621	1149	30	0.292
		Hamming	621	1149	30	2.075	621	1149	30	0.772	621	1149	30	0.307
	Symmetric	Proposed	462	894	18	2.071	462	894	18	0.772	462	894	18	0.140
		Kaiser	462	894	18	2.073	462	894	18	0.763	462	894	18	0.299
		Bartlett	462	894	18	2.071	462	894	18	0.772	462	894	18	0.142
		Blackmann	462	894	18	2.060	462	894	18	0.770	462	894	18	0.288
		Hamming	462	894	18	2.070	462	894	18	0.761	462	894	18	0.296

4.3.2 Sequence ECG Denoising Architecture

The whole analysis is performed post-synthesis through which resource utilization and power consumption are calculated. Table 4.1 signifies the utilization of basic units (Slice LUT, Slice register, DSP) for proposed sequence architectures of ECG denoising block using window functions. It also incorporates the anti-symmetric and symmetric for windows function architectures of the core structure. For simulation, the authors have considered three types of FPGA board: Virtex, Kintex, and Zedboard and compared their resource utilization and on-chip power for the proposed architectures

Table 4.2: Resource & power utilization of Sequence denoising

Filter Architecture	Selection of Coefficients		Virtex Board				Kintex Board				Zedboard			
			Resource Utilization			On-Chip Power (W)	Resource Utilization			On-Chip Power (W)	Resource Utilization			On-Chip Power (W)
			Slice LUT	Slice Registers	DSP	Total	Slice LUT	Slice Registers	DSP	Total	Slice LUT	Slice Register	DSP	Total
Sequence	Anti-symmetric	Proposed	621	1149	30	2.074	621	1149	30	0.772	621	1149	30	0.140
		Kaiser	621	1149	30	2.076	621	1149	30	0.774	621	1149	30	0.299
		Bartlett	621	1149	30	2.075	621	1149	30	0.773	621	1149	30	0.142
		Blackmann	621	1149	30	2.066	621	1149	30	0.761	621	1149	30	0.292
		Hamming	621	1149	30	2.075	621	1149	30	0.772	621	1149	30	0.307
	Symmetric	Proposed	462	894	18	2.074	462	894	18	0.770	462	894	18	0.138
		Kaiser	462	894	18	2.067	462	894	18	0.762	462	894	18	0.289
		Bartlett	462	894	18	2.076	462	894	18	0.772	462	894	18	0.140
		Blackmann	462	894	18	2.072	462	894	18	0.758	462	894	18	0.281
		Hamming	462	894	18	2.060	462	894	18	0.769	462	894	18	0.295

The three different boards are used for the simulations on the proposed architectures using windows (anti-symmetrical & symmetrical) techniques. The proposed methodology performance is evaluated based on resource utilization and on-chip power consumption. The inference from Table 4.1 has been drawn that our proposed Collateral architecture yields minimum on-chip power 0.142W and 0.140 W when using anti-symmetric and symmetric window technique for the proposed window function. The symmetric design of collateral architecture used 462 LUTs, 894 slice registers, and only 18 DSPs on targeting the Zynq-7000 board.

Table 4.2 tabulated that the sequence architecture has consumed the same number of resources as collateral on the expense of 0.140 W and 0.138 W power consumption by anti-symmetric and symmetric design respectively on Zed board. Figure 4.5 represents the RTL schematic of the selected symmetric design of sequence architecture.

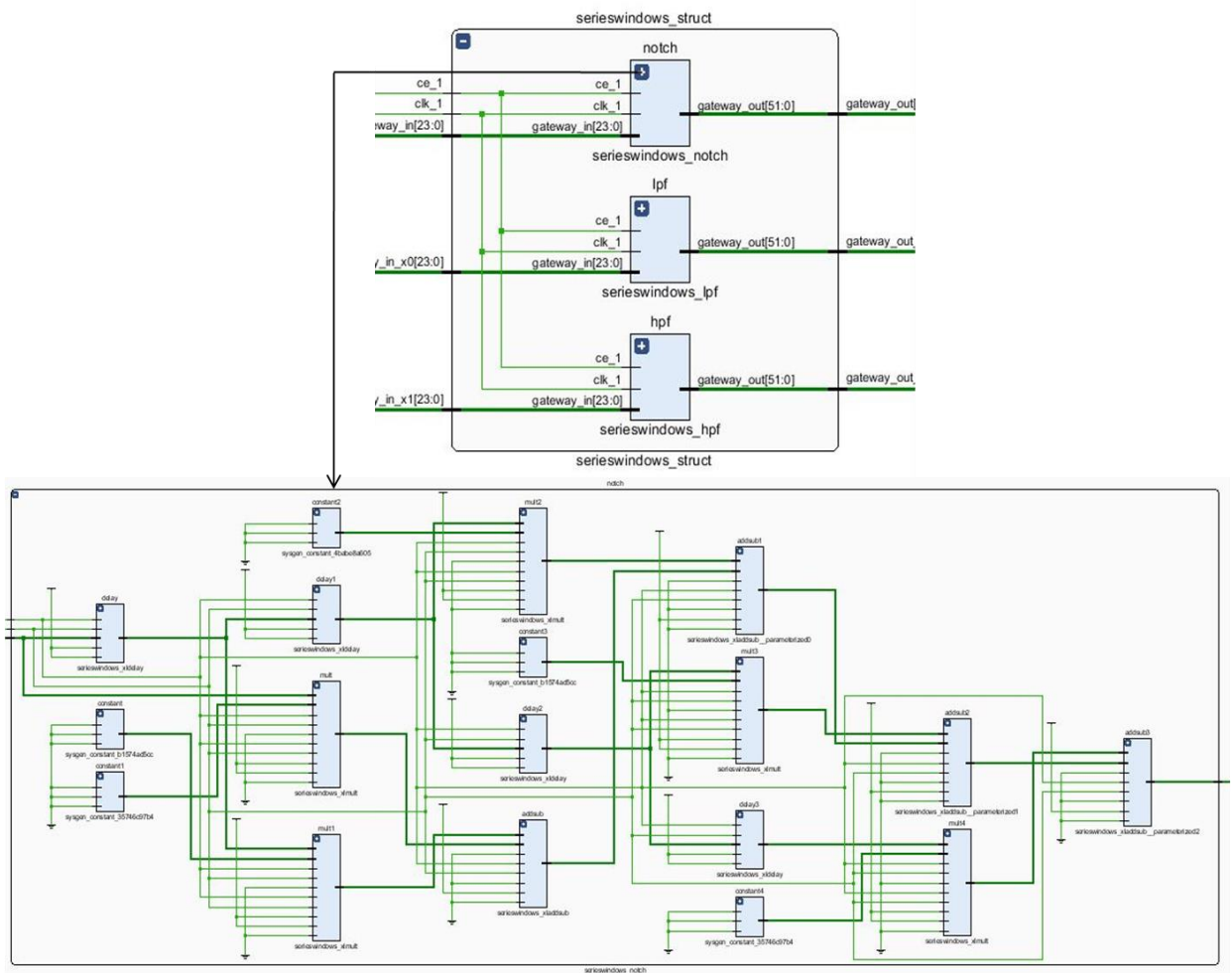


Figure 4.6: RTL schematic of ECG denoising block and its core structure

Figure 4.6 illustrates the ECG denoising block having three digital filters: HPF, LPF, and Notch for the elimination of unwanted signals present in the ECG. It also signifies the inclusion of basic components (adder, multiplier, and delay) for the designing of these digital filters for its core structure. The authors have also validated the proposed architectures with the popular technique of wavelet transform.

4.4 VALIDATION OF RESULTS

The wavelet transition is very popular in the field of signal processing. It can provide time and frequency information in parallel, consequently resulting in the signal time-frequency representation [146]. Spectral information about the signal is provided by the Conventional Fourier Transform. In addition to this, it only works for static signals. The codes may be inconsistent in many real-world applications. Wavelet Transform is used for the processing of non-stationary signals. Real-time signal processing is which is done by Wavelet Transform is gaining a lot of traction these days. This has to lead to an increase in the requirement for an effective structure to implement the wavelet transitions. In the wake of increasing requests and technology for portable ECG equipment and its real-time applications, it demands the system to be created with low power dissipation & high-speed output. In this research, the proposed structure for discrete wavelet transform filter is designed that is realized using FPGA tools. Resource consumption and power consumption are the design criteria used for each architecture that are researched so that an appropriate structure can be selected basis application requirements [147].

The non-static signal for analysis and processing is done by the due to its wavelet transition characteristics. Due to the growing number of different sectors, it is necessary to explore the hardware implementation options of the Discrete Wavelet Transform (DWT) [148]. Wavelet Transform is a time-domain function that has been used for many years for various applications, but most applications are linked to signal compression. Wavelets are recently been employed to solve complications in ECG signals such as data compression, detection of QRS complex. It simply works to separate the constituents of the signal into

different levels based on their frequency and analyze each level with a reasonable solution. Therefore, the wavelet transform uses a low time interval to analyze high-frequency variables and long-term intervals to analyze low-frequency variables. The wavelet transform has the benefit of separating the signal into different resolutions related to detecting the characteristic point from a non-stationary signal such as an ECG. The DWT function is expressed by Eq. (4.1)

$$W_{\psi}(j, k) = \frac{1}{\sqrt{m}} \sum x(n) \psi_{j,k}(n) \quad (4.1)$$

where $x(n)$ = input signal, $1/\sqrt{m}$ is a normalizing term, m is the number of samples in the sequence and n is integer = 0, 1, 2,..... $m-1$. Discrete wavelet transform is computed by passing the input signal to a chain of LPF (L) and HPF (H) as per the decomposition arrangement invented by Mallat. In each decomposition level, the LPF & HPF and high-pass filters are immediately followed by a down-sampling operator having operation as $(X \downarrow 2)[n] = X[2n]$, decreasing the rate of sampling by a factor of 2. To achieve these requirements, power consumption, area, throughput, etc, should be taken to create an efficient design. Power consumption and application size are some of the most crucial problems for making an efficient design. Therefore, all these factors should be taken into consideration while designing.

In this thesis, FPGAs are used to run DWT's hardware. The FPGA application has a specific integrated circuit (ASIC) features with a reusable utility. The ASIC has interconnects which are programmed to fit a specific application. These interconnect consist of a series of logic cells and routing channels. Due to the increasing demand for DSP based applications, the FPGA-based ASIC market is expanding rapidly. The general-purpose DSP processors have good arithmetic capabilities compared to FPGA, and it makes the FPGA implementation challenges. Nevertheless, the reproducibility of FPGA is the most important advantage which makes it a viable option over others. In traditional ASIC models, any addition or editing is cost-intensive, whereas in FPGA these could be done at no extra cost.

Table 4.3 tabulated the utilization of the resources and power by the proposed architectures. It represents that the sequence architecture using the Haar wavelet consumes minimum resources and power. The Haar wavelet used 309 LUT, 597 Registers, and 18 DSP by targeting Zedboard.

Table 4.3: Validation of results by employing wavelet transform

Filter Architecture	Selection of Coefficients		Virtex Board				Kintex Board				Zedboard			
			Resource Utilization			On-Chip Power (W)	Resource Utilization			On-Chip Power (W)	Resource Utilization			On-Chip Power (W)
			Slice LUT	Slice Register	DSP	Total	Slice LUT	Slice Register	DSP	Total	Slice LUT	Slice Register	DSP	Total
Collateral	Wavelet	Haar	309	597	18	2.041	309	597	18	0.728	309	597	18	0.262
		Daubechies	729	1337	34	2.082	729	1337	34	0.781	729	1337	34	0.316
		Coiflets	729	1337	34	2.079	729	1337	34	0.777	729	1337	34	0.313
		Biorthogonal	729	1337	34	2.073	729	1337	34	0.770	729	1337	34	0.301
Sequence		Haar	309	597	18	2.041	309	597	18	0.729	309	597	18	0.260
		Daubechies	729	1337	34	2.082	729	1337	34	0.785	729	1337	34	0.312
		Coiflets	729	1337	34	2.086	729	1337	34	0.779	729	1337	34	0.310
		Biorthogonal	729	1337	34	2.090	729	1337	34	0.781	729	1337	34	0.307

The Haar wavelet function consumes 33% fewer resources are compared proposed window function but in terms of power utilization the selected Haar wavelet consumes 122 mW more power than the selected window function.

4.5 COMPARISON OF PROPOSED ARCHITECTURES WITH EXISTING LITERATURE

The collateral and sequence ECG denoising architecture has been proposed by the authors to diminish all the ECG noises simultaneously. These architectures assure to consume the low resources and power; which is favorable to the wearable ECG devices. Table 4.4 tabulated the comparison of proposed ECG denoising modules with existing literature. The three FPGA boards (Virtex, Kintex, and Zedboard) are directed to calculate the resources & power utilization for the presented modules. The symmetric sequence architecture has been chosen due to low resource utilization and power consumption. It

utilizes only 0.86% of LUTs, 11.7% of registers, and 8.18% of DSPs. It consumes only 138 mW of power and attains 28.86% improvement in comparison to the recent literature.

Table 4.4: Comparison of Proposed architecture with recent literature

References	Filter design technique	Noises Removed	FPGA	Resource Utilization (%)			Power Consumption (mW)	Percentage Improvement
				LUT	Slice Register	I/O Block		
Proposed Architecture	Proposed Technique	EMG, BLW,PLI	ZedBoard (Zynq-7000 AP SoC)	0.86	0.514	8.18	138	Selected
[132]	Least-square approximation	BLW	Zedboard (Zynq-7000 AP SoC)	0.46	0.44	7.58	142	2.81%
[71]	Kaiser	EMG	Spartan 3E (XC3S500e-4fg320)	1.19	1.67	7.32	167	17.36 %
[133]	Kaiser	PLI	Spartan 3E (XC3S500e-4fg320)	2.1	2.4	9	194	28.86 %

4.6 CONCLUSION

The work in this thesis describes a consistent & efficient methodology for ECG denoising by utilizing different windowing and wavelet functions. The benefits of windows function and its ability to acquire useful information from the signal have been in focus in this research. To implement the ECG denoising block on hardware is a challenging task to attain low resource capacity and power consumption. In this chapter, to acquire the useful ECG signal from the noisy signal validation of the results is done by employing DWT-based denoising using five wavelet functions (haar, daubechies, coiflet, symlet and biorthogonal). The morphology of the ECG waveform did not alter in all the five wavelets. The hardware implementation of the proposed block is not done on DSP and MCU, but FPGA. The proposed collateral and sequence methods were implemented using windows and wavelet techniques are simulated on FPGA. Among collateral and sequence architecture; sequence architecture provides better results as it acquires only 462 Slice LUTs, 894 Slice registers, and only 18 DSP for proposed window function. Only 0.138W of on-chip power is consumed in the proposed architecture. The execution speed &

utilization represents the capability to perform the transform employing the proposed methodology. For the proposed ECG denoising block the result leads to conclude only 0.86% of LUTs, 5.13% of registers and 8.18% of DSP is the resource consumption & 138mW is on-chip power is consumed by Zedboard; which is less as compared to Virtex and Kintex FPGA board [149].

Figure 4.7 represents an expert system for ECG denoising block for the removal of ECG noises simultaneously. The 2-tier and 3-tier architectures have been purposed to remove ECG noises simultaneously by utilizing minimum resources. These architectures are used in the stationary ECG modules where power consumption is not an important criterion.

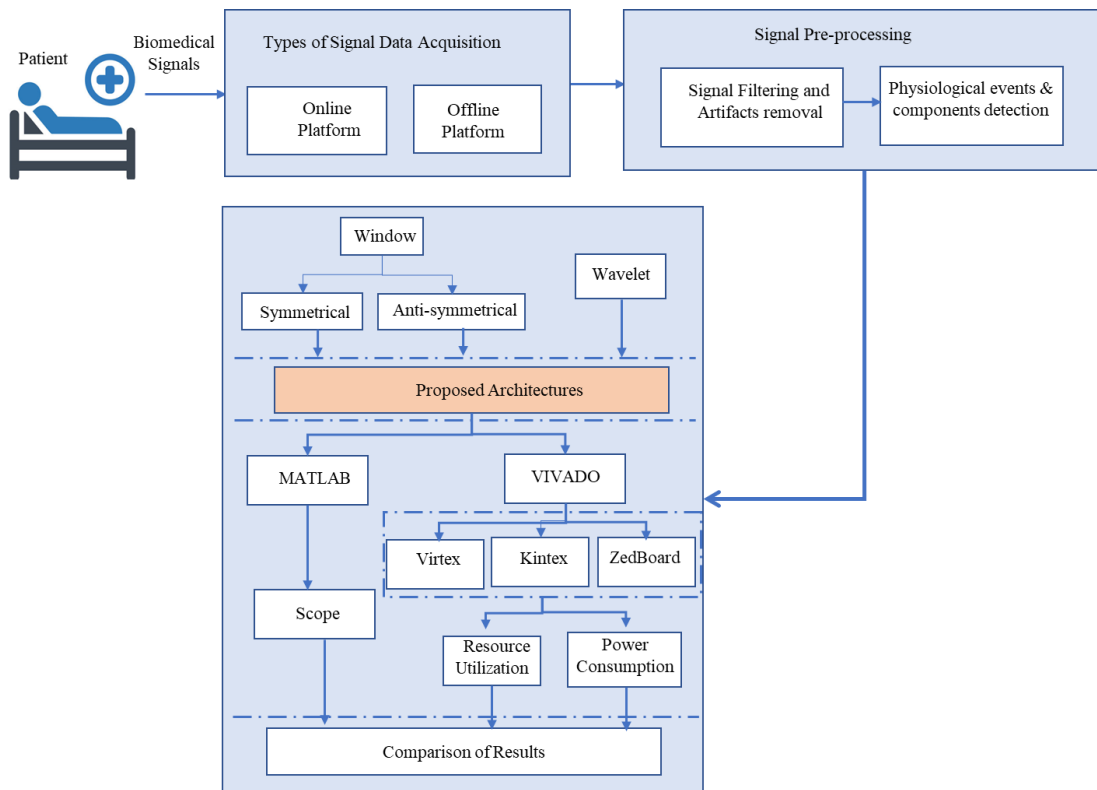


Figure 4.7: An Expert system for ECG denoising block

To attain low power criterion collateral and sequence architectures have been proposed. To research the next level sequence architecture has been selected because it consumes minimum resources along with minimum power consumption. The sequence architecture is very useful for the wearable and portable ECG module. This architecture helps to design an overall expert system for the classification of several CVDs.

CHAPTER 5
MULTISTAGE HEART RATE
VARIABILITY CLASSIFICATION
SYSTEM

CHAPTER 5

MULTISTAGE HEART RATE VARIABILITY CLASSIFICATION SYSTEM

5.1 INTRODUCTION

The nervous system directs all body functions and allows a person to adapt to any internal or external stimuli, like circadian changes, exercise, and emotions. It is composed of two core divisions: the peripheral & central nervous system (NS). The central NS comprises the brain & spinal cord although the peripheral NS consists of the autonomic nervous system (ANS), the cranial nerves, and spinal nerves. The vast ANS innervates all internal organs and carries messages from the brain and neuroendocrine regulatory center to the organs. The parasympathetic nervous system (PNS) & sympathetic nervous system (SNS) are the two core parts of ANS. The SNS exits the spinal cord and enters the small ganglia near the cord to form a chain that spreads the nervous impulse to the post-ganglionic neurons, which reach the organs and glands. The generalized physiological response of the SNS is commonly known as “fight and flight”, which is contrary to the PNS that controls the body’s “rest and digest” functions.

The SNS and PNS work together with specialized heart nerves and fibers, to propagate electrical impulses throughout the heart’s muscle cell networks, which participate in cardiac function control. At rest, the PNS controls the heart by slowing heartbeats through branches of the vagus nerve. In times of stress or activity, the SNS stimulates the heart’s nerves and fibers to stimulate conduction and make the ventricles

contract more forcefully; thereby increasing heartbeats [91]. A schematic representation of the electrical pathway from the nervous system to the heart is shown in Figure 5.1.

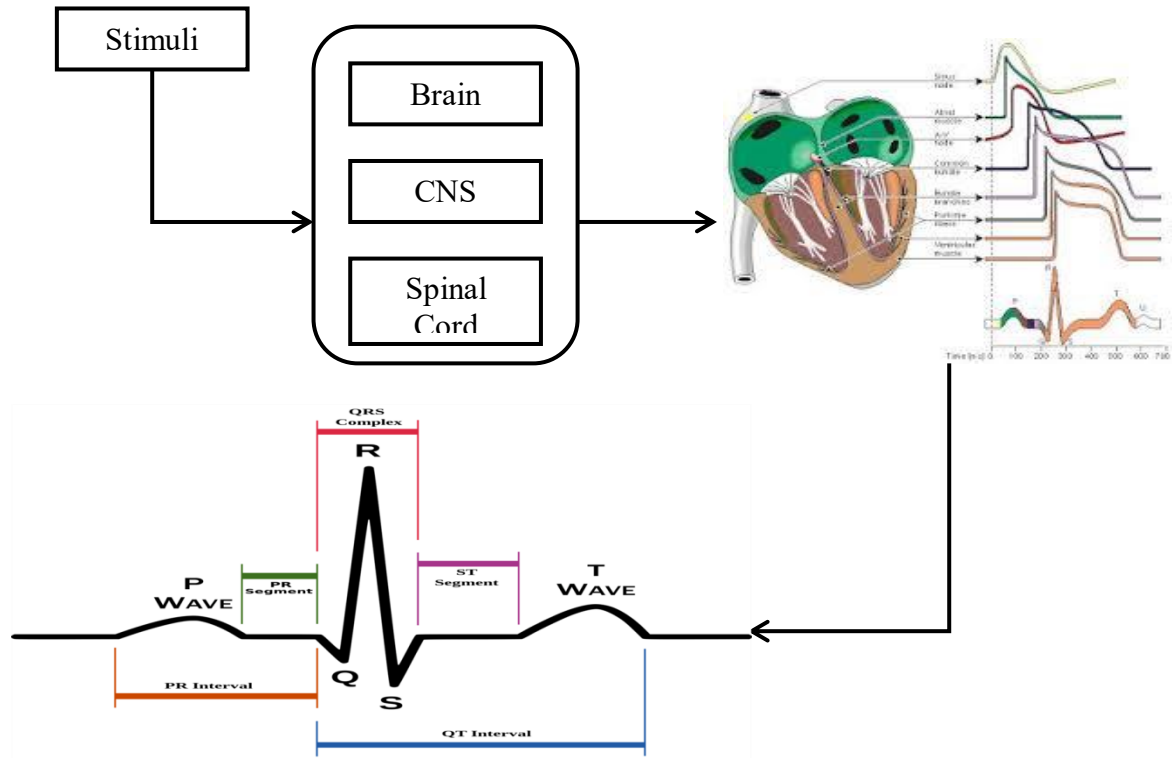


Figure 5.1: ECG waveform generation from various stimuli

HRV appears to be very popular these days for the researchers; it helps in specialist care of their patient’s performance, & recovery. Many academicians & professional specifies HRV as one of the crucial markers for the evaluation of wellness & performance of a patient’s health.

5.1.1 Heart Rate Variability

HRV is controlled by the ANS and its parasympathetic & sympathetic branches. It is frequently recognized as a non-invasive marker of ANS activity. The production of the first continuous and accurate recording of the electrical activity of the heart was invented by W. Einthoven in the late 1890s. By integrating the galvanometer with photography, Einthoven made it possible to assess the variation within beat-to-beat in the heart rhythm

[3, 4]. Heart rate is not stable, even at rest, the time between heartbeats varies slightly. Consecutive *RR*-intervals can be used to calculate the variability in the HR termed as HRV. The *RR*-interval variability is synchronous with respiration, whereby HR increases during inhalation and decreases in the course of expiration, which was eventually denoted as Respiratory Sinus Arrhythmia (RSA). It is the variation of heart rate in the frequency range of respiration, which is a component of HRV, and thus its frequency differs with breathing rate. During the 1960s research on HRV was popularized and focused on:

- a) The physiological mechanisms mediating HR,
- b) The relationship between HRV and clinical status, and
- c) The relationship between psychological processes and HRV.

5.2 PROPOSED METHODOLOGY

This section describes the different ECG dataset and the proposed methodology. It includes the selection of features, statistical analysis techniques, and machine learning algorithms applied for the proposed methodology.

The methodology for HRV based classification consisting acquiring data from an online ECG database, ECG denoising by employing digital FIR filters, QRS complex detection, extraction of features from different domains: time-domain, frequency-domain, and geometric-domain, statistical analysis technique by employing *t*-test, ANOVA, and machine learning algorithms for classification.

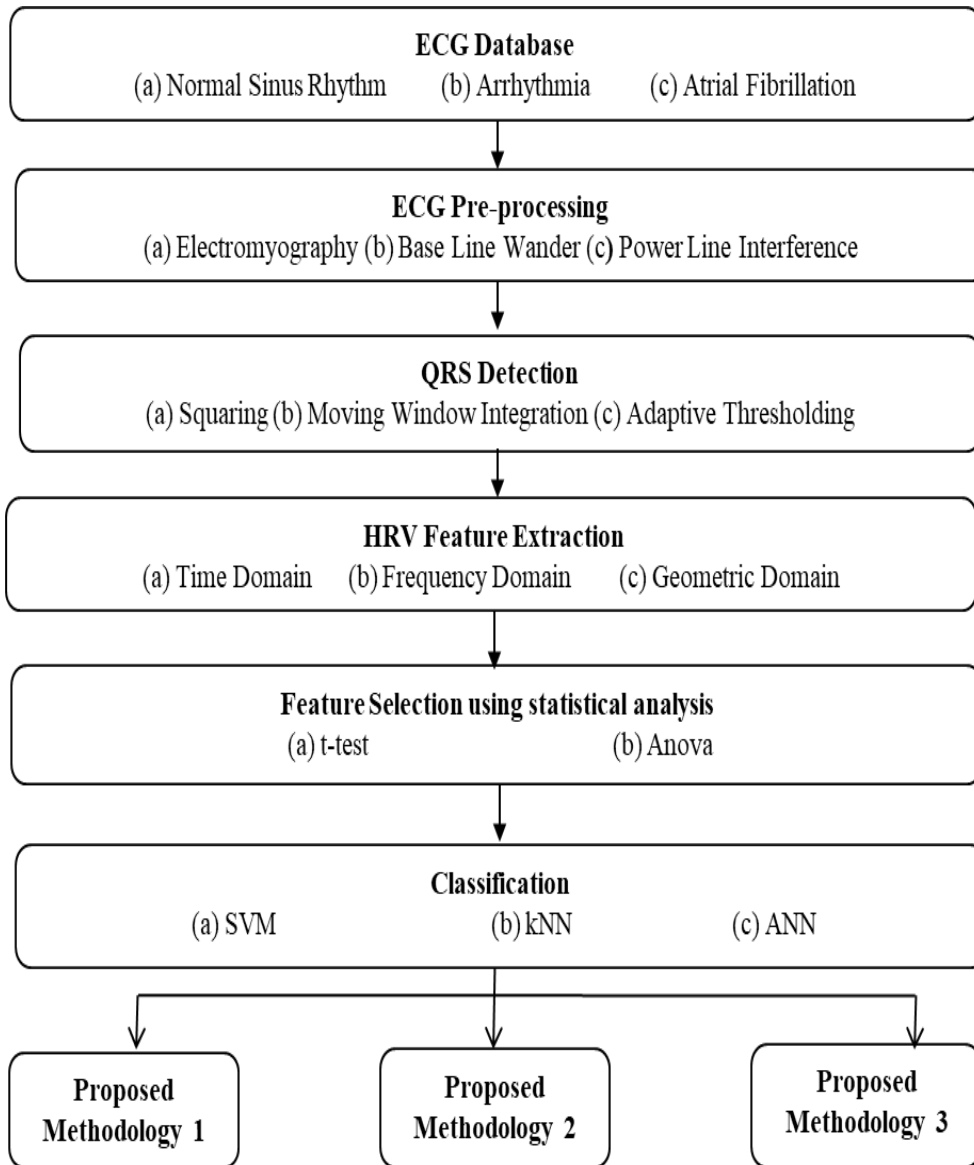


Figure 5.2: Proposed methodology for HRV classification

HRV Feature Extraction

There are three main approaches for analyzing HRV from an ECG: time domain, frequency domain & geometric domain methods. Table 5.1 tabulates the description of HRV features in different domains.

Table 5.1: HRV Feature Description

Domain	Features	Description	Formula	Unit
Time domain	<i>mean RR</i>	Mean of all <i>RR</i> interval	$mean\ RR = 1/N \sum_{i=1}^N (RR_i)$	ms
	<i>SDNN</i>	Standard deviation of <i>NN</i> interval	$SDNN = \sqrt{\frac{\sum_{i=1}^N (RR_i - mean(RR))^2}{N}}$	ms
	<i>SDSD</i>	Standard deviation of <i>SD</i>	$SDSD = \sqrt{\frac{\sum_{i=1}^N (SD_i - mean(SD))^2}{N}}$	ms
	<i>RMSSD</i>	Root Mean Square of <i>SD</i>	$RMSSD = \sqrt{\frac{\sum_{i=1}^{N-1} (RR_i - mean(RR))^2}{N-1}}$	ms
	<i>NN50</i>	Number of <i>SD</i> >50ms	<i>NN50</i> = number of <i>SD</i> > 50ms	nu
	<i>pNN50</i>	Percentage of <i>NN50</i> >50ms	<i>NN50</i> * 100	%
	Max-Min HR	Mean difference between maximum-minimum HR	<i>Max-Min HR</i> = Max(HR) - Min(HR)	bpm
	mean HR	Mean of total HR	$Mean\ HR = 1/N \sum_{i=1}^N HR_i$	bpm
Geometrical domain	<i>HRVTI</i>	Ratio of integral of density distribution of <i>RR</i> interval to the maximum intensity distribution.	$HRVTI = \left(\frac{Totalnumber(NN)}{max(NN)} \right)$	nu
Frequency domain	<i>aULF</i>	Absolute power of ULF (≤ 0.003 Hz)	$aULF = \sum_0^{0.003} p(k)$	ms ²
	<i>aVLF</i>	Absolute power of VLF (0.033-0.04 Hz)	$aVLF = \sum_{0.033}^{0.04} p(k)$	ms ²
	<i>aLF</i>	Absolute power of LF (0.04-0.15 Hz)	$aLF = \sum_{0.04}^{0.15} p(k)$	ms ²
	<i>aHF</i>	Absolute power of HF (0.15-0.4 Hz)	$aHF = \sum_{0.15}^{0.4} p(k)$	ms ²
	<i>aTotal</i>	Absolute power of total frequency spectrum	$aTotal = \sum_0^{0.4} p(k)$	ms ²
	<i>pVLF</i>	Relative power of VLF	$pVLF = \left(\frac{aVLF}{aTotal} \right) \times 100$	%
	<i>pLF</i>	Relative power of LF	$pLF = \left(\frac{aLF}{aTotal} \right) \times 100$	%
	<i>pHF</i>	Relative power of HF	$pHF = \left(\frac{aHF}{aTotal} \right) \times 100$	%

	Lf_{norm}	Normalized variation of Total power on LF	$Lf_{norm} = \left(\frac{a_{LF}}{a_{Total} - a_{VLF}} \right) \times 100$	nu
	Hf_{norm}	Normalized variation of Total power on HF	$Hf_{norm} = \left(\frac{a_{HF}}{a_{Total} - a_{VLF}} \right) \times 100$	nu
	LF/HF	Ratio of LF power to HF power	$LF/HF = \left(\frac{a_{LF}}{a_{HF}} \right) \times 100$	%
<p><i>NN</i>: Successive Difference between normal to normal R to R peak (exclude abnormal and ectopic beats). <i>N</i>: Total number of RR or NN intervals <i>p(k)</i>: Power Spectral Density of frequency spectrum <i>SD</i>: Successive Difference between consecutive RR intervals. <i>bpm</i>: beats per minute <i>nu</i>: No units</p> <p><i>ULF</i>: Ultra Low Frequency <i>LF</i>: Low Frequency <i>VLF</i>: Very Low Frequency <i>HF</i>: High Frequency</p>				

(a) Time Domain

HRV is computed by various techniques, but the time-domain parameters are the simplest among other parameters. The measures are calculated by utilizing the intervals between consecutive normal rhythms. The RR intervals and HR is determined by correct QRS complex detection. Time-domain features are computed including the mean of NN interval or RR interval, the difference within the longest & shortest NN interval (max-minRR), maxRR, minRR and mean RR. The simplest and most commonly used time-domain HRV measures constitute of the standard deviation of NN-intervals (SDNN) & root mean square of the successive changes of NN-intervals (RMSSD). The SDNN reproduces an estimate of all the cyclic features accountable for change in the duration of recording (i.e. overall estimate of HRV) encompassing both short term high-frequency changes & the lowest frequency features [93]. An average of normal R-R intervals (SDANN) is an equivalent technique that controls the ECG records length. A different and more reliable time domain parameter is RMSSD. It is a common parameter based on differences between the longest and shortest NN-interval and corresponds to short-term HRV changes [94].

Figure 5.3 represents the transformation of the ECG into R-R interval spectrum. The recorded ECG is utilized to form the successive beat-to-beat variation. The variations have been plotted as a tachogram and measured in milliseconds versus interval number.

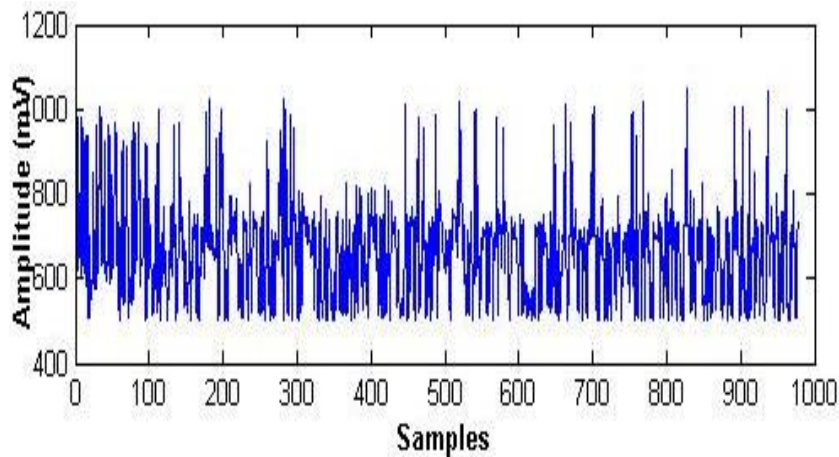


Figure 5.3: Beat to Beat variation of $R-R$ intervals (Tachogram)

(b) Frequency Domain

In the 70s and 80s, several academic groups started to apply power spectral techniques or frequency domain measures of HRV expanding the current time-domain techniques. This technique would add insight into the nature of HR fluctuations by separating the overall variability into its frequency components [95]. In the analysis of power spectral decomposition, the series of RR -interval is considered as a complex sum of waveforms. The FFT algorithm is considered to decompose the total variance of the HR into specific frequency bands. The total variance of HR mainly consists of total power, with the variance of all NN-interval at ≤ 0.4 hertz (Hz), High frequency (HF) found between the 0.15 Hz – 0.4 Hz frequency range, low-frequency (LF) between the 0.04-0.15 Hz frequency range, and very low frequency (VLF) between the 0.003-0.04 Hz frequency range. The physiological significance of HF is that it is aided by Para-sympathetic variations and represents the respiratory variation while the LF expressed the modulation by both SNS and PNS and is affected by baroreflex feedback loops. The VLF represents the influence of thermoregulatory, peripheral vasomotor, or renin-angiotensin systems. The proportion of low frequency to high frequency is used as the reflection of the sympathetic modulations but later, the interpretation has been criticized.

The short term recording (2 to 5 minutes) helps to calculate the three spectral parameters from the PSD. The fluctuation in HR varies as per the central frequency and power distribution of LF and HF variations. For an effective VLF measure, long term recordings are needed as it measures frequency variation having cycle length between 25

to 250 seconds (>4 minutes). To acquire reasonable estimates of power from FT; it needs more than 40 minutes of recording. Degradation in the accuracy is observed for short term recordings of VLF. The Ultra-low frequency (ULF) is an added parameter that is occasionally utilized all through HRV recordings. The FFT helps to convert the tachogram into a power spectrum and separate them into its corresponding frequencies comprising VLF, LF, and HF as represented in Figure 5.4. These frequency measures are computed in absolute values of power (milliseconds squared) as aVLF, aLF and aHF.

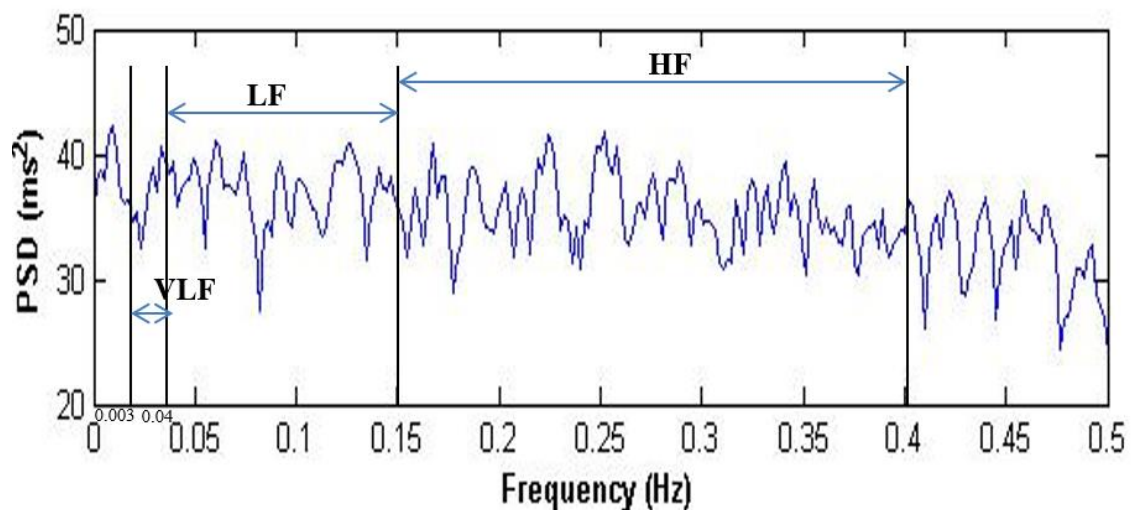


Figure 5.4: PSD for *R-R* interval

The LF and HF are computed in the normalized units resulting in relative value for each frequency measure in proportion to the absolute total power (aTotal) minus the VLF component. The Lfnorm & Hfnorm represents the normalized components that highlight the balanced and controlled behavior of PNS and SNS.

(c) Geometric Domain

These features are computed by generating the histogram of the successive difference of the *RR* interval. HRV Triangular Index (HRVTI) is one of the geometric domain features that are the ratio of the maximum value in the histogram to the length of the histogram.

Statistical Analysis

The science of collecting data and analyzing its trends and patterns is termed statistical analysis. There are several HRV measures calculated in various domains (time-domain, frequency-domain, and geometric domain); only a few represent a prominent effect on the system's performance. Due to this, the correlation among HRV measures is computed at 95% and 99%. For statistical analysis, various techniques are applied namely *t*-test & one way ANOVA, two way ANOVA, many more. In this research, *t*-test & one way ANOVA is considered. The *t*-test is used to compare two groups of ECG dataset and the ANOVA test is employed for three groups. The *t*-test verifies two hypotheses about the HRV features sample data; one is the null hypothesis and the other is the alternative hypothesis. In this design, two tail *t*-tests are employed for analysis, and its formulation is specified in Eq. (5.1).

$$t = \frac{\bar{x} - \mu_{H_0}}{\sigma_s / \sqrt{n}} \quad (5.1)$$

Annotations: \bar{x} is the sample mean, μ_{H_0} represents the mean of the null hypothesis, σ_s is the standard deviation of the sample and n is the number of samples.

A two-tailed test is effective in determining the difference between the two datasets. It is due to the utilization of both the positive and negative tails of the distribution in the *t*-test. In other words, it testifies the options of positive or negative differences. When there is a comparison between more than two groups ANOVA technique is employed. This method also considered two hypotheses expressed in Eq. (5.2).

$$H_0: \mu_1 = \mu_2 = \mu_3 \quad (5.2)$$

H_1 : at least one of the mean is unequal

Where μ_1 is the mean of the NSR HRV parameter, μ_2 is the mean of the AR HRV parameter & μ_3 is the mean of the AF HRV parameter.

Classification

To analyze the effectiveness of statistical analysis after HRV feature extraction, several classification methods are used. These classifiers investigate the performance of HRV measures to distinguish between normal and abnormal ECG signals. Some of the classifiers utilized in this thesis are SVM, kNN & ANN [150]. The authors have utilized the training dataset as 70% and the testing dataset as 30%. The performance of these classifiers is improvised by employing 5-fold cross-validation. It has been perceived that the overall accuracy of classification is increased after feature selection by employing statistical analysis [151-156].

(a) Support Vector Machine (SVM)

SVM represents the theory of maximum margin theory and is a supervised learning algorithm. Binary classification is a widespread algorithm for real-time problems [157-160]. A three-dimensional plane termed as a hyperplane in SVM helps to separate the different classes present in the dataset. The vector present nearest to the hyperplane is labeled as SV (Support Vector). The longest distance towards SV which aims to maximize the margin between hyper-plane and reduce the generalization error is termed as functional margin. SVM classification is a two-level concept: training and testing. The best feature among trained data is chosen, and then it is applied to unseen data during the testing period. The given set of training data (X_i) lies in between ($X_1, X_2, X_3, \dots, X_n$) of n point represented by Eq. (5.3):

$$(\vec{X}_1, O_1), \dots, \dots, (\vec{X}_n, O_n) \quad (5.3)$$

The output ($O_1, O_2, O_3, \dots, O_n$) can be -1 or 1, which represent different classes for input data ($X_1, X_2, X_3, \dots, X_n$) during binary classification. The generalized equation for hyperplane which separates the classes is given by Eq. (5.4).

$$\vec{W} \cdot \vec{X} - B = 0 \quad (5.4)$$

Annotations: \vec{W} is weight vector, \vec{X} is the input vector and B is the bias.

SVM classification is based on the selection of kernel selection as it comprises of various SVM kernels: linear, Gaussian radial basis function (RBF) kernel, polynomial,

etc. These types of kernels are tested on HRV features but Gaussian Radial Basis Function (GRBF) gives better accuracy due to higher dimensional space to separate the training data in their respective classes. The researchers have employed cubic and coarse Gaussian Radial Basis Function in this work. The non-linear equation of GRBF is represented by Eq. (5.5).

$$f(X) = \sum_{i=1}^n W_i K(X - X_i) + B \quad (5.5)$$

$$\text{where } K(X, X_i) = \exp\left(-\frac{\sum\|X-X_i\|^2}{2\sigma^2}\right) \quad (5.6)$$

Where X , is the input vector, X_i is the support vector, B is bias and weight vector, W is weight, σ is the Gaussian distribution.

(b) k-Nearest Neighbor (kNN)

The kNN classifier is the simplest and widely employed supervised classification algorithm. The kNN is firstly theorized [19], that further developed by [20] to conceptualize the weighted kNN[20]. It is based on the theory of the Nearest Neighbor rule as it assigns a point 'x' to the class maximum that existed amongst the 'k' points in the training set nearest to 'x'. The decision is chosen on the foundation of the points which are nearest to the Euclidean distance. The whole points in the neighborhood append equally to the conclusion for 'x'. The ease of implementation and efficiency helps authors to select kNN, but it has less accuracy as compared to other classifiers. For the improvisation of this drawback, weighted kNN and cubic kNN are considered. The general equation for weighted kNN is represented in Eq. (5.7).

$$\arg \max_c \sum_{i=1}^K I_c(n_i) w_{n_i} \rightarrow x \quad (5.7)$$

In the weighted kNN, every neighbor $n_i \in n_e$ of kNN is equipped with a weight w_{n_i} . Where $I_c(n_i)$ is the function to determine the class 'c'.

(c) Artificial Neural Network (ANN)

For developing an intelligent system for classification numerous research has been done in the literature [35, 36]. Most of these systems are inspired by the human brain including how they process the information. The high performance of the ANN classification process required a high number of interconnected neurons [161-164]. A node is the basic computational unit in artificial neurons; it receives the input from the environment or the external source. Each node is associated with some weight that calculates the function of the weighted sum of its input. The selection of learning rules and activation functions is an essential structure of a neural network. The feed-forward networks and feedback networks are two types of neural network architectures [167]. The basic architecture of ANN comprising three types of layers: input, hidden & output. The neurons that existed in the input layer represented as ' x_{ij} ' (input vector) are fed to the neurons of the hidden layer. The neurons of this layer termed as ' j ' also with its input signals ' x_i ' are assigned with respective weight vector ' w_{ij} '. The overall input of the activation block, net_j , is calculated by the addition of the inner product of the input, weight vector, and bias having ' n ' number of neurons in Eq. (5.8) and the output of the activation function(O_j) is expressed by Eq. (5.9) [36].

$$net_j = bias_j + \sum_{i=1}^n w_{ij} x_i \quad (5.8)$$

$$O_j = \varphi(net_j) \quad (5.9)$$

where φ denotes the activation function of the neuron. These machine learning techniques help the authors to propose different methodologies to notice the effect of statistical analysis on classification accuracy.

In the proposed methodology as shown in Figure 5.2, the authors have conducted three types of pilot studies by employing different domain features and statistical analysis.

- a) Classification of AR and NSR by employing time-domain features
- b) Computer-Aided Diagnostic for Feature-Based Classification (CAD-FSC)
- c) Multi-Stage Heart Rate Variability Classification System

5.2.1 HRV Classification by employing Time-domain features

The proposed methodology comprises of AR and NSR dataset. The FIR Kaiser Window function helps to eradicate the artifacts from the raw signal. The Pan-Tompkins algorithm is utilized to detect QRS complex from the signal, which helps to compute the HR from the ECG waveform. Time-domain HRV features are computed by utilizing HR parameters and a *t*-test is employed for statistical analysis. SVM and kNN machine learning algorithms are applied for classification as shown in Figure 5.5.

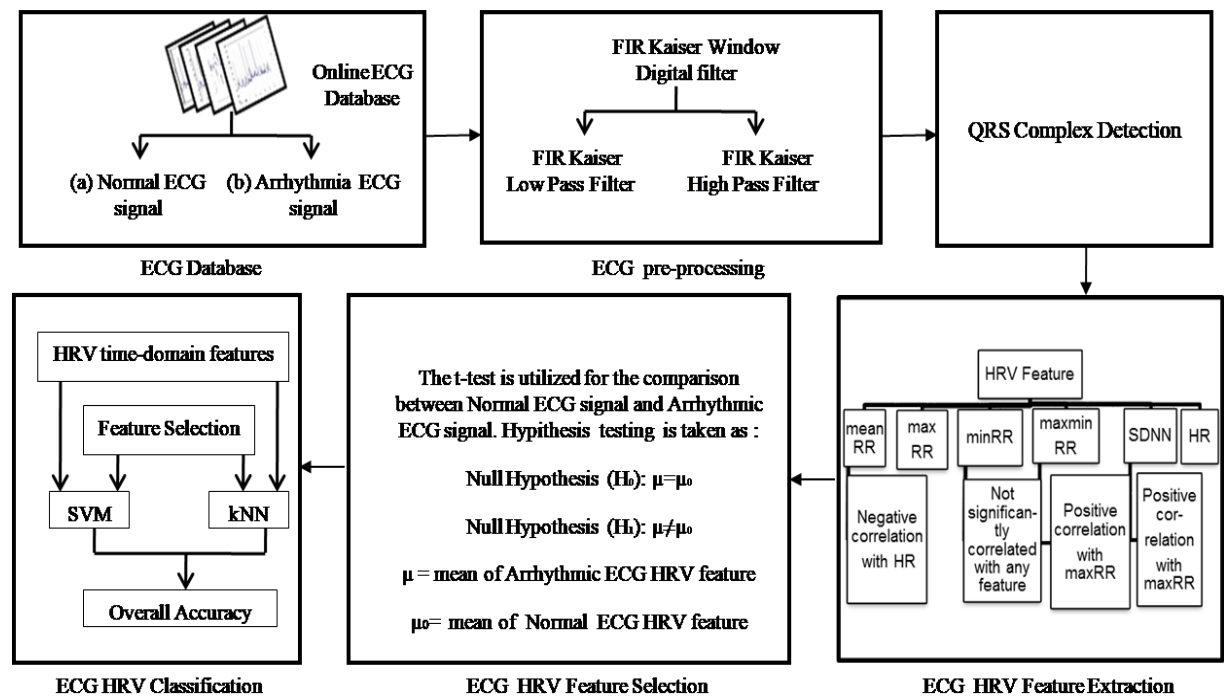


Figure 5.5: Proposed Methodology of time-domain HRV classification

The time-domain HRV classification utilized only time-domain features. To enhance the performance of the classification methodology the authors have used frequency, geometric domain attributes also.

5.2.2 HRV Classification by employing CAD-FSC system

The CAD-FSC system consists of NSR, AR, and AF dataset from the online platform. The different noises of ECG are eliminated by employing digital FIR filters. The QRS detection helps to compute the HR which is an essential parameter for evaluation of HRV features using different domains (time domain, frequency domain).

The four types of classifiers namely Cubic SVM (*C-SVM*), Coarse Gaussian SVM (*CG-SVM*), Cubic kNN (*C-kNN*), and Weighted kNN (*W-kNN*) are utilized to compute the performance parameters for the methodology [169-171]. The proposed methodology also observes the effect in classification accuracy before feature selection and after feature selection as represented in Figure 5.6.

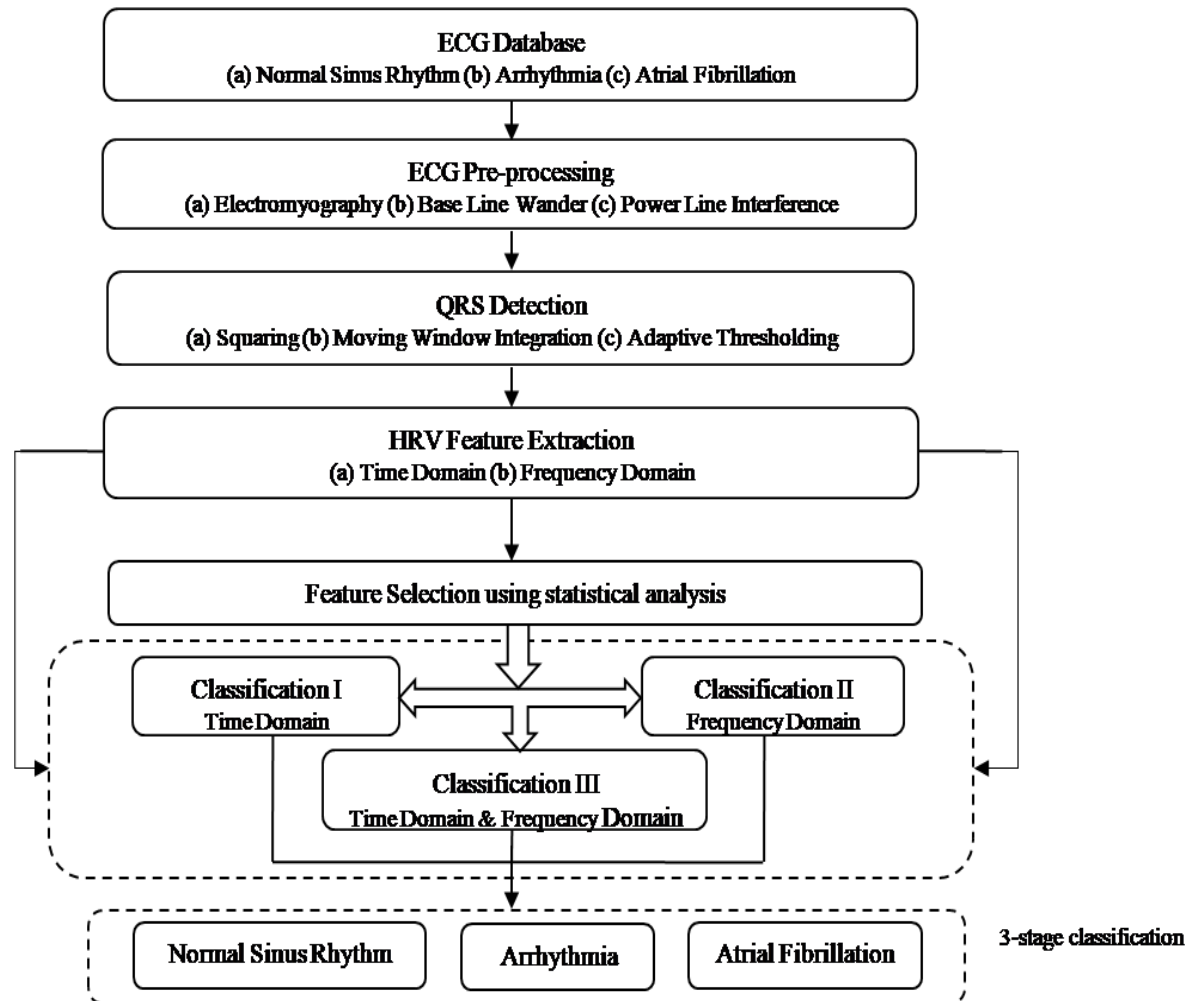


Figure 5.6: Proposed CAD-FSC Methodology

The CAD-FSC system utilizes all domain features & monitors the effect of statistical analysis on the performance of the presented methodology. A stage-wise classification has also been performed to categorize the HRV based CVDs.

5.2.3 HRV Classification by employing MSHVC system

ECG filtering techniques are applied on the ECG databases and *R*-peaks are identified using the Pan-Tompkins system [153]. Various HRV measures are obtained in time, frequency & geometrical domain. The classification is performed using SVM, kNN, and ANN classifiers as represented in Figure 5.7.

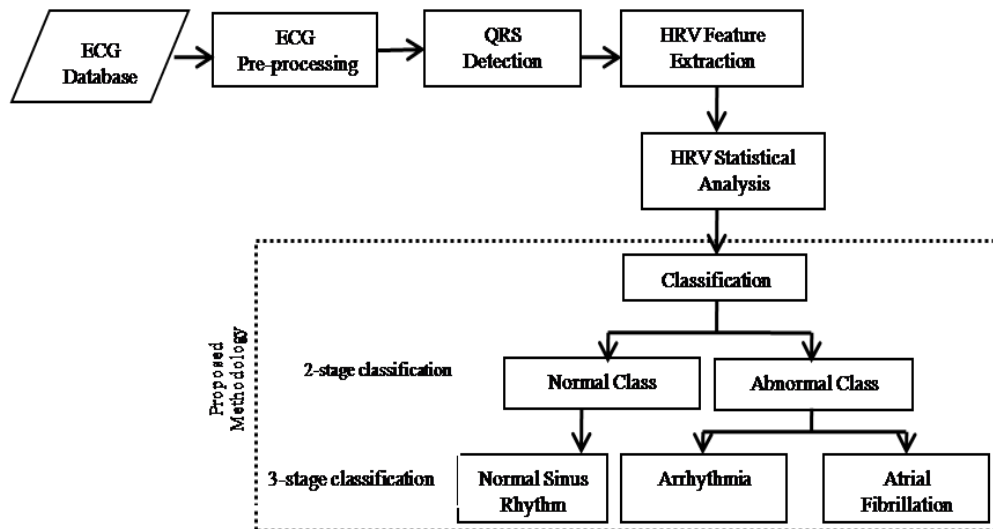


Figure 5.7: Proposed methodology for the classification of Heart diseases

The proposed methodology comprises of a two-stage and a three-stage classification. For the two-stage classification normal (NSR) and abnormal ECG (AR and AF) are separated; which is followed by the distribution of the abnormal ECG into AR and AF for three-stage classification. The novelty of this study lies in extensive feature selection employed on the extracted feature set to choose the most significant measures that give additional useful information than others. The extraction of features is done from a filtered signal which is a crucial part of the design process. HRV measures are distributed in three domains: time, geometric & frequency. The spectrum of power of the tachogram is represented in Figure 5.2. Table 5.2 tabulated the brief explanation of all the HRV measures along with their formulation and units. In this design processing, the ANOVA technique is employed for the selection of the evident HRV attributes.

5.3 RESULTS & DISCUSSION

This segment elucidates the three kinds of proposed methodologies and their findings in terms of sensitivity, specificity, accuracy, and PPV. The percentage improvement in the overall accuracy after employing statistical analysis techniques is showcased.

5.3.1 HRV Classification by employing Time-domain features

The normalization of the dataset is the initial step before applying a statistical test on different HRV [168]. The Graphical and Exact methods are used to verify the normal data distribution in the statistical analysis. The graphical method helps to visualize the normality by using the histogram plot, Q-Q plot and box plot, etc. Figure 5.8, Figure 5.9, & Figure 5.10 represented the histogram plot, Q-Q plot, and box plot respectively to visualize the normality of different HRV features. From Figure 5.8, it has been interpreted that the data is approximately normally distributed. Figure 5.9 represents that most of the data lie on the straight line or at a minimal distance from it, signifying that data is normally distributed. Figure 5.10 explains the symmetrical property of the HRV features with the mean, median, and center. In meanRR and max-min RR feature, one outlier is present; however, the data is approximately distributed.

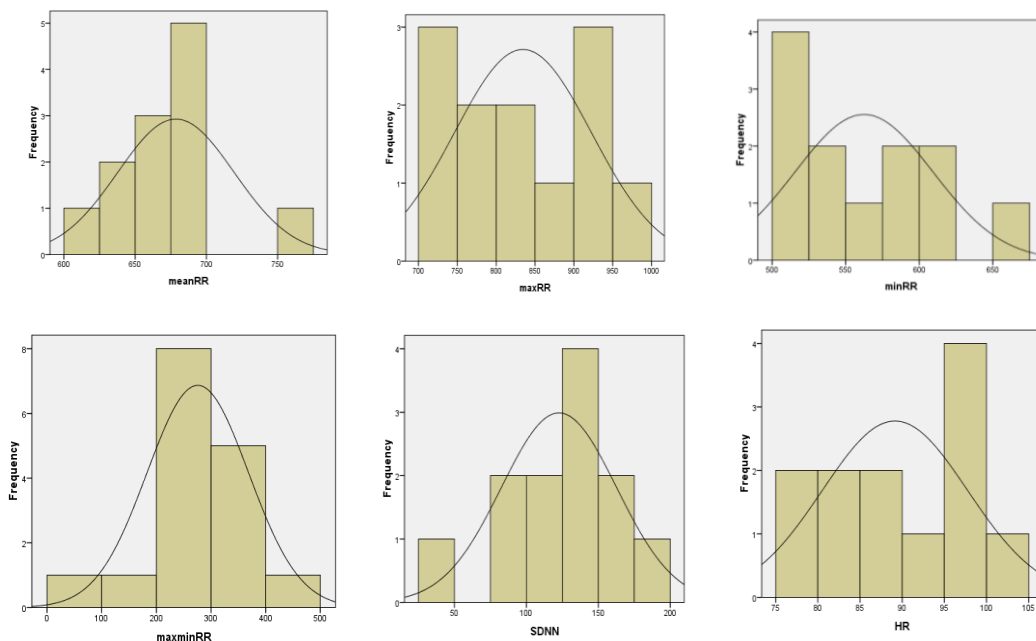


Figure 5.8: Histogram Plot (a) meanRR (b) maxRR (c) minRR (d) maxminRR (e) SDNN (f) HR

Multistage Heart Rate Variability Classification System

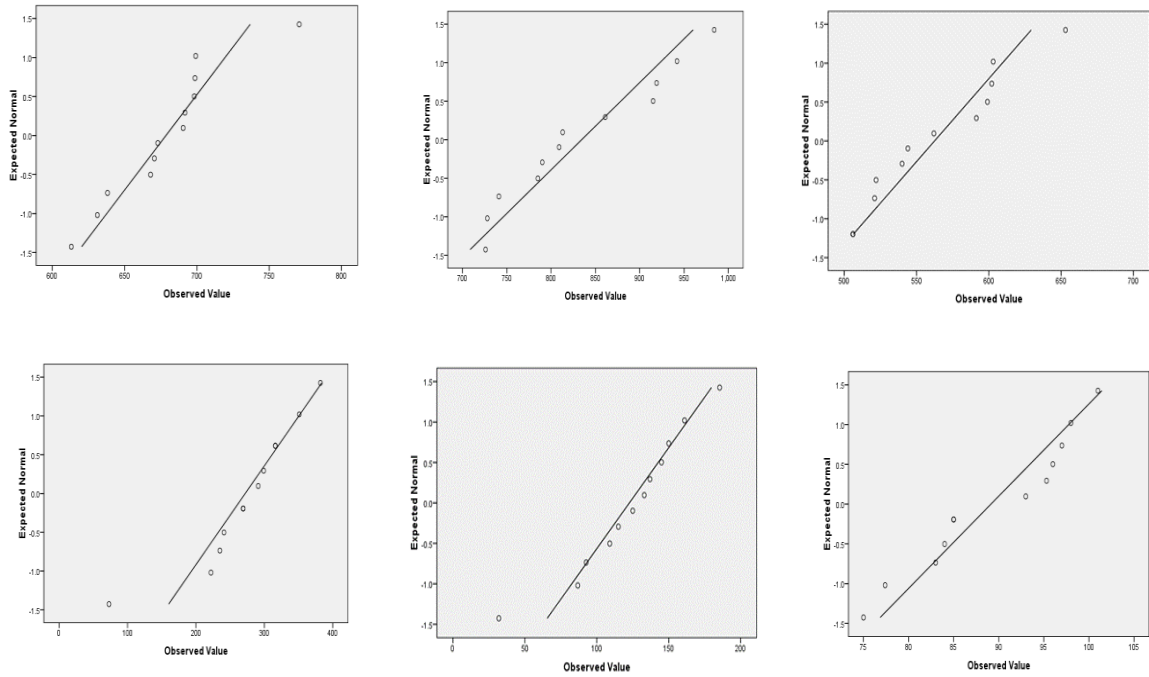


Figure 5.9: Q-Q Plot (a) meanRR (b) maxRR (c) minRR (d) maxminRR (e) SDNN (f) HR

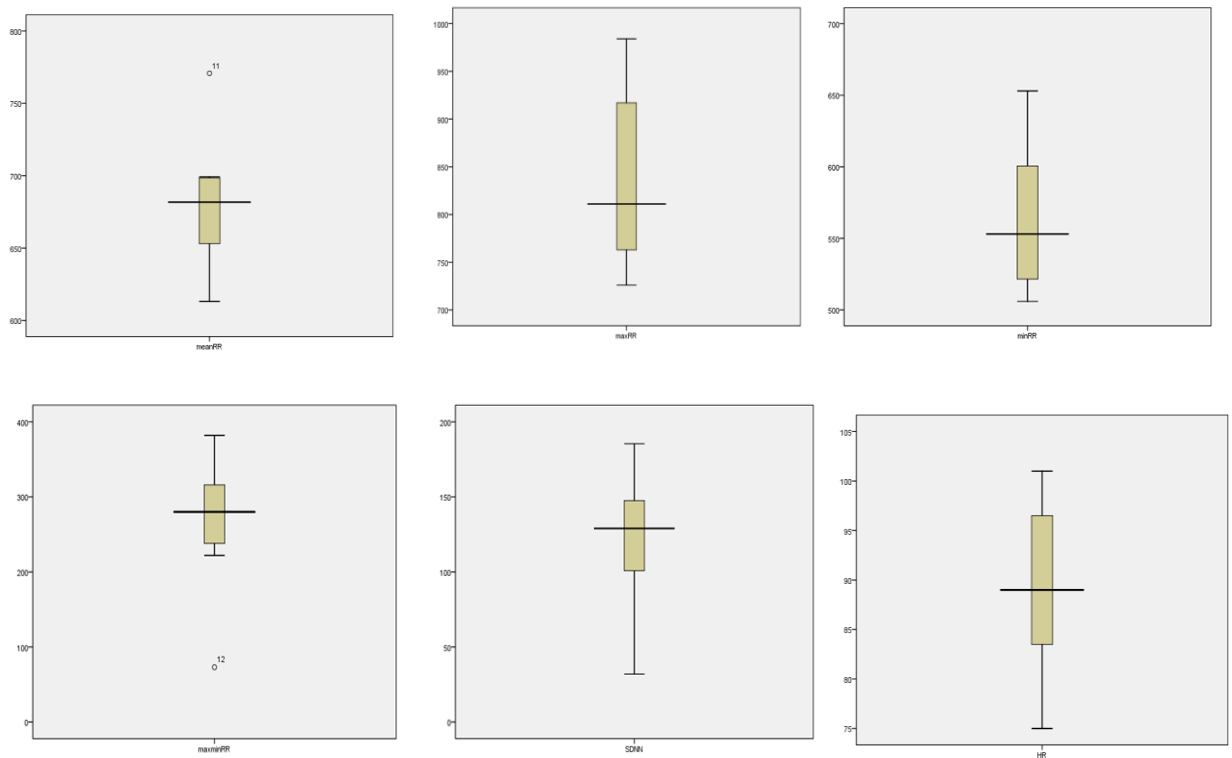


Figure 5.10: Box Plot(a) meanRR (b) maxRR (c) minRR (d) maxminRR (e) SDNN (f) HR

In the *Exact method*, numerical values are extracted and compared with the standard range of normality distribution. The ‘z’ value of the data is considered to find the

skewness and kurtosis, which must lie in between -1.96 to +1.96. The ‘z’ and ‘p’ values of different HRV features are illustrated in Table 5.2.

Table 5.2 : z & p value of HRV parameters

HRV Features	Skewness(z)	Kurtosis(z)	p value ($p>0.05$)
meanRR	0.89	1.245	0.334
maxRR	0.55	-0.99	0.322
minRR	0.714	-0.59	0.306
maxminRR	-2.14	2.69	0.142
SDNN	-1.28	1.14	0.789
HR	-0.40	-1.06	0.317

Table 5.3: Correlation of HRV features

HRV Features	mean RR	max RR	minRR	max-min RR	SDNN	HR
mean RR	1	0.26	0.57	0.29	0.50	-0.66*
max RR	0.26	1	0.45	0.99**	0.92**	0.19
minRR	0.57	0.45	1	0.44	0.37	0.15
max-minRR	0.23	0.99**	0.44	1	0.91**	0.22
SDNN	0.50	0.92**	0.37	0.91**	1	0.15
HR	-0.61*	0.19	0.15	0.22	-0.15	1

** Significance value at 0.01 level (2-tailed)

* Significance value at 0.05 level (2-tailed)

From Table 5.2, it is illustrated that skewness and kurtosis ‘z’ values for HRV features lie between -1.95 to +1.96. This illustrates that the database considered are approximately normally distributed. There are several features present in the ECG signal, out of which few features contain more useful information than others. Feature selection plays an important role in which the correlation of features with each other is considered. Subsequently, to test the sample data for a particular condition for different time-domain HRV features a statistical hypothesis test termed as *t*-test is utilized as represented in Eq. (5.1). Spearman correlation is used for observing the correlation between different HRV

features. It defines the relationship between different HRV features. Table 5.3 tabulates the correlation matrix among different HRV features.

Table 5.3 tabulated that minRR is not related to other HRV parameters. The t -test is used for statistical analysis, which calculates the ' p ' value for different HRV features signifies the comparison between normal and arrhythmic ECG signal expressed in Table 5.4. In the table, if values lie in the range $0.05 < p \leq 0.10$ it is suggestive significant if it is $0.01 < p \leq 0.05$ then it is moderately significant and value is $p \leq 0.01$ than strongly significant. where table defines Mean \pm Standard Deviation value.

Table 5.4: Comparison of normal ECG and arrhythmic ECG

HRV Features	Normal ECG(sec)	Arrhythmia ECG(sec)	p value
meanRR	666.58 \pm 115.65	678.61 \pm 40.88	$p > 0.05$
maxRR	666.83 \pm 115.44	834.41 \pm 88.22	$p < 0.01$
minRR	666.33 \pm 115.874	562.41 \pm 46.83	$p < 0.01$
maxminRR	0.5 \pm 1.73	272 \pm 78.48	$p < 0.01$
SDNN	0.35 \pm 1.22	122.8 \pm 40.07	$p < 0.01$
HR	93 \pm 53	89 \pm 9	$p > 0.05$

From Table 5.4, it is observed that meanRR and HR values have suggestive significant changes. All other features such as maxRR, minRR, maxminRR, and SDNN have strong significant changes. It signifies that if a person has these types of variations in HRV features; probably he will be suffering from arrhythmia disease. This is because of the inverse relation between RR interval and HR interval ($60/RR$ sec), for arrhythmia signal, the RR interval gets decreased with an increase in HR in contrast to a normal ECG signal. The statistical analysis of the time-domain HRV feature illustrates that out of six features; four features have strong significant changes and the other two have suggestive significant changes. This selected HRV features help in the classification of AR ECG and NSR ECG.

To analyze the effectiveness of our proposed methodology the ECG classification has been done by using different machine learning algorithms. It has been observed that the overall accuracy of classification is increased after feature selection by *t*-test. The overall accuracy attained by SVM and kNN classifiers is 78.7% and 75.4 % respectively. After considering a two-tail *t*-test for feature selection, the accuracy has been improved to 80.3% and 82% for SVM and kNN respectively.

(a) Percentage Improvement during time-domain classification

This study represents the statistical study of time-domain HRV features for arrhythmia disease. The SVM classifier signifies 2% improvement and kNN illustrates 14.02% percent improvement in the overall accuracy after feature selection. This methodology is capable to classify arrhythmia and normal sinus rhythm with 82% overall accuracy when only time-domain features are present.

5.3.2 HRV Classification by employing CAD-FSC

The suggested CAD-FSC system is distributed into three levels of feature consideration.

- a) Performance parameter of CAD-FSC before & after applying statistical analysis by considering time-domain features.
- b) Performance parameter of CAD-FSC before & after using statistical analysis by considering only frequency-domain features.
- c) Performance measures of CAD-FSC before and after employing statistical analysis by considering the time and frequency-domain features.

These levels are further classified into two sections: the accuracy computed before applying statistical analysis and the accuracy achieved after removing redundant features using ANOVA test as shown in Figure 5.11.

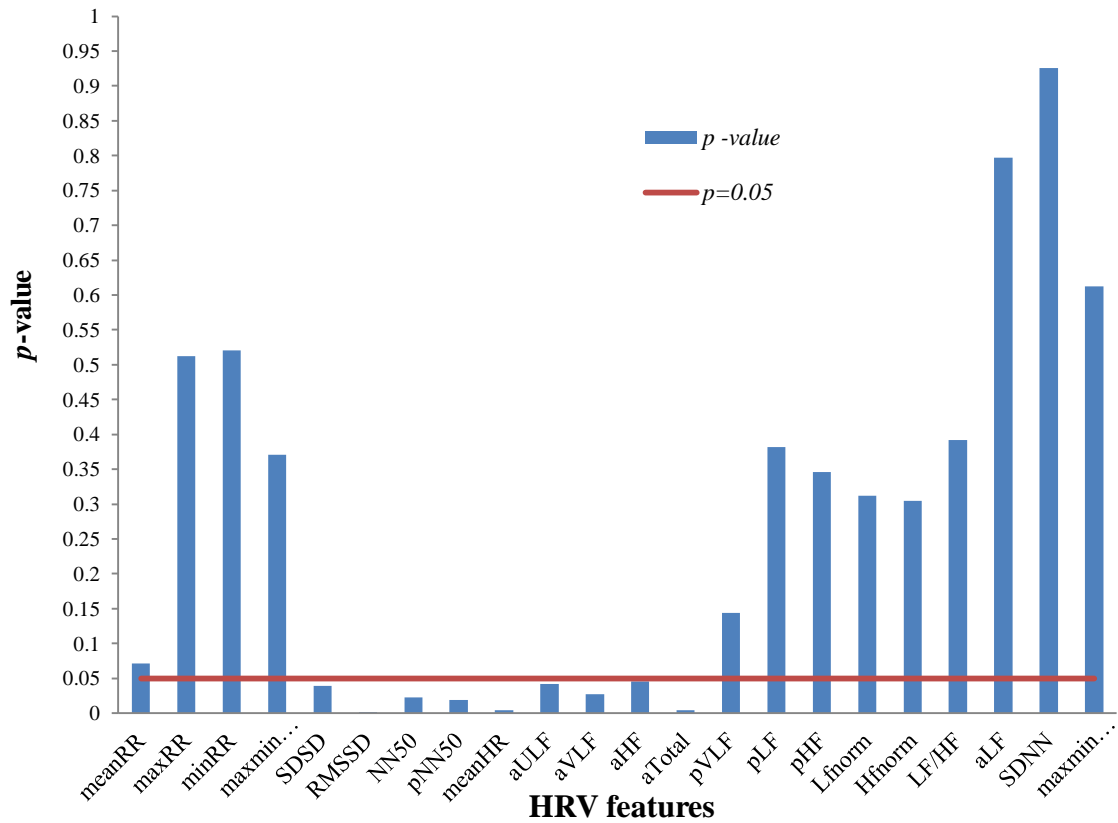


Figure 5.11: Feature selection criteria based upon the p -value

HRV features that provide significant variation between mean values: weak significant (WS) & strong significant (SS) are deliberated when the p -value is greater than 0.05 & less than or equal to 0.05 respectively. The prominent variation in HRV features of different databases denoted by mean \pm standard deviation (SD) notation. The parameters that accomplished $p \leq 0.05$ are chosen & additional parameters that acquired $p > 0.05$ are rejected are represented in Figure 5.11.

Case A: Performance parameter of CAD-FSC before & after applying statistical analysis technique by considering time-domain.

The CAD-FSC system's overall accuracy is low for the chosen classifiers before employing statistical analysis. The highest accuracy of 78.7% & 65.6% are attained by employing C-SVM & CG-SVM respectively but it is very less for the achieves only 65.6% accuracy, which is very low for notable classification illustrated in Table 5.5.

Table 5.5: Performance parameter of classification system utilizing time-domain parameters before & after HRV statistical analysis

Classification Technique		C-SVM		CG-SVM		C-kNN		W- kNN	
		Before	After	Before	After	Before	After	Before	After
PPV	PPV ₀	86.66%	93.33%	94.44%	94.44%	94.44%	94.44%	89.47%	89.47%
	PPV ₁	66.66%	68%	0%	87.50%	60%	80.95%	77.27%	77.27%
	PPV ₂	86.36%	85.71%	53.48%	62.85%	60.71%	80.95%	89.47%	85%
Sen.	Sen ₀	72.20%	77.77%	94.44%	94.44%	94.44%	94.44%	94.44%	94.44%
	Sen ₁	80%	85%	0%	35%	45%	80%	85%	85%
	Sen ₂	42%	78.26%	100%	95.65%	73.91%	73.91%	73.91%	73.91%
Sp.	Sp ₀	95.30%	97.67%	97.67%	97.67%	97.67%	97.67%	95.34%	95.34%
	Sp ₁	80.48%	80.48%	100%	97.56%	85.36%	85.36%	66.66%	87.80%
	Sp ₂	92.10%	92.10%	48.64%	65.78%	71.05%	89.47%	92.10%	92.10%
Acc.	Acc ₀	88.52%	91.80%	96.72%	96.72%	96.72%	96.72	95.08%	95.08%
	Acc ₁	80.32%	81.96%	65.57%	77.04%	72.13%	83.60	86.88%	86.88%
	Acc ₂	88.52%	86.88%	67.21%	77.04%	72.13%	88.52%	85.24%	85.24%
Overall Accuracy		78.7%	80.3%	80.3%	75.4%	75.4%	82%	82%	83.6%
AUC		0.95	0.96	0.96	0.95	0.95	0.94	0.94	0.94

After employing the feature selection method prominent development is perceived in the classification accuracy of the system. In which C-SVM achieves 80.3% & CG-SVM acquires 75.4% overall accuracy to categorize the dataset in three CVD groups.

Case B: Performance parameter of CAD-FSC before & after using statistical analysis by considering only frequency-domain features.

On consideration of frequency-domain HRV measure before the feature selection, only C-SVM & CG-SVM attains 49.2% & 41 % of classification accuracy as represented in Table 5.6.

Table 5.6: Performance parameter of classification system on utilizing frequency domain parameters before & after using statistical analysis

Classification Technique		C-SVM		CG-SVM		C-kNN		W- kNN	
		Before	After	Before	After	Before	After	Before	After
PPV	PPV ₀	54.16%	38.46%	0%	0%	32.43%	44.73%	40%	55.55%
	PPV ₁	45.45%	31.57%	100%	80%	40%	60%	30%	57.14%
	PPV ₂	46.66%	50%	38.98%	41.05%	44.44%	75%	31.25%	65%
Sen.	Sen ₀	72.22%	55.55%	0%	0%	66.66%	94.44%	55.55%	83.33%
	Sen ₁	50%	30%	10%	20%	30%	45%	30%	40%
	Sen ₂	30.43%	34.78%	100%	83.33%	17.30%	26.08%	21.73%	56.52%
Sp.	Sp ₀	74.41%	62.79%	100%	100%	41.86%	51.16%	65.11%	72.09%
	Sp ₁	78.37%	68.29%	100%	100%	87.80%	78.57%	65.85%	85.36%
	Sp ₂	78.94%	78.94%	5.2%	13.15%	86.84%	94.73%	71.05%	81.57%
Acc.	Acc ₀	73.77%	60.65%	70.49%	70.49%	49.18%	63.93%	62.29%	75.40%
	Acc ₁	63.93%	55.73%	70.49%	72.13%	62.29%	72.13%	54.09%	70.49%
	Acc ₂	60.65%	62.29%	40.98%	45.90%	60.65%	68.85%	52.45%	72.13
Overall Accuracy		49.2%	39.3%	39.3%	44.3%	44.3%	52.5%	52.5%	59%
AUC		0.72	0.82	0.82	0.62	0.62	0.67	0.67	0.74

The W-kNN algorithm attains 59% overall accuracy for the classification. A noticeable increment in the overall accuracy is observed on consideration of both the time & frequency domain HRV parameters as shown in Table 5.7. It has been perceived that C-SVM achieves a maximum of 96.72% accuracy before employing statistical analysis methods & after using these techniques the classification accuracy able to accomplish 98.4%; which is very effective to categorize three CVD classes.

Case C: Performance parameters of CAD-FSC before and after employing statistical analysis by considering time and frequency-domain.

Table 5.7: Performance parameters of the classification system on utilizing time-domain & frequency domain before & after employing statistical analysis

Classification Technique	Performance Metrics	C-SVM		CG-SVM		C-kNN		W- kNN	
		Before	After	Before	After	Before	After	Before	After
PPV	PPV ₀	100%	100%	100%	100%	100%	100%	100%	100%
	PPV ₁	90.47%	95%	0%	100%	41.17%	70%	63.63%	84.21%
	PPV ₂	100%	100%	55.81%	72.72%	53.84%	78.26%	62.5%	87.50%
Sen.	Sen ₀	100%	100%	100%	100%	100%	100%	100%	100%
	Sen ₁	100%	100%	0%	52.63%	36.84%	73.68%	36.84%	84.21%
	Sen ₂	91.66%	95.83%	100%	100%	58.33%	75%	83.33%	87.50%
Sp.	Sp ₀	100%	100%	100%	100%	100%	100%	100%	100%
	Sp ₁	95.23%	97.61%	100%	100%	76.19%	85.71%	90.47%	92.85%
	Sp ₂	100%	100%	48.64%	75.67%	67.56%	86.48%	67.56%	91.89%
Acc.	Acc ₀	96.72%	100%	100%	100%	100%	100%	100%	100%
	Acc ₁	96.72%	98.36%	70.49%	85.24%	63.93%	81.96%	73.77%	90.16%
	Acc ₂	96.72%	98.36%	68.85%	85.24%	63.93%	81.96%	73.77%	90.16%
Overall Accuracy		96.72%	98.4%	98.4%	85.2%	85.2%	82%	82%	90.2%
AUC		0.97	1	1	0.93	0.93	0.91	0.91	0.86

The proposed methodology concludes that the C-SVM classification algorithm is chosen when the HRV parameters from both the domains are taken after exercising the ANOVA test.

(a) The Percentage Improvement throughout the proposed system

The enhancement in percentage is calculated to validate the performance at different stages of the presented system. It has computed the percentage improvement designed for three classes:

i. *Percentage Improvement in classification accuracy & AUC by considering Time-domain measures:* The development in CAD-FSC system carried by time-domain parameters before & after employing the feature selection methods. The C-kNN attains

determining improvement in AUC of 4.25% & classification accuracy of 14.02% respectively as shown in Figure 5.12.

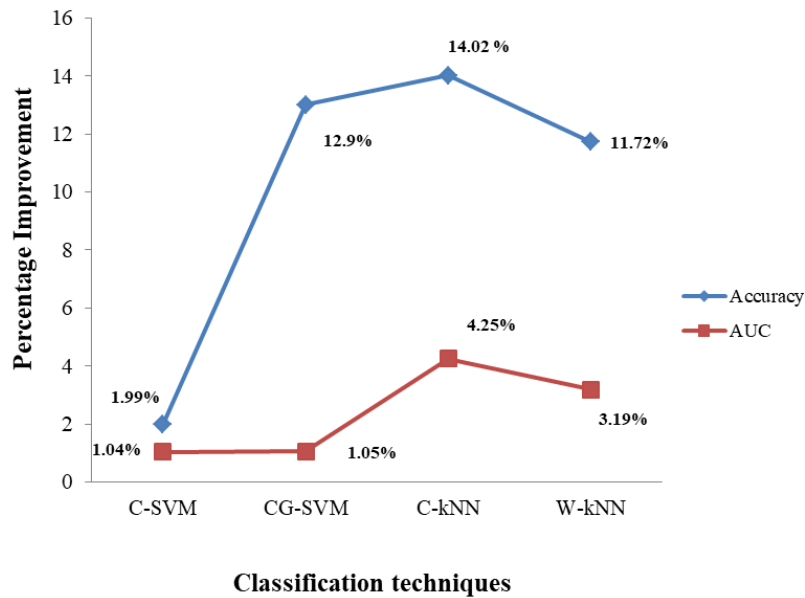


Figure 5.12: Percentage improvement for AUC and accuracy by utilizing Time-domain

ii. *Percentage Improvement in classification AUC & Accuracy by considering Frequency-domain measures:* The consideration of frequency-domain HRV parameter for the system attains 41.69% of classification later employing the ANOVA technique. The C-kNN algorithm attained 17.91% enhancement in AUC after the selection of features as illustrated in Figure 5.13.

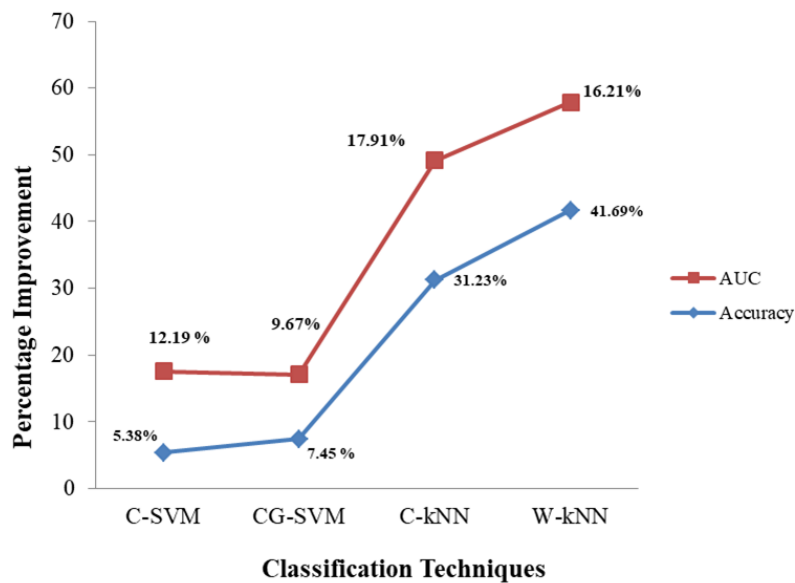


Figure 5.13: Percentage improvement for AUC and Accuracy by utilizing Frequency-domain

- iii. *Percentage Improvement in classification AUC & Accuracy by considering during Time and Frequency-domain:* When both time & frequency-domain features are taken then the classification accuracy gets improved significantly. The C-kNN classifier attains 22.07% classification accuracy enhancement & W-kNN achieves 16.28% enhancement in AUC as shown in Figure 5.14.

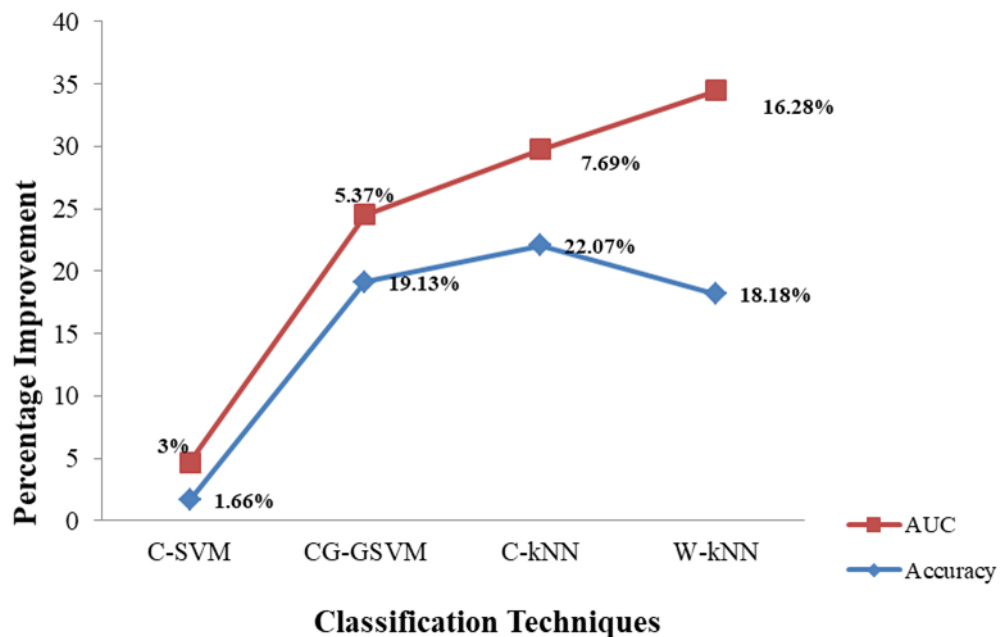


Figure 5.14: Percentage enhancement for accuracy and AUC by utilizing Time-domain and Frequency-domain

Multiple studies have been proposed for feature-based classification using HRV features. The nineteen HRV measures from the time & frequency domain are obtained. The classification accuracy is enhanced by removing the unnecessary features employing the ANOVA method. The nine HRV measures are chosen due to their valuable significance. The parameters are SDS, NN50, RMSSD, mean HR, pNN50, aVLF, aULF, aTotal & aHF. There have been six cases are considered based on feature selection to validate the classification accuracy. The system of CAD-FSC is justified by taking four classifiers (C-SVM, CG-SVM, C-kNN & W-kNN). The interpretation of the outcomes that the overall classification accuracy has been enhanced up to 99% after employing feature selection by taking all domains HRV features.

5.3.3 HRV Classification by employing MSHVC

Table 5.8 tabulates the comparative outcomes of the ANOVA method which depicts the prominent distinction among the features of different databases. It shows the value in Mean \pm Standard Deviation (SD) form.

Table 5.8: Comparison table of HRV measures by ANOVA test

Domain	HRV Features	MIT/BIH NSR Database	MIT/BIH AR Database	MIT/BIH AF Database	<i>p</i> -value
Time Domain	<i>mean RR</i>	6.63e2 \pm 6.72	6.71e2 \pm 14.40	6.77e2 \pm 25.96	<i>p</i> >0.05
	<i>SDNN</i>	1.44e2 \pm 3.89	1.42e2 \pm 17.20	1.46e2 \pm 9.17	<i>p</i> >0.05
	<i>SDSD</i>	1.98e2 \pm 5.53	1.84e2 \pm 20.76	1.97e2 \pm 13.47	<i>p</i> <0.05
	<i>RMSSD</i>	1.98e2 \pm 5.64	1.84e2 \pm 20.75	1.97e2 \pm 13.47	<i>p</i> <0.05
	<i>NN50</i>	7.88e2 \pm 19.23	5.37e2 \pm 28.54	8.09e2 \pm 50.45	<i>p</i> <0.05
	<i>pNN50</i>	52.28 \pm 0.89	55.51 \pm 2.65	54.80 \pm 3.12	<i>p</i> <0.05
	<i>Max-Min HR</i>	61.11 \pm 0.76	61.78 \pm 1.00	61.28 \pm 1.18	<i>p</i> >0.05
	<i>mean HR</i>	97.05 \pm 1.83	93.78 \pm 4.05	94.89 \pm 5.32	0.01 < <i>p</i> \leq 0.05
Geometrical Domain	<i>HRVTI</i>	22.24 \pm 3.63	26.92 \pm 5.23	21.49 \pm 6.50	<i>p</i> <0.01
Frequency Domain	<i>aULF</i>	0.07 \pm 0.008	0.073 \pm 0.007	0.76 \pm 0.008	<i>p</i> <0.05
	<i>aVLF</i>	1.34 \pm 0.03	1.33 \pm 0.058	1.37 \pm 0.041	<i>p</i> <0.05
	<i>aLF</i>	4.08 \pm 0.60	4.01 \pm 0.11	3.95 \pm 0.66	<i>p</i> >0.05
	<i>aHF</i>	9.34 \pm 0.082	9.13 \pm 0.25	8.89 \pm 1.90	<i>p</i> <0.05
	<i>aTotal</i>	14.76 \pm 0.14	14.47 \pm 0.37	14.81 \pm 0.29	<i>p</i> <0.05
	<i>pVLF</i>	9.07 \pm 0.18	9.17 \pm 0.28	9.27 \pm 0.30	<i>p</i> >0.05
	<i>pLF</i>	27.64 \pm 0.27	27.72 \pm 0.47	27.72 \pm 0.36	<i>p</i> >0.05
	<i>pHF</i>	63.28 \pm 0.21	63.04 \pm 0.58	63.06 \pm 0.57	<i>p</i> >0.05
	<i>Lfnorm</i>	0.30 \pm 0.002	0.30 \pm 0.005	0.30 \pm 0.004	<i>p</i> >0.05
	<i>Hfnorm</i>	0.70 \pm 0.002	0.69 \pm 0.005	0.69 \pm 0.004	<i>p</i> >0.05
<i>LF/HF</i>	0.44 \pm 0.005	0.44 \pm 0.01	0.44 \pm 0.009	<i>p</i> >0.05	

The HRV measures values depend on the waveform duration and sampling frequency of the signal utilized during processing. In this design, the results are taken at a sampling frequency of 1000 Hz for a lengthy ECG dataset. After investigating the result of the

ANOVA method, it is perceived that some HRV parameters (SDSD, RMSSD, NN50, pNN50, HRVTI, aULF, aVLF, aHF, and aTotal) provide a strong caution to reject H_0 . It signifies that these HRV features provide a prominent change in its mean value. The remaining HRV measures signify weak sign against to reject H_0 , except mean HR that delivers moderate significant variation. Normally, the HRV measure explains a strong significant variation that signifies there is a substantial difference arises among different databases. After validating the p -value of ANOVA a prominent variation in different datasets is chosen. The selected features are mean HR SDSD, aTotal, NN50, aULF, aVLF, RMSSD, aHF & pNN50. Table 5.9 tabulates the performance of classifiers in the MSHVC system.

Table 5.9: List of experiments performed for MSHRV system

Case	Level	Experiments	Description
1.	2- Stage Classification	<i>EXP 1</i>	The performance measure of MSHVC before statistical analysis
		<i>EXP 2</i>	The performance measure of MSHVC after statistical analysis
2.	3- Stage Classification	<i>EXP 3</i>	The performance measure of MSHVC before statistical analysis
		<i>EXP 4</i>	The performance measure of MSHVC after statistical analysis

- i. *The performance measure of MSHVC before statistical analysis:* Two-stage classification classifies the dataset into normal and abnormal ECG signals. The first level images are signified as Normal ECG and Abnormal ECG. The outcomes of 2- stage classification before statistical analysis using SVM, kNN, and ANN are tabulated in Table 5.10.

For two-class classification before statistical analysis, the features determining the normal and abnormal ECG gives 86.9% using SVM classifier, 95 % using kNN, and 96.7 %

accuracy using the ANN technique. The best results were obtained using ANN having 100% specificity and 95.3% sensitivity.

ii. *Performance measure of MSHVC after statistical analysis:* Two-stage classification classifies the dataset into normal and abnormal ECG signal. The first level images are signified as Normal ECG and Abnormal ECG. The outcomes of 2- stage classification after statistical analysis using SVM, kNN, and ANN are tabulated in Table 5.11.

Table 5.10: Performance measure of the classification system for two-stage classification before HRV statistical analysis

Features	Classification Technique for 2-stage without feature selection	Confusion Matrix			Sensitivity	Specificity	Accuracy	PPV	AUC
			N	AN					
HRV features (TD,FD,GD)	SVM	N	10	8	100%	55.5%	86.9%	84.3%	0.94
		AN	0	43					
	kNN	N	18	1	95.23%	94.73%	95%	94%	0.95
		AN	2	40					
	ANN	N	18	0	95.3%	100%	96.7%	100%	0.96
		AN	2	41					
N – Normal, AN – Abnormal, PPV- Positive Prediction Value, AUC- Area under the curve									

Table 5.11: Performance measure of classification system for two-stage classification after HRV statistical analysis

Features	Classification Technique for 2-stage with feature selection	Confusion Matrix			Sensitivity	Specificity	Accuracy	PPV	AUC
			N	AN					
HRV features (TD,FD,GD)	SVM	N	18	1	95.23%	94.73%	95%	94%	0.95
		AN	2	40					
	kNN	N	18	1	97.6%	94.7%	96.7%	97.6%	0.96
		AN	1	41					
	ANN	N	18	0	97.67%	100%	98.36%	100%	0.98
		AN	1	42					
N – Normal, AN – Abnormal, PPV- Positive Prediction Value, AUC- Area under the curve									

For two-stage classification after statistical analysis, the features determining the normal and abnormal ECG gives 95% employing SVM classifier, 96.7 % using kNN, and 98.36% accuracy by ANN technique. The best results were obtained using ANN having 100% specificity and PPV along with 97.67% sensitivity. It can be seen that classification accuracy has been improved after feature selection.

The 3-stage classification divides the abnormal ECG into two types of heart disease: Arrhythmia and Atrial Fibrillation. The evaluation parameters of classification are tabulated in Table 12 and Table 13.

- i. *The performance measure of MSHVC before statistical analysis:* The result of 3-stage classification before statistical analysis using SVM, kNN, and ANN is tabulated in Table 5.12.

Table 5.12: Performance measure of classification system for 3-stage classification before HRV statistical analysis

Classification Technique		SVM			kNN			ANN		
		Performance Metrics								
Confusion Matrix		<i>N</i>	<i>AR</i>	<i>AF</i>	<i>N</i>	<i>AR</i>	<i>AF</i>	<i>N</i>	<i>AR</i>	<i>AF</i>
	<i>N</i>	9	2	7	15	1	2	18	0	0
	<i>AR</i>	0	3	17	0	6	14	1	17	0
	<i>AF</i>	0	0	23	0	0	23	2	1	22
PPV	PPV₀	100%			100%			85.71%		
	PPV₁	60%			35.29%			94.44%		
	PPV₂	48.93%			58.97%			100%		
Sen.	Sen₀	50%			83.33%			100%		
	Sen₁	15%			30%			94.44%		
	Sen₂	100%			100%			88%		
Sp.	Sp₀	100%			100%			93.02%		
	Sp₁	92.85%			97.56%			97.60%		
	Sp₂	36.84%			57.89%			100%		
Acc.	Acc₀	85.24%			95.08%			95.08%		
	Acc₁	68.85%			75.40%			96.72%		
	Acc₂	60.65%			35.29%			95.08%		

Overall Accuracy	59%	72.13%	93.4%
AUC	0.91	0.93	0.96

For 3- stage HRV classification, SVM employs only 59%, weighted kNN depicts 72.13 % and ANN provides 93.4% overall accuracy for classification. The better results are obtained from ANN having more AUC of 0.96 than other classifiers.

- ii. *The performance measure of MSHVC after statistical analysis:* The result of 3-stage classification after statistical analysis using SVM, kNN, and ANN is tabulated in Table 5.13.

Table 5.13: Performance measure of classification system for three stage classification after HRV statistical analysis

Classification Technique		SVM			kNN			ANN		
		Performance	Metrics							
Confusion Matrix		<i>N</i>	<i>AR</i>	<i>AF</i>	<i>N</i>	<i>AR</i>	<i>AF</i>	<i>N</i>	<i>AR</i>	<i>AF</i>
	<i>N</i>	15	2	1	18	0	0	18	0	0
	<i>AR</i>	0	7	13	1	17	0	0	20	0
	<i>AF</i>	0	0	23	2	1	22	1	0	22
PPV	PPV₀	100%			85.71%			94.73%		
	PPV₁	77.77%			94.44%			100%		
	PPV₂	62.16%			100%			100%		
Sen.	Sen₀	83.33%			100%			100%		
	Sen₁	23.33%			94.44%			100%		
	Sen₂	100%			88%			95.65%		
Sp.	Sp₀	100%			93.02%			100%		
	Sp₁	95.12%			97.60%			100%		
	Sp₂	63.15%			100%			100%		
Acc.	Acc₀	95.08%			95.08%			99%		
	Acc₁	75.40%			96.72%			100%		
	Acc₂	77.04%			95.08%			99%		
Overall Accuracy		73.77%			93.4%			99%		
AUC		0.92			0.94			1.00		

After statistical analysis of 3-stage classification, an increment in the overall accuracy has been observed. For 3- stage HRV classification, SVM results in 73.77% of overall accuracy, weighted kNN gives 93.4% and ANN results in 99% overall accuracy for classification. The remarkable results are obtained using ANN and a significant improvement is observed in overall accuracy after feature selection.

(a) Percentage Improvement in MSHVC system at various level of abstraction

The percentage enhancement is deliberated to justify the performance at various levels of abstraction in the classification system. The computation is done in three parts: percentage improvement of 2-stage classification, percentage improvement of 3-stage classification, and percentage improvement of MSHVC system.

- i. Percentage improvement of 2-stage classification:* For the 2-stage classification phase, a significant percentage improvement in the performance parameters for all the classification approaches before HRV statistical analysis and after HRV statistical analysis using three classifiers is observed. SVM provides the maximum percentage improvement of 11.7% in the overall accuracy and ANN depicts a maximum of 3 % improvement for Area underneath the Receiver Operating Characteristics (ROC) curve. Figure 5.15 visually represents the percentage improvement in accuracy and AUC.

A significant percentage improvement has been drawn during multistage classification. For 2 –stage classification system SVM, kNN, and ANN give 11.7 %, 1.6 %, and 3.3 % of improvement respectively. For 3-stage classification the presented system observed noticeable improvement, it gives 20.02% in SVM, 26.66% in kNN, and 6.6% in the ANN classification system.

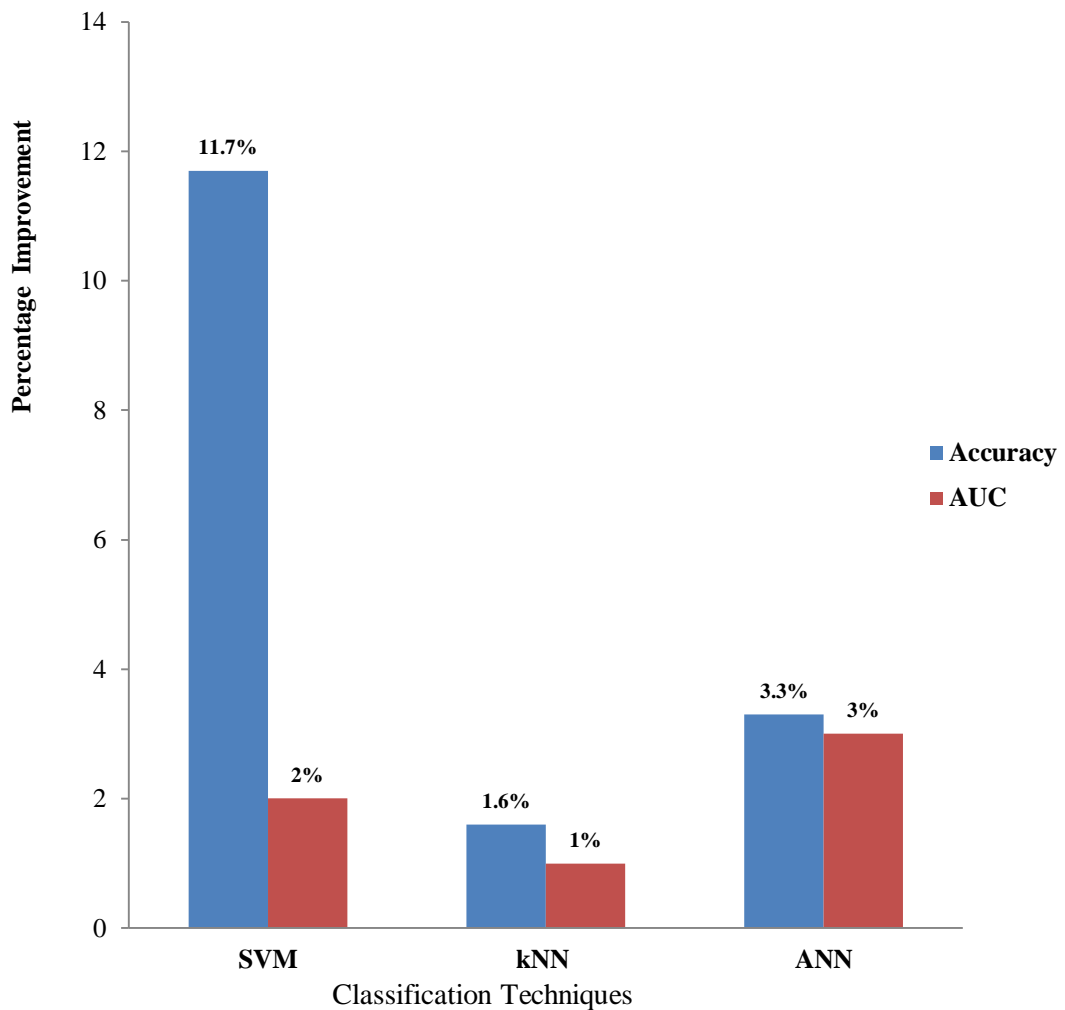


Figure 5.15: Percentage Improvement for accuracy and AUC during 2-6 classification.

- ii. *Percentage improvement during 3-stage classification:* For the 3-stage classification phase noteworthy percentage improvement in the accuracy and AUC parameters is seen before HRV statistical analysis and after HRV statistical analysis. kNN achieved the maximum percentage improvement of 26.63% in the overall accuracy and SVM gives 7.14% improvement for Area under the Receiver Operating Characteristics (ROC) curve. Figure 5.16 depicts the percentage improvement in accuracy and AUC for 3-stage classification.

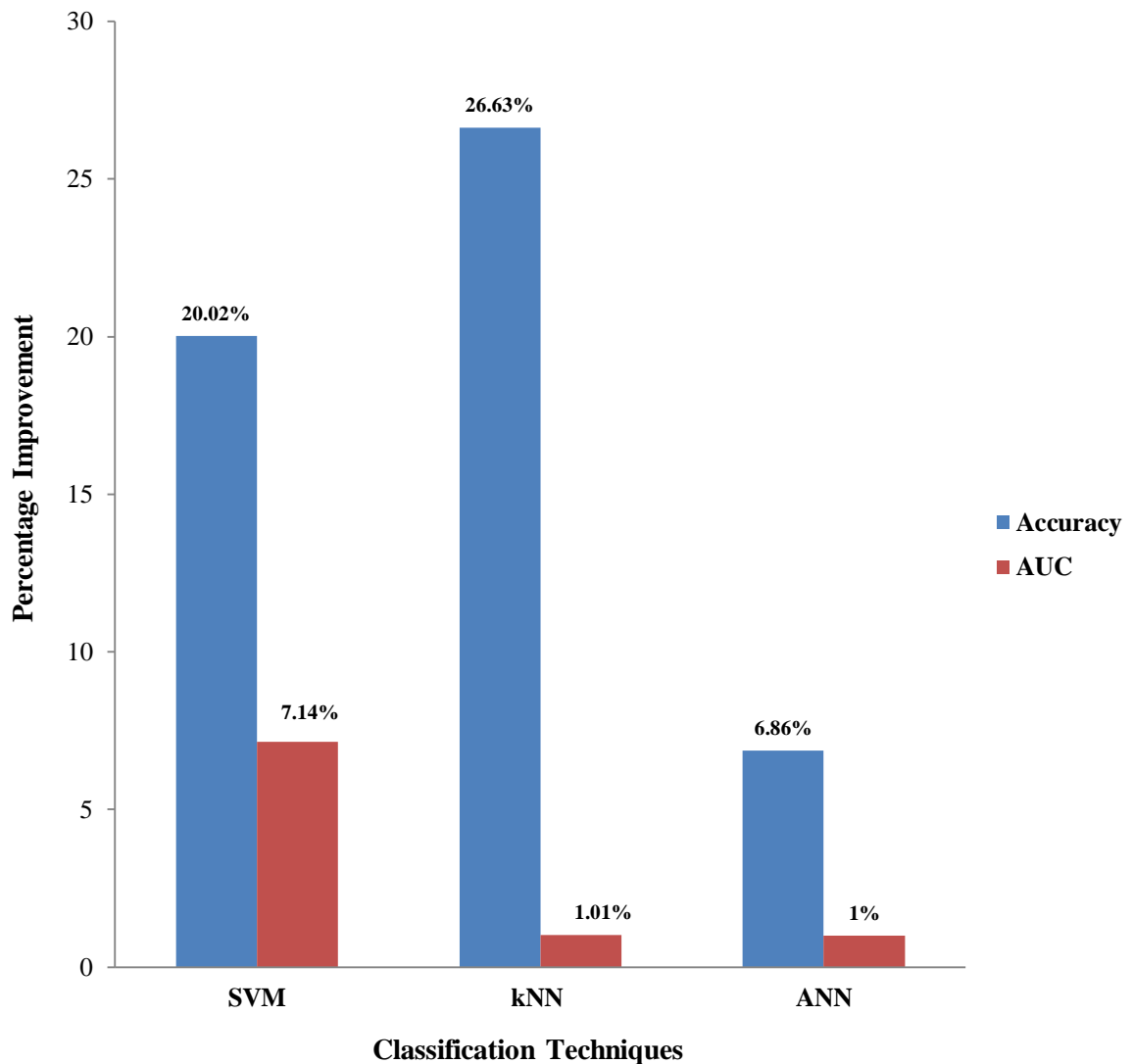


Figure 5.16: Percentage Improvement for accuracy and AUC during 3-stage classification.

- iii. *Percentage improvement in MSHVC system:* A considerable percentage improvement has been drawn during the MSHVC system demonstrated in Figure 5.17. For 2 –stage classification system SVM, kNN, and ANN result in 11.7 %, 1.6 %, and 3.3 % improvement respectively. For the 3-stage classification, the proposed system observed noticeable improvement. It results in 20.02% for SVM, 26.66% for kNN, and 6.6% for the ANN classification system.

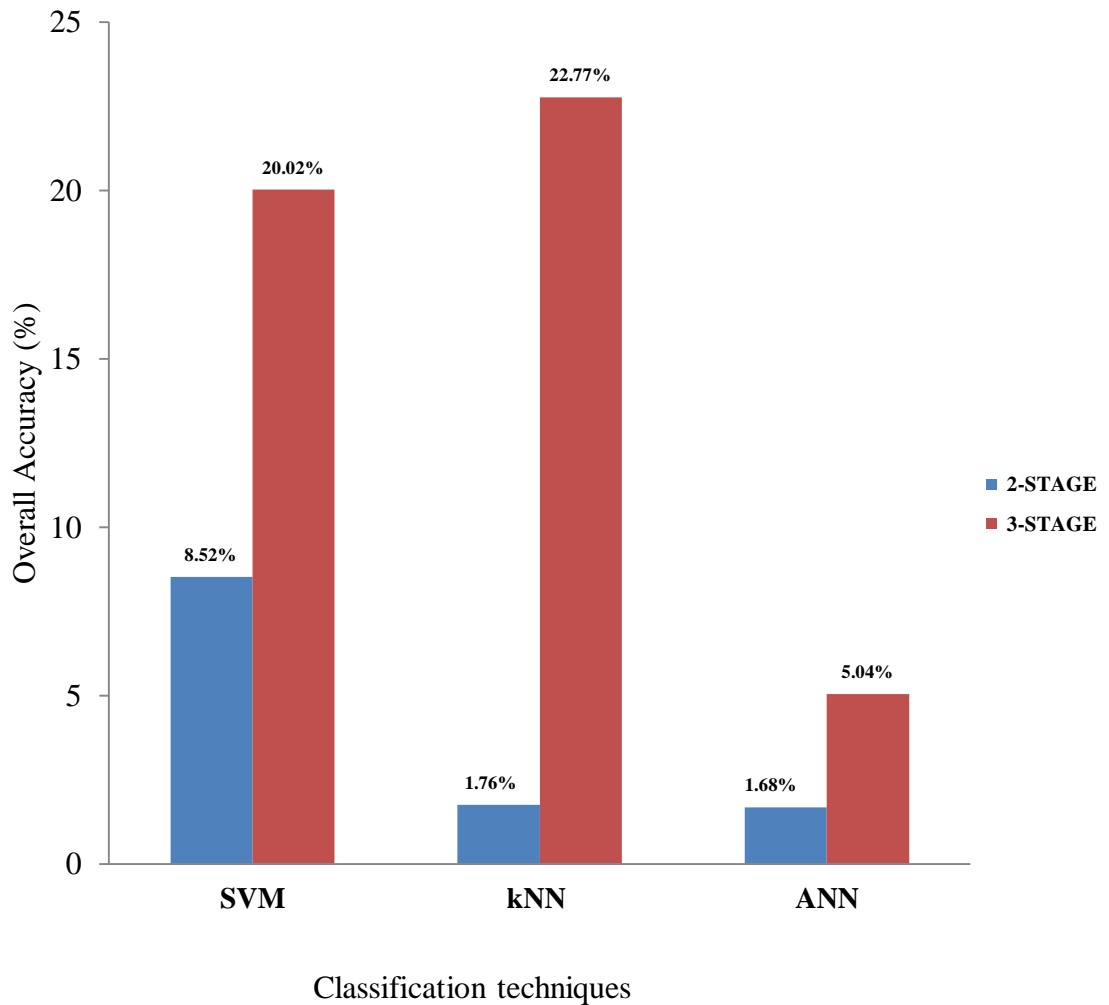


Figure 5.17: Percentage improvement during MSHVC classification.

An MSHVC system illustrates the detection of AR, AF, and NSR ECG. Detection of these diseases is done based on long-term HRV analysis. The twenty features in the time-domain, frequency-domain, and geometrical domain were extracted. Only 9 parameters are chosen namely RMSSD, SDDSD, HRVTI, NN50, pNN50, aHF, , aVLF, aULF, & aTotal. A total of four experiments has been performed two each in 2-stage classification and 3-stage classification. All the performance parameters are evaluated before statistical analysis and after statistical analysis. The SVM, kNN, and ANN classifiers are compared with the MSHVC system. The conclusion has been drawn that for the proposed system ANN has attained 99% overall accuracy at 2-stage and 3-stage classification. The innovation of this work manifested in the statistical study, which is used to extract the most significant features via the ANOVA technique. It is observed that classification

performance parameters of 2-stage and 3-stage classification are significantly improved after statistical analysis.

5.4 COMPARISON OF PROPOSED METHODOLOGIES WITH RECENT LITERATURE

The three proposed methodologies are compared with the recent classification techniques. The presented methodology implemented multi-stage classification to diagnose AR, AF & NSR ECG. Table 5.14 tabulates the comparison by considering the database utilized, the number of features used, time length, classification algorithm employed, and performance parameters. The presented methodology contributes to multistage classification of AR, AF, and NSR long-term ECG by extracting twenty HRV features from frequency-domain, time-domain, and geometrical-domain. Popular classification techniques namely SVM, kNN, and ANN are applied on nine significant features computed from ANOVA. It is observed that ANN shows remarkable results for MSHVC classification.

Table 5.14: Comparison with existing literature

Previous Work (Year)	Database used	Number of features	Time length	Classification Technique	Accuracy	Specificity	Sensitivity	Overall Accuracy Improvement
<i>Time domain</i>	<i>NSR and AR</i>	4	24-h	<i>kNN</i>	82%	90.83%	82.7%	17%
<i>MSHVC Technique</i>	<i>NSR, AR and AF</i>	9	24-hr	<i>MSHVC</i>	99%	100%	98.55%	Selected
<i>CAD-FSC</i>	<i>NSR, AR and AF</i>	9	24-h	<i>CAD-FSC</i>	97%	99.20%	98.61%	2.02%
[173]	NSR, CHF	34	5-min	3-stage classifier	98.2%	98.1%	97%	0.4%
[107]	NSR, CHF	9	2- hr	SVM	94.44%	98.33%	86.67%	4.60%
[107]	NSR, CHF	3	5 min	SVM	96.67%	98.33%	93.33%	2.35%
[172]	NSR, CHF	9	5-min	SVM	90.95%	90.03%	91.31%	8.13%
[105]	AFPDB	25	5-min	SVM	87.7%	88.7%	86.8%	11.41%
[108]	NSR, CHF, Long term ST-T	3	24-hr	Ensemble of bagged decision tree	98.1%	99.3%	98.57%	1%
[115]	NSR, CHF	4	1000 RR-intervals	kNN	87.9%	94.4%	80%	11.44%
[110]	AFPDB	26	15-min	SVM	79.3%	81.1%	79.3%	19.89

A 3-stage classifier to Detect Congestive Heart Failure (CHF) from NSR is proposed in [173]. He extracted thirty-four features for 5-min of time length and obtained 98.8%, 98.1% and 100% of accuracy, specificity and sensitivity respectively. In [107] classifies

similar database using SVM for 2-hour & 5-minute frames length is taken. It attains 94.44% & 96.67% classification accuracy respectively. In [172] practice SVM with CHF and NSR on nine feature and attained 90.95% of accuracy, 90.03 % of specificity, and 91.31% of sensitivity. An Atrial Fibrillation Prediction (AFPDB) system is presented in 2016 and 2018 to classify paroxysmal atrial fibrillation employing SVM & acquiring 79.3% of accuracy in 15-minute duration and improved accuracy of 87.7% for the 5-minute time length of ECG [105, 110]. Ensemble classifier is applied by [108] to diagnose CHF, NSR, and long-term ST-T database based on three HRV features, he obtained 98.1%, 100% and 98.57 % of accuracy, specificity, and sensitivity respectively [108]. Lastly, kNN is applied to detect CHF and NSR using four HRV feature for 1000 RR-intervals and attained 79.3 % accuracy, 81.1% specificity, and 79.3 % sensitivity [115]. Our proposed system outperforms all the recent techniques and attained 99% overall accuracy.

5.5 CONCLUSION

The main aim of this chapter is to detect the most appropriate HRV features for the classification of sinus rhythm, arrhythmia, and atrial fibrillation diseases. The elimination of the unwanted noise is done using a digital filter and a QRS detection algorithm is employed to calculate HR from the ECG waveform. The HR helps to compute several HRV features; which performs a significant role to classify heart disease to deliver a precise non-invasive diagnosis. All the HRV measures provide diverse information of the ANS and PNS. The statistical analysis helps to select these significant features from the group of HRV features by eliminating redundant and irrelevant features. Only a few attributes signify a prominent effect on the classification accuracy and by utilizing these features three methodologies are proposed to develop an algorithm for better classification. A maximum of 82%, 97%, and 99% of overall accuracy is obtained by time-domain methodology, CAD-FSC system, and MSHVC system respectively by applying SVM, kNN, and ANN classifiers.

CHAPTER 6
CONCLUSION AND FUTURE
SCOPE

CHAPTER 6

CONCLUSION AND FUTURE SCOPE

6.1 CONCLUSION

The objective of the conclusion chapter is to summarize the crux of the presented research that aims to design an expert system for low power wearable ECG module. This research focuses on the FPGA based ECG de-noising architectures using digital filters. The noise-free ECG signals is very decisive in the detection of various HRV based CVDs. Many windows based digital FIR filter architectures are utilized to eradicate the EMG, BLW & PLI noise. The clean ECG facilitate good performance in the classification process of various CVDs. Several findings have been observed during the research, which is concluded chapter-wise in this section. The future scope has also been discussed at the end of this chapter.

The detailed functioning of the human cardiac system has been discussed in the first chapter. The cardiac system regulates the flow of blood in the entire body. The repolarization & depolarization in cardiac cells leads to generating the ECG waveform that helps to diagnose various CVDs. Different kinds of low & high-frequency noises that contaminate the ECG signal during the acquisition that deteriorates the informatory ECG signal has been deliberated. This study focuses on the noise removal techniques and extraction of useful ECG signals.

An extensive literature survey has been carried out in the second chapter. A review has been performed in the field of QRS detection algorithms, several kinds of CVDs, FPGA implementation of digital filter design. An extensive study on the machine learning algorithms based on HRV is accomplished. The exhaustive study of the popular and recent literature assists the researchers to discover some of the research gaps. Based on these research gaps, different objectives were framed for this research work.

The execution of various Bio-signal processing approaches for the eradication of artifacts from the raw ECG signal is described in the third chapter. A low resource, real-time acquisition of ECG signal denoising circuit is simulated in VIVADO software by

targeting the Zynq-7000 board. It is analyzed to find the effectiveness of the circuit to acquire real-time noise-free ECG signals. The FIR window-based functions for the simultaneous removal of ECG noises are applied. A modified hamming window has also been proposed & selected for its better frequency response. The modified window consumes fewer resources in comparison to classical window functions due to its symmetrical nature. It consumes less than 1% of the resources that existed in the latest FPGA board. The proposed XSG architecture consumed more power in comparison to the existed literature. These architectures have been utilized in stationary ECG module, where power consumption is not an important parameter.

The wearable & portable ECG system needs a large battery life, which is an important parameter. It is achieved by introducing a power-efficient ECG denoising module. In the fourth chapter power-efficient collateral & sequence XSG, architecture has been designed & evaluated. These architectures attain the low power criterion along with simultaneous removal of all the ECG noises. The simulation & synthesization of the XSG model is done on the VIVADO tool using the Verilog HDL language. The sequence XSG model has been selected because it consumes only 0.138 Watt of on-chip power. The selected sequence XSG architecture using modified window function sequence consumes low resources & power in comparison to existing literature which is favorable for handheld ECG devices. A noiseless & clean ECG signal is very important to categorize the CVDs by employing machine learning approaches.

The fifth chapter of this work proposes a novel approach and methodology for the HRV based classification system. It incorporates various machine learning algorithms namely SVM, kNN & ANN. A multistage HRV based classification system has been introduced for the classification of Arrhythmia, Atrial Fibrillation & Normal Sinus Rhythm. A total of 21 HRV features are extracted from the time, frequency & geometric domain. The SPSS tool has been utilized to remove redundant features. The *t*-test & ANOVA technique helps to remove the irrelevant features & only 9 features have been selected that give a prominent effect on the classification accuracy. The three classification system namely time domain, CAD-FSC & MSHVC has been introduced to classify arrhythmia, atrial fibrillation & normal sinus rhythm based on extracted features, feature selection technique & classifier used. The MSHVC system attains 99% overall accuracy that facilitates the ECG classification system to classify the CVDs accurately.

This thesis work finally proposed a low power expert system developed for HRV based multi-stage classification as shown in Figure 5.18.

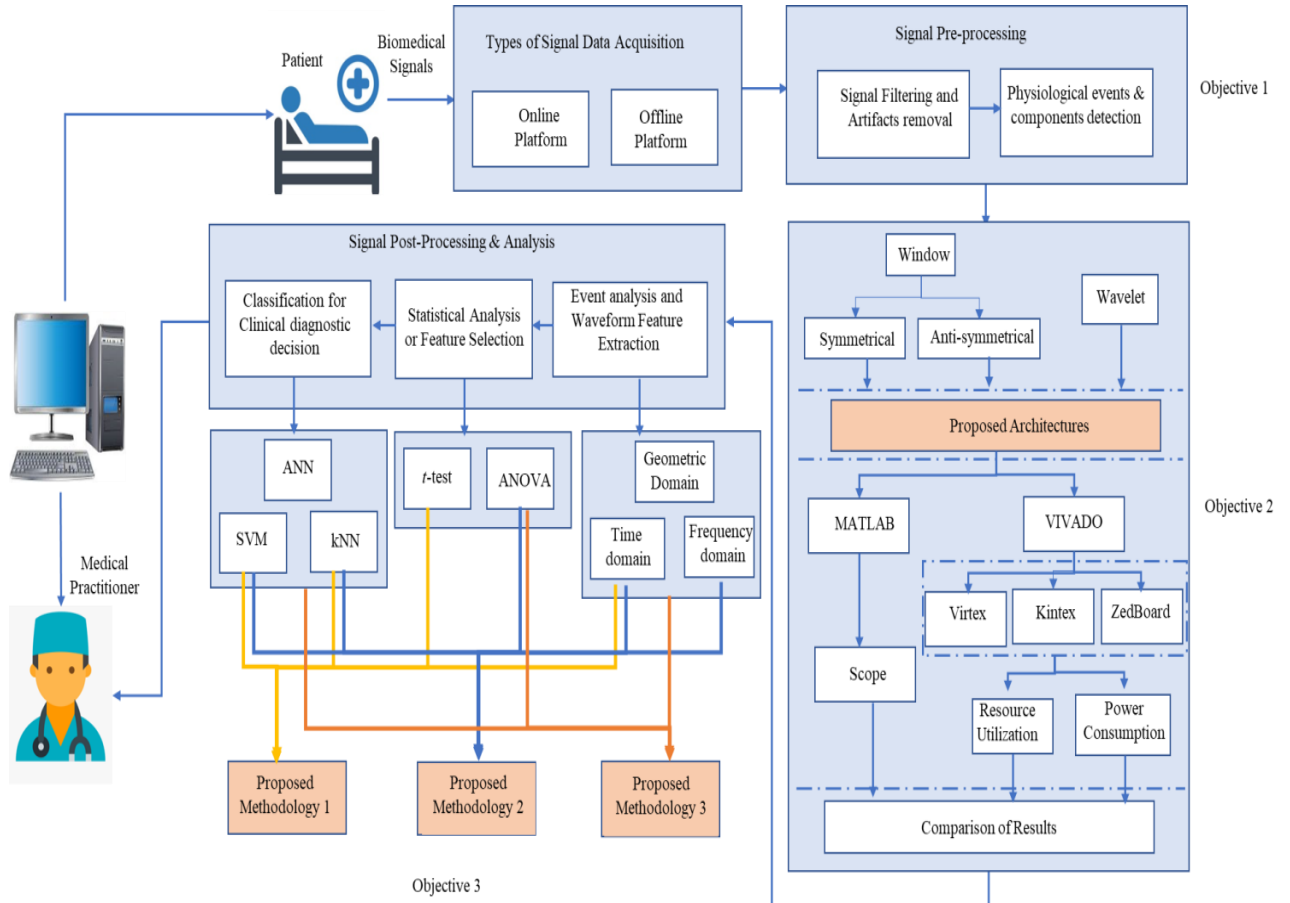


Figure 6.1: An expert system for low power wearable ECG module

It incorporates the proposed ECG denoising architecture for the pre-processing block. The expert system also comprises of proposed methodologies, which are based on different types of feature extraction, statistical analysis & classifiers utilized to categorize the arrhythmia, atrial fibrillation & normal sinus rhythm.

An expert low power wearable multistage HRV based classification system is introduced during this research work that will help the individual in monitoring cardiac

health. Finally, the methodology of a power-efficient wearable ECG expert system for HRV based classification has been presented.

6.2 FUTURE SCOPE

Based on the results attained in this research, work improvement has been done concerning a recent study. The possibility in the application areas of ECG wearable modules is exhaustive & time-consuming. This research focuses on the knowledge escalation on the clinical utilization of biomedical devices. Future research examined the possible area for the new technology in biomedical ECG devices.

1. In this study, the ECG signal assists to classify various CVDs. To enhance the overall diagnostic accuracy other bio-signals such as Atrial Blood Pressure (ABP), Pulsatile cardiovascular signals (PPG) & ECG-Derived Respiration (EDR) signal must be considered.
2. The hardware implementation of a low-power ECG denoising module on VIVADO has been achieved in this work. The work can be further extended by implementing the classification methodologies on FPGA. Thus, an overall expert system for wearable ECG device can be designed.
3. The wireless protocol can be utilized to enhance the applicability of the research work. IoT based design can be employed in the design methodology for wearable ECG module. By using this feature patients can directly connect to their clinicians using its dedicated android app.
4. All the existed work incorporates the time plane features & amplitude information. A further investigation can be done by considering the fusion of these HRV based features & their effect on the classification accuracy.
5. Apart from the Arrhythmia & Atrial Fibrillation CVD utilized in this work. A robust classifier can be designed by considering other types of abnormalities.

6. The proposed research is based on a small group of subjects. To apply the classification on a large dataset, Deep Neural Network (DNN) can be employed to verify the feasibility in this application. DNN can easily handle a large number of databases, as it reduces the execution of complex computations during the extraction of features.

7. The proposed design is verified with physionet database. Real-time data can be taken from hospitals, which consider different sex, age, disease community to authenticate the applicability area of the presented methodology.

LIST OF PUBLICATIONS

LIST OF PUBLICATIONS

1. Kirti, Harsh Sohal and Shruti Jain, “Design and Implementation of Low Power ECG Pre-processing Module on Xilinx FPGA”, *IETE Journal of Research*, 2020

(SCI Indexed) (IF: 1.03)

2. Kirti, Harsh Sohal, and Shruti Jain, “Multistage Classification of Arrhythmia and Atrial Fibrillation on Long- Term Heart Rate Variability”, *Journal of Engineering Science and Technology*, Vol. 15 (2), 2020

(ESCI Indexed)

3. Kirti, Harsh Sohal and Shruti Jain, “Statistical analysis of HRV parameters for the detection of Arrhythmia”, *International Journal of Imaging and Graphics*,

(In Press) (ESCI Indexed)

4. Kirti, Harsh Sohal and Shruti Jain, “Computer Aided Diagnostic System for Feature Based Classification using Heart Rate Variability”, *Biomedical Engineering Applications, Basis and Communications*, Vol. 32 (2), 2020.

(ESCI Indexed)

5. Kirti, Harsh Sohal and Shruti Jain, “Comparative Analysis of Heart Rate Variability Parameters for Arrhythmia and Atrial Fibrillation using ANOVA”, *Biomedical and Pharmacology Journal*, vol. 11, pp. 1841-1849, 2018.

(Scopus Indexed)

6. Kirti, Harsh Sohal and Shruti Jain, “FPGA implementation of Power-Efficient ECG pre-processing block”, *International Journal of Recent Technology and Engineering*, vol. 8 (1), pp. 2899-2904, 2019.

(Scopus Indexed)

7. Kirti, Harsh Sohal and Shruti Jain, “Interpretation of Cardio Vascular Diseases using Electrocardiogram: A Study”, 5th, IEEE International Conference on Parallel, Distributed and Grid Computing (PDGC), Jaypee University of Information Technology, Waknaghat, Solan, H.P, India, Dec. 20-22, 2018.

8. Kirti, Harsh Sohal and Shruti Jain, “Review and Comparison of QRS Detection Algorithms for Arrhythmia”, 5th International Conference on Signal Processing, Computing and Control (ISPC), Jaypee University of Information Technology, Waknaghat, Solan, H.P, India, Oct. 10-12, 2019.

REFERENCES

REFERENCES

- [1] Rakshit, Manas. "Real-time Electrocardiogram (ECG) signal analysis and Heart Rate determination in FPGA platform." PhD diss., 2015.
- [2] World Health Organization. Cardiovascular diseases. Available: <https://www.who.int/healthtopics/cardiovascular-diseases>.
- [3] Prabhakaran, Dorairaj, Panniyammakal Jeemon, and Ambuj Roy. "Cardiovascular diseases in India: current epidemiology and future directions." *Circulation* 133, no. 16 1605-1620, 2016.
- [4] Huseby, Miriam Kirstine. "FPGA Based Development Platform for Biomedical Measurements: ECG Module." Master's thesis, 2013.
- [5] C. Bearzi, M. Rota, T. Hosoda, J. Tillmanns, A. Nascimbene, A. De Angelis, S. Yasuzawa-Amano, I. Tromova, R. W. Siggins, N. Lecapitaine, S. Cascapera, A. P. Beltrami, D. A. D'Alessandro, E. Zias, F. Quaini, K. Urbanek, R. E. Michler, R. Bolli, J. Kajstura, A. Leri, and P. Anversa, Human cardiac stem cells. *Proceedings of the National Academy of Sciences of the United States of America*, vol. 104, pp. 1406814073, 2007.
- [6] D. S. Park and G. I. Fishman, *The cardiac conduction system*, pp. 904915, 2011.
- [7] A. A. Grace and D. M. Roden, *Systems biology and cardiac arrhythmias*. *Lancet*, vol. 380, pp. 1498508, 2012.
- [8] ECG waveform. Available: <https://www.researchgate.net/publication/287200946>
- [9] Ghosh, Ria. "Hardware Implementation of Real-Time Beat Detection and Classification Algorithm for Automated ECG Analysis." PhD diss., 2018.
- [10] Hamilton, Pat. "Open source ECG analysis." In *Computers in cardiology*, pp. 101-104. IEEE, 2002.
- [11] Seema Nayak, Manoj Nayak, Pankaj Pathak. "Chapter 1: A Review on FPGA-Based Digital Filters for De-Noiseing ECG Signal" , IGI Global, 2020.
- [12] Seema, Bhogeshwar Sande. "Synthesis and analysis of digital filters on FPGA for denoising ECG signal.", 2017
- [13] I. I. Christov, Real time electrocardiogram QRS detection using combined adaptive threshold. *Biomedical engineering online*, vol. 3, p. 28, 2004.
- [14] A. L. Goldberger, L. A. Amaral, L. Glass, J. M. Hausdor, P. C. Ivanov, R. G. Mark, J. E. Mietus, G. B. Moody, C. K. Peng, and H. E. Stanley, PhysioBank, PhysioToolkit, and

PhysioNet: components of a new research resource for complex physiologic signals. *Circulation*, vol. 101, pp. E215-E220, 2000.

[15] Mirzei, Shahnam. *Design methodologies and architectures for digital signal processing on fpgas*. University of California, Santa Barbara, 2010.

[16] Herniter, Marc E. *Programming in MATLAB*. Brooks/Cole Publishing Co., 2000.

[17] Líčko, Miroslav, Jan Schier, Milan Tichý, and Markus Köhl. "Matlab/simulink based methodology for rapid-fpga-prototyping." In *International Conference on Field Programmable Logic and Applications*, pp. 984-987. Springer, Berlin, Heidelberg, 2003.

[18] Mittal, Sparsh, Saket Gupta, and S. Dasgupta. "System generator: The state-of-art FPGA design tool for dsp applications." In *Third International Innovative Conference On Embedded Systems, Mobile Communication And Computing (ICEMC2 2008)*, pp. 187-190. 2008.

[19] Valters, Gatis. "Initial version of MATLAB/SIMULINK based tool for VHDL code generation and FPGA implementation of Elementary Generalized Unitary Rotation." In *2011 NORCHIP*, pp. 1-6. IEEE, 2011.

[20] Dabney, James B., and Thomas L. Harman. *Mastering simulink*. Pearson, 2004.

[21] Lu, Dengsheng, and Qihao Weng. "A survey of image classification methods and techniques for improving classification performance." *International journal of Remote sensing* 28, no. 5 (2007): 823-870.

[22] Kim, Hye-Geum, Eun-Jin Cheon, Dai-Seg Bai, Young Hwan Lee, and Bon-Hoon Koo. "Stress and heart rate variability: a meta-analysis and review of the literature." *Psychiatry investigation* 15, no. 3 (2018): 235.

[23] J. Pan and W. J. Tompkins, "A real-time QRS detection algorithm," *IEEE transactions on biomedical engineering*, pp. 230-236, 1985.

[24] P. S. Hamilton and W. J. Tompkins, "Quantitative investigation of QRS detection rules using the MIT/BIH arrhythmia database," *IEEE transactions on biomedical engineering*, pp. 1157-1165, 1986.

[25] D. Benitez, P. Gaydecki, A. Zaidi, and A. Fitzpatrick, "A new QRS detection algorithm based on the Hilbert transform," in *Computers in Cardiology 2000*, 2000, pp. 379-382.

[26] N. M. Arzeno, Z.-D. Deng, and C.-S. Poon, "Analysis of first-derivative based QRS detection algorithms," *IEEE Transactions on Biomedical Engineering*, vol. 55, pp. 478-484, 2008.

- [27] C. Li, C. Zheng, and C. Tai, "Detection of ECG characteristic points using wavelet transforms," *IEEE Transactions on biomedical Engineering*, vol. 42, pp. 21-28, 1995.
- [28] S. Rekik and N. Ellouze, "Enhanced and Optimal Algorithm for QRS Detection," *IRBM*, vol. 38, pp. 56-61, 2017.
- [29] S. Farashi, "A multiresolution time-dependent entropy method for QRS complex detection," *Biomedical Signal Processing and Control*, vol. 24, pp. 63-71, 2016.
- [30] Y.-C. Yeh and W.-J. Wang, "QRS complexes detection for ECG signal: The Difference Operation Method," *Computer methods and programs in biomedicine*, vol. 91, pp. 245-254, 2008.
- [31] L. D. Sharma and R. K. Sunkaria, "A robust QRS detection using novel pre-processing techniques and kurtosis based enhanced efficiency," *Measurement*, vol. 87, pp. 194-204, 2016.
- [32] P. Phukpattaranont, "QRS detection algorithm based on the quadratic filter," *Expert Systems with Applications*, vol. 42, pp. 4867-4877, 2015.
- [33] M. Merino, I. M. Gómez, and A. J. Molina, "Envelopment filter and K-means for the detection of QRS waveforms in electrocardiogram," *Medical engineering & physics*, vol. 37, pp. 605-609, 2015.
- [34] K. Arbateni and A. Bennis, "Sigmoidal radial basis function ANN for QRS complex detection," *Neurocomputing*, vol. 145, pp. 438-450, 2014.
- [35] T. Sharma and K. K. Sharma, "QRS complex detection in ECG signals using locally adaptive weighted total variation denoising," *Computers in Biology and Medicine*, vol. 87, pp. 187-199, 2017.
- [36] Y. Li, X. Tang, Z. Xu, and H. Yan, "A novel approach to phase space reconstruction of single lead ECG for QRS complex detection," *Biomedical Signal Processing and Control*, vol. 39, pp. 405-415, 2018.
- [37] Hou, Zhongjie, Yonggui Dong, Jinxi Xiang, Xuewu Li, and Bin Yang. "A Real-Time QRS Detection Method Based on Phase Portraits and Box-Scoring Calculation." *IEEE Sensors Journal* 18, no. 9 (2018): 3694-3702.
- [38] Chin, Wen-Long, Cheng-Chieh Chang, Cheng-Lung Tseng, Ying-Zhe Huang, and Tao Jiang. "Bayesian Real-Time QRS Complex Detector for Healthcare System." *IEEE Internet of Things Journal* (2019).
- [39] R. B. Hinton and K. E. Yutzey, "Heart valve structure and function in development and disease," *Annual review of physiology*, vol. 73, pp. 29-46, 2011.

- [40] D. P. Zipes, P. Libby, R. O. Bonow, D. L. Mann, and G. F. Tomaselli, *Braunwald's Heart Disease E-Book: A Textbook of Cardiovascular Medicine: Elsevier Health Sciences*, 2018.
- [41] M. Rivera-Ruiz, C. Cajavilca, and J. Varon, "Einthoven's string galvanometer: the first electrocardiograph," *Texas Heart Institute Journal*, vol. 35, p. 174, 2008.
- [42] J. Cloutier, C. Hayes, and D. Allen, "Reducing Delay to Treatment Of St-Elevation Myocardial Infarction With The Use Of Software Electrocardiographic Interpretation And Electronic Transmission (SCINET)," *Canadian Journal of Cardiology*, vol. 34, pp. S150-S151, 2018.
- [43] A. Gacek and W. Pedrycz, *ECG signal processing, classification and interpretation: a comprehensive framework of computational intelligence: Springer Science & Business Media*, 2011.
- [44] P. Kligfield, L. S. Gettes, J. J. Bailey, R. Childers, B. J. Deal, E. W. Hancock, et al., "Recommendations for the standardization and interpretation of the electrocardiogram: part I: the electrocardiogram and its technology a scientific statement from the American Heart Association Electrocardiography and Arrhythmias Committee, Council on Clinical Cardiology; the American College of Cardiology Foundation; and the Heart Rhythm Society endorsed by the International Society for Computerized Electrocardiology," *Journal of the American College of Cardiology*, vol. 49, pp. 1109-1127, 2007.
- [45] J. W. Mason, E. W. Hancock, and L. S. Gettes, "Recommendations for the standardization and interpretation of the electrocardiogram: part II: electrocardiography diagnostic statement list a scientific statement from the American Heart Association Electrocardiography and Arrhythmias Committee, Council on Clinical Cardiology; the American College of Cardiology Foundation; and the Heart Rhythm Society Endorsed by the International Society for Computerized Electrocardiology," *Journal of the American College of Cardiology*, vol. 49, pp. 1128-1135, 2007.
- [46] R. G. Afkhami, G. Azarnia, and M. A. Tinati, "Cardiac arrhythmia classification using statistical and mixture modeling features of ECG signals," *Pattern Recognition Letters*, vol. 70, pp. 45-51, 2016.
- [47] S. Rana, S. Jain, and J. Virmani, "Classification of focal kidney lesions using wavelet-based texture descriptors," *International Journal of Pharma and Bio Sciences*, vol. 7, pp. 646-652, 2016.

- [48] S. Bhusri and S. Jain, "Analysis of breast lesions using laws' mask texture features," in *Parallel, Distributed and Grid Computing (PDGC), 2016 Fourth International Conference on*, 2016, pp. 56-60.
- [49] N. Parashar, S. Jain, M. Sood, and J. Dogra, "Review of biomedical system for high performance applications," in *Signal Processing, Computing and Control (ISPCC), 2017 4th International Conference on*, 2017, pp. 300-304.
- [50] A. Dhiman, S. Dubey, S. Jain, "Design of Lead II ECG Waveform and Classification Performance for Morphological features using Different Classifiers on Lead II," *Research Journal of Pharmaceutical, Biological and Chemical Sciences (RJPBCS)*, vol. 7, pp. 1226-1231 July-Aug 2016.
- [51] R. Martinek, R. Kahankova, J. Nedoma, M. Fajkus, and K. Cholevova, "Fetal ECG Preprocessing Using Wavelet Transform," in *Proceedings of the 10th International Conference on Computer Modeling and Simulation*, 2018, pp. 39-43.
- [52] S. Jain. S. Rana , J. Virmani "SVM-Based Characterization of Focal Kidney Lesions from B-Mode Ultrasound Images," *Research Journal of Pharmaceutical, Biological and Chemical Sciences (RJPBCS)*, vol. 7, pp. 837- 846, July- Aug 2016.
- [53] G. Baroldi, "Different types of myocardial necrosis in coronary heart disease: a pathophysiologic review of their functional significance," *American heart journal*, vol. 89, pp. 742-752, 1975.
- [54] Tragardh, E. and Schlegel, T. T. (2006) "High-Frequency ECG", USA.
- [55] Sadabadia, H., Ghasemia, M. and Ghaffaria, A.(2007) "A Mathematical Algorithm For ECG Signal denoising Using Window Analysis", *Biomed Pap Med FacUnivPalacky Olomouc Czech Repub*,7, Vol. 151, No. 1, pp.73–78.
- [56] Sayadi, O. and Shamsollahi, M.B., (2008) "ECG Denoising and Compression Using a Modified Extended Kalman Filter Structure", *IEEE Transactions On Biomedical Engineering*, Vol. 55, No. 9, pp. 2240-2248.
- [57] Kaur, M., Singh, B. and Seema (2011) "Comparisons of Different Approaches For Removal of Baseline Wander From ECG Signal", in *2nd International Conference and workshop on Emerging Trends in Technology 2011*, Proceedings published by *International Journal of Computer Applications*, pp.30-36.
- [58] Zaman, M.T.U., Hossain, D., Arefin, M.T., Rahman, M.A., Islam, S.N. and Haque, A.K.M. F. (2012) "Comparative Analysis of De-Noising on ECG Signal", *International Journal of Emerging Technology and Advanced Engineering*, Vol. 2, No.11, pp. 479- 486.

- [59] Chandrakar, B., Yadav, O.P. and Chandra, V.K, “A Survey of Noise Removal Techniques For ECG Signals”, *International Journal of Advanced Research in Computer and Communication Engineering*, Vol. 2, No. 3, pp. 1354-1357,2013.
- [60] Joshi, P. J., Patkar, V. P., Pawar, A.B., Patil, P. B., Bagal, U.R. and Mokal, B. D. “ECG Denoising Using MATLAB”, *International Journal of Scientific & Engineering Research*, Vol.4, No.5, pp.1401-1405, 2013.
- [61] Barik, R. K., Dwibedi, S.K., Rout, S.S. and Sahu, S.R. “An Improved and Efficient MAC Unit and Its Implementation in FPGA”, *International Journal of Review in Electronics & Communication Engineering*, Vol. 2, No. 2, pp. 71-74, 2014.
- [62] Bortolan, G. and Christov, I. “Dynamic Filtration of High-Frequency Noise in ECG Signal”, *Computing in Cardiology* , ISSN 2325-8861, Vol. 41, pp.1089-1092, 2014.
- [63] 1. J. Xiang, Y. Dong, X. Xue, and H. Xiong, “Electronics of a wearable ECG with level crossing sampling and human body communication, ”*IEEE Transaction Biomedical Circuits System*, Vol.13,pp.68–79,2019.
- [64] K.K.Parhi,VLSI Digital Signal Processing Systems: Design and Implementation. NewYork:Wiley,1999.
- [65] K.Tripathi, P.Narkhede, R.Kottath, V.Kumar, and S.Poddar, “Design considerations of orientation estimation system,” *IEEE Conference on Wireless Networks and Embedded Systems*, Chitkara University, Rajpura, pp.1–6, 2016.
- [66] F. F. Daitx, V. S. Rosa, E. Costa, P. Flores, and S. Bampi, “VHDL generation of optimized FIR filters,” *2nd International Conference on Signals, Circuits and Systems*, Tunisia,pp.1–5, 2008.
- [67] A. A. H. Ab-Rahman, I. Kamisian, and A. Z. Shaameri, “ASIC modeling and simulation of adaptive FIR filter,” *Proceedings of International Conference on Electronic Design*,Penang,pp.1–4, 2008.
- [68] A. H. A. Razak, M. I. Abu Zaharin, and N. Z. Haron, “Implementing digital finite impulse response filter using FPGA”,*Proceedings of Asia-Pacific Conference on Applied Electromagnetic*,Melaka, Vol.12,pp.1–5, 2007.
- [69] P. K. Meher, S. Chandrasekaran, and A. Amira, “FPGA realization of FIR filters by efficient and flexible systolization using distributed arithmetic, ”*IEEE Trans. Signal Processing*, Vol. 56, no.7, pp.3009–17, 2008.

- [70] 10. J. Talmon, J. Kors, and J. Van Bommel, "Adaptive Gaussian filtering in routine ECG/VCG analysis," *IEEE Trans. Acoustic Speech Signal Processing*, Vol.34, pp.527–34, 1986.
- [71] P.C.Bhaskar and M.Uplane, "High frequency electromyogram noise removal from electrocardiogram using FIR low pass filter based on FPGA," *Procedia Technology*, Vol.25, pp. 497–504, 2016.
- [72] S. B. Jadhav and N. N. Mane, "A novel high speed FPGA architecture for FIR filter design," *Int. J. Reconfigurable Embedded Systems*, Vol.1 ,no.1, pp.1–10, ISSN:2089-4864, 2012.
- [73] Nabih-Ali, Mohammed, El-Sayed A. El-Dahshan, and Ashraf S. Yahia. "Heart diseases diagnosis using intelligent algorithm based on PCG signal analysis." *International Journal of Biology and Biomedicine*, 2017
- [74] L. Chmelka, J. Kozumplik. "Wavelet-Based Wiener Filter for Electrocardiogram Signal Denoising." *Computers in Cardiology 2005*;32: 771-774. IEEE 2005.
- [75] Omid Sayadi, Mohammed Begher Shamsollahi, "ECG Denoising with Adaptive Bionic wavelet transform", *proceedings of 28Th IEEE, EMBS Annual International conference*, New York, 2008.
- [76] M. Velasco, B. Weng, K.E. Barner, "ECG signal denoising and baseline wander correction based on the empirical mode decomposition". *Computers in Biology and Medicine* 38, 1 – 13, 2008.
- [77] D. Thakur, S.S. Rathore, "Comparison of ECG signal De-noising in FIR and wavelet domains", *International Journal of Engineering Research and General Science* Volume 3, Issue 6, November-December, 2016.
- [78] Chou, C.J., Mohana krishnan, S. and Joseph, B. "FPGA Implementation of Digital Filters", *Evans, Proc. ICSPAT '93*, 1993.
- [79] Kuon, I. and Rose, J. "Measuring The Gap Between FPGAs and ASICs", *IEEE Transactions on Computer-Aided Design of Integrated Circuits and Systems*, Vol. 26, No.2, pp. 203–215, 2007
- [80] Ravikumar, M. "Electrocardiogram Signal Processing on FPGA For Emerging Healthcare Applications", *International Journal of Electronics Signals and Systems*, Vol.1, No.3, pp.91-96, 2012.

- [81]Dixit, H.V. and Gupta V. “IIR Filters Using System Generator For FPGA Implementation”, International Journal of engineering Research and Applications, Vol. 2, No. 5, pp. 303-306, 2012
- [82]Chauhan, S., Sharma, L. and Mehra, R. “Cost Analysis of Digital FIR Filter Using Different Window Techniques”, International Journal of Electrical, Electronics and Data Communication, ISSN: 2320-2084, Vol. 1, No. 6, pp. 25-29, 2013.
- [83]Kasetwar, A. R. and Gulhane, S. M. “Adaptive Power Line Interference Canceller: A Survey”, International Journal of Advances in Engineering & Technology, Vol. 5, No. 2, pp. 319-326, 2013.
- [84]Pawar, D.J. and Bhaskar, P.C. “FPGA Based FIR Filter Design for Enhancement of ECG Signal by Minimizing Base-line Drift Interference “, International Journal of Current Engineering and Technology, INPRESSCO, ISSN 2277 – 4106, pp. 1775-1778, 2013.
- [85]Yadav, S.K. and Mehra, R. (2014) “Analysis of Different IIR Filter based on Implementation Cost Performance”, International Journal of Engineering and Advanced Technology, Vol. 3, No. 4, ISSN: 2249 – 8958, pp. 267-270.
- [86]Bokde, P.R. and Choudhari, N.K. (2015) “Implementation of Digital Filter on FPGA For ECG Signal Processing”, International Journal of Emerging Technology and Innovative Engineering, Vol. 1, No. 2, pp.175-181.
- [87] Agarwal S. and Wadhvani A., Analysis of Heart Rate Variability During Meditative and Non-Meditative State Using Analysis of Variance. *International Journal of Advanced Biological and Biomedical Research*;1: 728-736(2013).
- [88] Parashar N., Jain S., Sood M.,Semiautomatic Detection of Cardiac Diseases employing Dual Tree Complex Wavelet Transform. *Periodicals of Engineering and Natural Sciences (PEN)*;6:129-140 (2018).
- [89] Dhiman A., Dubey S.,Jain S., Design of Lead II ECG Waveform and Classification Performance for Morphological features using Different Classifiers on Lead II. *Research Journal of Pharmaceutical, Biological and Chemical Sciences*;7: 1226- 1231 (2016).
- [90] Kirti, Sohal H and Jain S, Comparative Analysis of Heart Rate Variability Parameters for Arrhythmia and Atrial Fibrillation using ANOVA, *Biomedical and Pharmacology Journal*, 11: 1849, 2018.
- [91] Shaffer F. and Ginsberg J. An overview of heart rate variability metrics and norms *Frontiers in public health* ;5: 258 (2017).

- [92] Li Y., Tang X., Xu Z., and Yan H. A novel approach to phase space reconstruction of single lead ECG for QRS complex detection. *Biomedical Signal Processing and Control*, **39**: 405-415 (2018).
- [93] Qin Z., Li M., Huang L., and Zhao Y., Stress level evaluation using BP Neural network based on time-frequency analysis of HRV. *IEEE International Conference on Mechatronics and Automation*:1798-1803 , (2017).
- [94] Agarwal S. and Wadhvani A., Analysis of Heart Rate Variability During Meditative and Non-Meditative State Using Analysis of Variance. *International Journal of Advanced Biological and Biomedical Research*; **1**: 728-736(2013).
- [95] Castaldo R, Xu W *et al.*, Detection of mental stress due to oral academic examination via ultra-short-term HRV analysis, *2016 38th Annual International Conference of the IEEE Engineering in Medicine and Biology Society (EMBC)*, 3805, 2016.
- [96] Castaldo R, Melillo P *et al.*, Fall prediction in hypertensive patients via short-term HRV Analysis, *IEEE journal of biomedical and health informatics* **21**: 399, 2017.
- [97] Isler Y and Kuntalp M, Combining classical HRV indices with wavelet entropy measures improves to performance in diagnosing congestive heart failure, *Computers in biology and medicine* **37**: 1502, 2007.
- [98] Liu G, Wang L *et al.*, A new approach to detect congestive heart failure using short-term heart rate variability measures, *PloS one* 9: e93399, 2014.
- [99] Pandey AK, Pandey P and Jaiswal K, Classification Model for the Heart Disease Diagnosis, *Global Journal of Medical Research* 14, 2014.
- [100] Poddar M, Birajdar AC and Virmani J, Automated Classification of Hypertension and Coronary Artery Disease Patients by PNN, KNN, and SVM Classifiers Using HRV Analysis, *Machine Learning in Bio-Signal Analysis and Diagnostic Imaging*, 99, 2019.
- [101] Goldberger AL, Amaral LA, Glass L *et al.*, PhysioBank, PhysioToolkit, and PhysioNet: components of a new research resource for complex physiologic signals, *Circulation* 101: e215, 2000.
- [102] Melillo P, Izzo R, Orrico A *et al.*, Automatic prediction of cardiovascular and cerebrovascular events using heart rate variability analysis, *PloS one* 10: e0118504, 2015.
- [103] Altan G, Kutlu Y and Allahverdi N, A new approach to early diagnosis of congestive heart failure disease by using Hilbert–Huang transform, *Computer methods and programs in biomedicine* 137: 23, 2016.

- [104] Borchini R, Veronesi G, Bonzini M, Gianfagna F, Dashi O, and Ferrario M, Heart rate variability frequency domain alterations among healthy nurses exposed to prolonged work stress, *International journal of environmental research and public health* 15: 113, 2018.
- [105] Boon K, Khalil-Hani M and Malarvili M, Paroxysmal atrial fibrillation prediction based on HRV analysis and non-dominated sorting genetic algorithm III, *Computer methods and programs in biomedicine* 153: 171, 2018.
- [106] Fonseca P, Long X, Radha M, Haakma R et al., Sleep stage classification with ECG and respiratory effort, *Physiological measurement* 36: 2027, 2015.
- [107] Hu, B. ; Wei, S.; Wei, D. ; Zhao, L.; Zhu, G. and Liu, C. Multiple Time Scales Analysis for Identifying Congestive Heart Failure Based on Heart Rate Variability. *IEEE Access*, 7, 17862-17871, 2019.
- [108] Mahajan, R.; Viangteeravat, T. and Akbilgic, O. Improved detection of congestive heart failure via probabilistic symbolic pattern recognition and heart rate variability metrics. *International journal of medical informatics*, 108, 55-63, 2017
- [109] Mufassirin, M. and Ragel, R. G. (2018). A novel filter-wrapper based statistical analysis approach for cancer data classification.
- [110] Boon, K. ; Khalil-Hani, M.; Malarvili, M. and Sia, C. Paroxysmal atrial fibrillation prediction method with shorter HRV sequences. *Computer methods and programs in biomedicine*, 134, 187-196, 2016
- [111] Yang, A. and Yin, H. Prediction of paroxysmal atrial fibrillation by footprint analysis. *Computers in Cardiology* , 28,401-404, 2001.
- [112] Isler, Y. and Kuntalp, M. Combining classical HRV indices with wavelet entropy measures improves to performance in diagnosing congestive heart failure. *Computers in biology and medicine*, 37, 1502-1510, 2007.
- [113] Liu, G. ; Wang, L.; Wang, Q.; Zhou, G.; Wang, Y. and Jiang, Q. (2014). A new approach to detect congestive heart failure using short-term heart rate variability measures. *PloS one*,. 9, e93399, 2014
- [114] Pandey, A. K. ; Pandey, P. and Jaiswal, K. Classification Model for the Heart Disease Diagnosis. *Global Journal of Medical Research*, 2014.
- [115] Cornforth, D. J. and Jelinek, H. F. (2016). Detection of congestive heart failure using Renyi entropy. *Computing in Cardiology Conference (CinC)*, 669-672.

- [116]N. Prashar, M. Sood, and S. Jain, "Semiautomatic Detection of Cardiac Diseases employing Dual Tree Complex Wavelet Transform," *Periodicals of Engineering and Natural Sciences (PEN)*, vol. 6, pp. 129-140, 2018.
- [117] N. Prashar, "Removal of electromyography noise from ECG for high performance biomedical systems," *Network Biology*, vol. 8, p. 12, 2018.
- [118]Underwood, K.D. and Hemmert, K.S. 2004. Closing the Gap: CPU and FPGA, Trends in Sustainable Floating-Point BLAS Performance. International Symposium on Field-Programmable Custom Computing Machines (FCCM), California, USA.
- [119]Zhuo, L. and Prasanna, V.K. 2005. Sparse Matrix-Vector Multiplication on FPGAs. International Symposium on Field Programmable Gate Arrays (FPGA), Monterey, CA, USA.
- [120] Meng, y., Brown A. P., Iltis, R. A., sherwood, t., lee, h. And kastner, R. 2005. MP Core: Algorithm and Design Techniques for Efficient Channel Estimation in Wireless Applications. Design Automation Conference (DAC), Anaheim, CA.
- [121]Hutchings, B. L. and Nelson, B. E., 2001. Gigaop DSP on FPGA. International Conference on Acoustics, Speech, and Signal Processing (ICASSP). Salt Lake, Utah.
- [122]Alsolaim, a., Becker, j., Glesner, m., and Starzyk, j. 2000. Architecture and Application of a Dynamically Reconfigurable Hardware Array for Future Mobile Communication Systems. International Symposium on Field Programmable Custom Computing Machines (FCCM). Napa, CA.
- [123]Melnikoff, S. J., Quigley, S. F., AND Russell, M. J. 2002. Implementing a Simple Continuous Speech Recognition System on an FPGA. International Symposium on Field-Programmable Custom Computing Machines (FCCM), Napa, CA.
- [124] Yokota, T., Nagafuchi, M., Mekada, Y., Yoshinaga, T., Ootsu, K., and Baba, T. 2002. A Scalable FPGA-based Custom Computing Machine for Medical Image Processing. International Symposium on Field-Programmable Custom Computing Machines (FCCM), Napa, CA.
- [125] Hosangadi, A., Fallah, F., and Kastner, R. 2006. Optimizing Polynomial Expressions by Algebraic Factorization and Common Subexpression Elimination. *IEEE Transactions on Computer-Aided Design of Integrated Circuits and Systems*, vol.25, issue 10, pp. 2012-2022.

- [126] Hauck, S., and Borriello, G. 1997. An evaluation of bipartitioning techniques. *IEEE Transactions on Computer-Aided Design of Integrated Circuits and Systems*, vol. 16, issue 8, pp 849-866.
- [127] A. Croisier, D. J. Esteban, M. E. Levilion, and V. Rizo, "Digital Filter for PCM Encoded Signals." United States Patent 3,777,130, December 3, 1973.
- [128] Wirthlin, M. J., and McMurtrey, B. 2001. Efficient Constant Coefficient Multiplication Using Advanced FPGA Architectures. *International Conference on Field Programmable Logic and Applications (FPL)*, Belfast, UK.
- [129] Crockett, Louise H., Ross A. Elliot, Martin A. Enderwitz, and Robert W. Stewart. *The Zynq Book: Embedded Processing with the Arm Cortex-A9 on the Xilinx Zynq-7000 All Programmable Soc*. Strathclyde Academic Media, 2014.
- [130] Jyoti, Adesh Kumar, and Anil Sangwan. "Designing of FIR Filter Using FPGA: A Review." *Nanoelectronics, Circuits and Communication Systems: Proceeding of NCCS 2017* 511 (2018): 493.
- [131] Kirti, H. Sohal and S. Jain, "Design and Implementation of Low Power ECG Pre-processing Module on Xilinx FPGA", *IETE Journal of Research*, 2020. <https://doi.org/10.1080/03772063.2020.1725660>
- [132] M. G. Egila, M. A. El-Moursy, A. E. El-Hennawy, H. A. El-Simary, and A. Zaki, "FPGA-based electrocardiography (ECG) signal analysis system using least-square linear phase finite impulse response (FIR) filter," *Journal of Electrical Systems and Information Technology*, vol. 3, pp. 513-526, 2019.
- [133] P. Bhaskar and M. Uplane, 'FPGA Based Notch Filter to Remove PLI Noise from ECG', *International Journal on Recent and Innovation Trends in Computing and Communication*, 2018, 3, pp. 2246-2250.
- [134] Verma, Gaurav. "Analysis of Power Reduction Techniques and Low Power Estimation Model for FPGA Implementations.", 2018.
- [135] Market Research Future. (2018, April). "Field Programmable Gate Array Market Available: <http://www.marketresearchfuture.com/reports/field-programmable-gate-arraymarket-1019>.
- [136] Kuon I., Rose J., "Measuring the Gap between FPGAs and ASICs", *IEEE Transaction on Computer Aided Design of Integrated Circuits and Systems*, vol. 26, no. 2, pp. 203-215, 2007.

- [137]Maxfield C., *The Design Warrior's Guide to FPGAs: Devices, Tools and Flows*, Newnes, Newton, MA, 2004.
- [138]Clarke P., *EE Times*, "Xilinx, ASIC Vendors Talk Licensing" June 22, 2001.
- [139]Yeap G. K., *Practical Low Power Digital VLSI Design*, Kluwer, Norwell, 1998.
- [140]The International Technology Roadmap for Semiconductors website. [Online]. Available: <http://public.itrs.net>
- [141]Verma G., *Embedded System Design for Students*, Shroff Publishers Pvt. Ltd., 2015.
- [142]Chattopadhyay S., *Embedded System Design*, PHI Learning Pvt. Ltd., 2010.
- [143]Xilinx, *Power Methodology Guide*, UG786 (v15.5) April 10, 2013.
- [144]Lorandel J., Prevotet J. C., Helard M., "Fast Power and Performance Evaluation of FPGABased Wireless Communication Systems", *IEEE Access*, vol.1-4, pp. 2005-2018, 2016.
- [145]Lamoureux J., Luk W., "An Overview of Low-Power Techniques for Field-Programmable Gate Arrays", in *proceedings of IEEE International Conference on Adaptive Hardware and Systems*, pp. 338-345, 2008.
- [146]Warrier, Prasanth M., B. R. Manju, and Rajkumar P. Sreedharan. "A Survey of Pre-processing Techniques Using Wavelets and Empirical-Mode Decomposition on Biomedical Signals." In *Inventive Communication and Computational Technologies*, pp. 993-1002. Springer, Singapore, 2020.
- [147] Nguyen, Thanh-Nghia, Thanh-Hai Nguyen, and Van-Thuyen Ngo. "Artifact elimination in ECG signal using wavelet transform." *Telkomnika* 18, no. 2 (2020): 936-944.
- [148]Zhao, Zhongyao, Chengyu Liu, Yaowei Li, Yixuan Li, Jingyu Wang, Bor-Shyh Lin, and Jianqing Li. "Noise rejection for wearable ECGs using modified frequency slice wavelet transform and convolutional neural networks." *IEEE Access* 7 (2019): 34060-34067.
- [149]Свид, І. В., О. С. Мальцев, Л. Ф. Сайківська, and О. В. Зубков. "Review of Seventh Series FPGA Xilinx." PhD diss., NURE, MC&FPGA, 2019.
- [150] Kirti, Harsh Sohal, and Shruti Jain, "Multistage Classification of Arrhythmia and Atrial Fibrillation on Long- Term Heart Rate Variability", *Journal of Engineering Science and Technology*, Vol. 15 (2), 2020.

- [151] Kirti, H. Sohal and S. Jain, "Computer Aided Diagnostic System for Feature Based Classification using Heart Rate Variability", *Biomedical Engineering Applications, Basis and Communications*, Vol. 32 (2), 2020.
- [152] Kirti, H. Sohal, Shruti Jain, "Review and Comparison of QRS Detection Algorithms for Arrhythmia", *5th International Conference on Signal Processing, Computing and Control (ISPCC)*, Jaypee University of Information Technology, Wagnaghat, Solan, H.P, India, pp. 159-164, 2018.
- [153] Yu, Qiong, Aili Liu, Tiebing Liu, Yuwei Mao, Wei Chen, and Hongxing Liu. "ECG R-wave peaks marking with simultaneously recorded continuous blood pressure." *PloS one* 14, no. 3 (2019): e0214443.
- [154] Tkacz, E. J., and P. Kostka. "An application of wavelet neural network for classification of patients with coronary artery disease based on HRV analysis." In *Proceedings of the 22nd Annual International Conference of the IEEE Engineering in Medicine and Biology Society (Cat. No. 00CH37143)*, vol. 2, pp. 1391-1393. IEEE, 2000.
- [155] Dallali, A., A. Kachouri, and M. Samet. "Fuzzy c-means clustering, Neural Network, WT, and HRV for classification of cardiac arrhythmia." *ARNP Journal of Engineering and Applied Sciences* 6, no. 10 (2011): 2011.
- [156] Stow, D., B. Burns, and A. Hope. "Mapping Arctic tundra vegetation types using digital SPOT/HRV-XS data A preliminary assessment." *International Journal of Remote Sensing* 10, no. 8 (1989): 1451-1457.
- [157] Kumar, Mohit, Ram Bilas Pachori, and U. Rajendra Acharya. "An efficient automated technique for CAD diagnosis using flexible analytic wavelet transform and entropy features extracted from HRV signals." *Expert Systems with Applications* 63 (2016): 165-172.
- [158] Pedley, Mike I., and Paul J. Curran. "Per-field classification: an example using SPOT HRV imagery." *Remote Sensing* 12, no. 11 (1991): 2181-2192.
- [159] Clark, Patrick E., Mark S. Seyfried, and Bob Harris. "Intermountain plant community classification using Landsat TM and SPOT HRV data." (2001).
- [160] Piotrowski, Zbigniew, and Małgorzata Szypulska. "Classification of falling asleep states using HRV analysis." *Biocybernetics and biomedical engineering* 37, no. 2 (2017): 290-301.

- [161]McIntyre, Chloe L., Nick J. Knowles, and Peter Simmonds. "Proposals for the classification of human rhinovirus species A, B and C into genotypically assigned types." *The Journal of general virology* 94, no. Pt 8 (2013): 1791.
- [162]Vijaya, G., Vinod Kumar, and H. K. Verma. "ANN-based QRS-complex analysis of ECG." *Journal of medical engineering & technology* 22, no. 4 (1998): 160-167.
- [163]Ozbay, Yuksel, and Bekir Karlik. "A recognition of ECG arrythihemias using artificial neural networks." In *2001 Conference Proceedings of the 23rd Annual International Conference of the IEEE Engineering in Medicine and Biology Society*, vol. 2, pp. 1680-1683. IEEE, 2001.
- [164]Bhalerao, Siddharth, Irshad Ahmad Ansari, and Anil Kumar. "Performance Comparison of SVM and ANN for Reversible ECG Data Hiding." In *Soft Computing: Theories and Applications*, pp. 197-207. Springer, Singapore, 2020.
- [165]Rakshit, Raj, V. Ramu Reddy, and Parijat Deshpande. "Emotion detection and recognition using HRV features derived from photoplethysmogram signals." In *Proceedings of the 2nd workshop on Emotion Representations and Modelling for Companion Systems*, pp. 1-6. 2016.
- [166]Tavassoli, Masih, Mohammad Mehdi Ebadzadeh, and Hamed Malek. "Classification of cardiac arrhythmia with respect to ECG and HRV signal by genetic programming." *Canadian Journal on Artificial Intelligence, Machine Learning and Pattern Recognition* 3, no. 1 (2012): 1-8.
- [167]Munla, Nermine, Mohamad Khalil, Ahmad Shahin, and Azzam Mourad. "Driver stress level detection using HRV analysis." In *2015 international conference on advances in biomedical engineering (ICABME)*, pp. 61-64. IEEE, 2015.
- [168]Nizami, Shermeen, James R. Green, J. Mikael Eklund, and Carolyn McGregor. "Heart disease classification through HRV analysis using parallel cascade identification and fast orthogonal search." In *2010 IEEE International Workshop on Medical Measurements and Applications*, pp. 134-139. IEEE, 2010.
- [169]Kumar, Prashant, Ashis Kumar Das, and Suman Halder. "Time-domain HRV Analysis of ECG Signal under Different Body Postures." *Procedia Computer Science* 167 (2020): 1705-1710.
- [170]Corredor-Matus, José R., and Fernando Riveros-Sanabria. "Analysis of parameters in electrocardiographic signals of patients with Chagas and time domain variables of the HRV using high resolution polygraph." *ORINOQUIA* 23, no. 2 (2019): 47-55.

- [171]Kim, Jeom Keun, and Jae Mok Ahn. "Effects of a spectral window on frequency domain HRV parameters." In *Advances in Computer Communication and Computational Sciences*, pp. 697-710. Springer, Singapore, 2019.
- [172]Wang, Y.; Wei, S. ; Zhang, S.; Zhang, Y. ; Zhao, L.; Liu, C. et al. (2018). Comparison of time-domain, frequency-domain and non-linear analysis for distinguishing congestive heart failure patients from normal sinus rhythm subjects. *Biomedical Signal Processing and Control*,42, 30-36.
- [173]Isler, Y.; Narin, A. ; Ozer, M. and Perc, M.. Multi-stage classification of congestive heart failure based on short-term heart rate variability. *Chaos, Solitons & Fractals*, 118, 145-151, 2019.

APPENDICES

APPENDICES

APPENDIX A

This section describes the Pan-Tompkins real-time QRS detection algorithm represented in Figure 1. The algorithm consists of a series of digital filters and signal processing implemented in a digital processing unit. The signal processed is the output from an ADC, at a sampling rate of 200 Hz. It passes through a lowpass filter and a highpass filter to eliminate noise before it continues through a filter that approximates a derivative. There is an amplitude squaring process before the signal passes through a moving-window integrator. The final step is an adaptive threshold method to determine the location of the signal peaks.

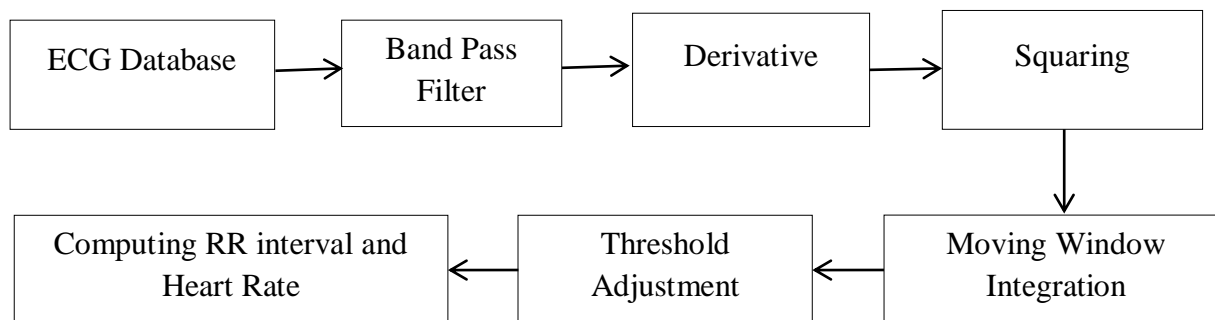


Figure 1: Pan-Tompkin's QRS Detection Algorithm

- i. **Bandpass Filter:** The bandpass filter reduces the influence of muscle noise, 50 Hz interference, baseline wander, and *T*-wave interference. The desired passband to maximize the *QRS* energy is approximately 5–15 Hz. The filters all have poles and zeros on the unit circle of the z plane. The cascading of low pass filter and high pass filter forms the bandpass filter. The lowpass filter has a cut-off frequency of about 11 Hz. The high pass filter having cutoff frequency is about 5 Hz. Figure 2 (b) represents the output of the filtered ECG signal.
- ii. **Derivative:** The signal is differentiated to provide the slope information of the *QRS* complex. A five-point derivative is used to approximate an ideal derivative between dc and 30 Hz. Figure 2 (c) shows the output of the derivative ECG signal.
- iii. **Squaring:** Squaring Function The signal is now squared point by point in the raw ECG signal. All data points are now made positive, and the squaring also does a nonlinear amplification of the derivative emphasizing the higher frequencies.

- iv. *Moving-Window Integration:* The moving-window integration results in waveform information and the slope of the R wave. The width of the window should be approximately the same as the widest possible QRS complex. A narrow window will produce several peaks in the integration waveform, while a wide window will merge the QRS and T waves. For a sample rate of 200 Hz, a window of 30 samples has proven to be a good size.
- v. *Threshold adjustment:* The time duration of the rising edge of the integration waveform corresponds to the duration of the QRS complex. Thresholds are automatically adjusted to float over the noise. Due to the good signal-to-noise ratio improved by the bandpass filter, low thresholds are possible. Two thresholds are used to detect a QRS complex. The higher the two thresholds will identifies the peaks of the signal. If no peaks have been identified within a certain time interval, the lower threshold is used to find a peak using a search back method. The thresholds are adjusted as the integrated signal moves forward. Figure 2(e) represents the QRS complex detection after employing thresholds.

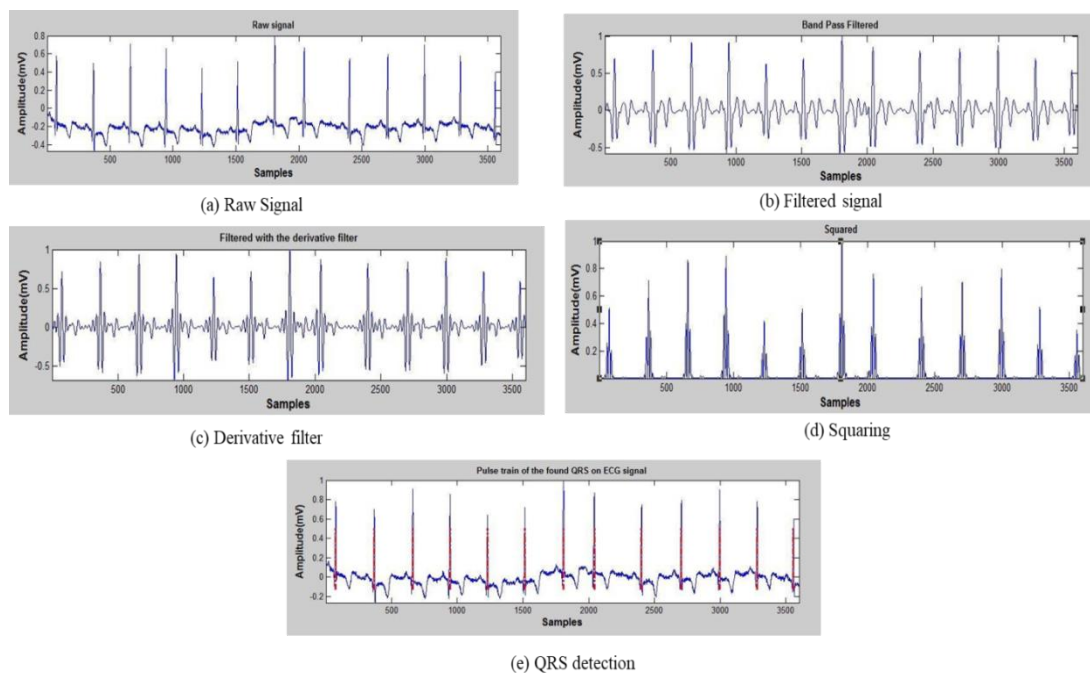


Figure 2: Simulation Results (a) Noisy ECG signal (b) Filtered Signal (c) Derivative signal (d) Squaring (e) QRS complex detection

- vi. *RR Intervals:* Two RR intervals are maintained. One is the average of the last eight beats, regardless of their values. The second is the average of the eight last beats

that fall within certain limits. The reason for this is to be able to adapt to quickly changing or irregular heartbeats.

- vii. *T-Wave Identification:* If the RR interval is less than 360 ms, the peak detected might be a peak from the T wave. If the maximal slope from the wave misses less than half of the preceding one, the peak is identified as a T wave. Otherwise, it is determined as a *QRS* complex.
- viii. *Heart Rate Variability:* Heart rate variability is the variation in the time between heartbeats. The RR interval calculations output the heartbeat. The difference between each of these outputs will give the heart rate variability measured over time.

APPENDIX B

The traditional window function description is given in this appendix.

Rectangular Window

It is a commonly utilized window function having advantages corresponding to the smallest main lobe width and the highest peak of the side lobe in various applications. For the past few years, researchers have not used it widely in signal processing applications due to its lack of flexibility. The rectangular window function is represented by equation 1.

$$w(n) = 1 \quad (1)$$

Hanning window

The Hanning window is named after Julius Von Hann and the raised cosine window. The endpoints of the Hann window just touch zero as compared to the hamming window function. The window function of hanning is represented by Eq. (2).

$$w(n) = 0.5 - 0.5 \cos\left(\frac{2\pi n}{M}\right) \quad (2)$$

Hamming window

It delivers good side-lobe attenuation in comparison to the rectangular window function. The hamming window function minimizes the highest side lobe, provide it a height of approximately 1/5th of the Hanning window. This window function is illustrated by Eq. (3)

$$w(n) = 0.54 - 0.46 \cos\left(\frac{2\pi n}{M}\right) \quad (3)$$

Kaiser Window

This window function is designed with minimum stop-band attenuation. It also provides maximum stop-band width to acquire the appropriate stop-band attenuation. It depends on various types of constraints like β dB (side-lobe attenuation), α (Kaiser window parameter) as it affects the side-lobe attenuation as represented by Eq. (4). Where, I_0 = zeroth-order modified Bessel function, β = parameter to allow a trade-off between side-lobe amplitude and main lobe width.

$$w(n) = I_0\left(\beta\sqrt{1 - \left(\frac{2n}{M} - 1\right)^2}\right) / I_0(\beta) \quad (4)$$

From the various literature, it has been inferred that the Kaiser window performs better as compared to other window functions because passband and stopband ripple size is not affected by the variation in the window length.

Bartlett window

This window function is relatable to the triangular window function. The triangular window has non-zeroes at first and last samples as compared to Bartlett which has zeroes at first and last samples. The weight function of the Bartlett window is signified in Eq. (5).

$$w(n) = 1 - \frac{2|n - \frac{M}{2}|}{M} \quad (5)$$

Blackmann window

Blackmann window is easily applicable to digital signal processing applications. It returns the L-point (positive integer) symmetric window in the column vector 'w'. Blackman window functions have somewhat wider central lobes along with minimum side-band leakage as compared to the same order Hamming and Hann window functions. Blackman window is defined by Eq. (6).

$$w(n) = 0.42 - 0.5 \cos\left(\frac{2\pi n}{M}\right) + 0.08 \cos\left(\frac{4\pi n}{M}\right) \quad (6)$$

APPENDIX C

Wavelet Functions

For the DWT special families of wavelet functions are developed. These wavelets are compactly supported, orthogonal or biorthogonal, and are characterized by low-pass and high-pass analysis and synthesis filters. From the filters, a wavelet function $\psi(t)$ and scaling function $\phi(t)$ can be derived.

1. Daubechies

The Daubechies family is named after Ingrid Daubechies who invented the compactly supported orthonormal wavelet, making wavelet analysis in discrete-time possible. The first order Daubechies wavelet is also known as the Haar wavelet, in which the wavelet function resembles a step function. The wavelet and scaling functions for the Daubechies functions with order 4 are represented in this section. The Haar wavelet or db1 can be written as Eq. 1 and represented in Figure 1.

$$\begin{aligned} \psi(t) &= \begin{cases} 1 & \text{if } x \in [0 \ 0.5] \\ -1 & \text{if } x \in [0.5 \ 1] \\ 0 & \text{if } x \notin [0 \ 1] \end{cases} \\ \phi(t) &= \begin{cases} 1 & \text{if } x \in [0 \ 1] \\ 0 & \text{if } x \notin [0 \ 1]. \end{cases} \end{aligned} \quad (1)$$

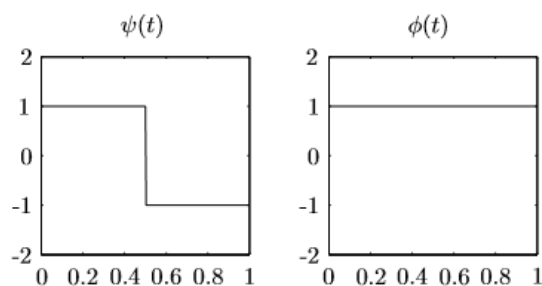


Figure 1: Haar wavelet

Higher-order Daubechies functions are not easy to describe with an analytical expression. The order of the Daubechies functions denotes the number of vanishing moments or the number of zero moments of the wavelet function. This is weakly related to the number of oscillations of the wavelet function. Larger the number of vanishing moments, the better

the frequency localization of the decomposition. The dependence between wavelet coefficients on different scales decays with increasing wavelet order [4].

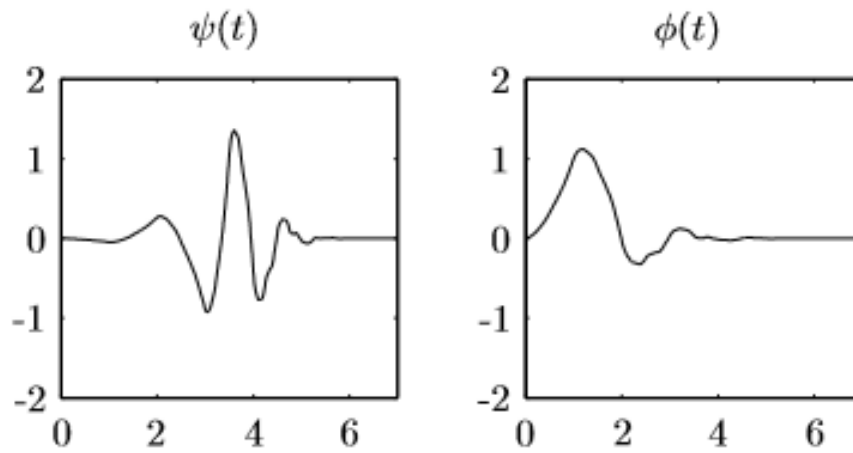


Figure 2: Daubechies 4 wavelet

The order of the wavelet functions can be compared to the order of a linear filter. The Daubechies wavelets are compactly supported orthogonal wavelets. The scaling filters are minimum-phase filters. Figure 2 illustrates the db4 wavelet.

2. Coiflets

Coiflets are also built by I. Daubechies at the request of R. Coifman. Coifman wavelets are orthogonal compactly supported wavelets with the highest number of vanishing moments for both the wavelet and scaling function for a given support width. The Coiflet wavelets are more symmetric and have more vanishing moments than the Daubechies wavelets as represented by Figure 3.

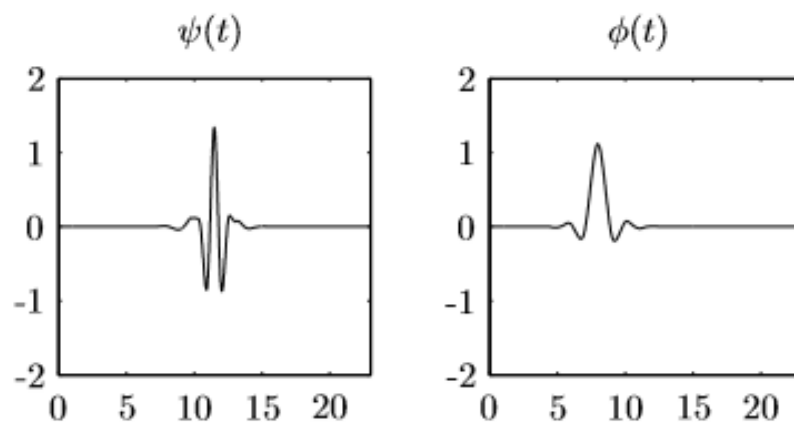


Figure 3: Coiflet 4 Wavelet

3. Symlets

Symlets are also orthogonal and compactly supported wavelets, which are proposed by I. Daubechies as modifications to the db family. Symlets are near symmetric and have the least asymmetry as signified in Figure 4. The associated scaling filters are near linear-phase filters. The properties of symlets are nearly the same as those of the db wavelets.

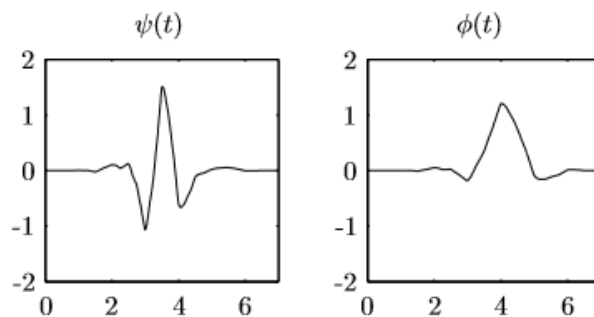


Figure 4: Symlet4 wavelet

5. Biorthogonal

The biorthogonal family contains biorthogonal compactly supported spline wavelets. With these wavelets, symmetry and exact reconstruction are possible using FIR (Finite Impulse Response) filters, which is impossible for the orthogonal filters (except for the Haar filters). The symmetry means that the filters have a linear phase. The biorthogonal family uses separate wavelet and scaling functions for the analysis and synthesis of a signal illustrated in Figure 5. The reverse biorthogonal family uses the synthesis functions for the analysis and vice versa.

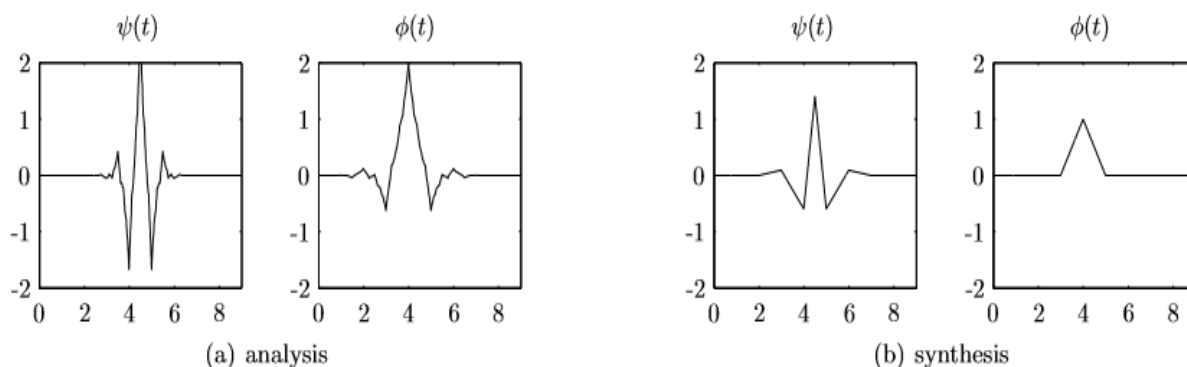


Figure 5: Biorthogonal wavelet

The wavelet coefficients in the different frequency bands of the DWT can be processed in several ways. By adjusting the wavelet coefficients the reconstructed signal of the

synthesis filter bank can be changed in comparison to the original signal. This gives the DWT some attractive properties over linear filtering. Compared to the CWT, the DWT is easier to compute and the wavelet coefficients are easier to interpret since no conversion from scale to frequency has to be made.